IDENTIFICATION OF SCAFFOLD PROTEINS RACK1 AND HIC-5 AS REGULATORS OF ENDOTHELIAL SPROUTING RESPONSES

A Dissertation

by

JUI MAYANK DAVE

Submitted to the Office of Graduate and Professional Studies of
Texas A&M University
in partial fulfillment of the requirements for the degree of

DOCTOR OF PHILOSOPHY

Chair of Committee,	Kayla Bayless
Committee Members,	Steve Maxwell
	Rajesh Miranda
	Veronica Sanchez
Head of Department,	Van Wilson

December 2014

Major Subject: Medical Sciences

ABSTRACT

Angiogenesis is defined as growth of new blood vessels from pre-existing ones and occurs during normal physiological development as well as pathological conditions like cancer. During angiogenesis, normally quiescent endothelial cells (ECs) are activated in response to external pro-angiogenic cues and undergo rapid morphogenic changes such as proliferation, migration, invasion, and lumen formation to extend new sprouts into surrounding three-dimensional (3D) matrix. To better understand angiogenic regulation, we utilized an in vitro model wherein sphingosine 1-phosphate (S1P) and pro-angiogenic growth factors (GF) synergize to induce rapid and robust endothelial sprouting in 3D collagen matrices.

In a proteomic screen designed to identify molecules relevant to angiogenesis, we found up-regulated levels of receptor for activated C kinase 1 (RACK1) and the intermediate filament protein, vimentin. RACK1 depletion reduced EC invasion. Silencing of vimentin or RACK1 decreased cell adhesion and attenuated with focal adhesion kinase (FAK) activation, which is indispensable for successful angiogenesis. Moreover, pro-angiogenic GFs enhanced RACK1 and vimentin association. RACK1, vimentin, and FAK, formed an intermolecular complex during S1P- and GF- induced invasion. Also, depletion of RACK1 decreased vimentin and FAK association, suggesting a role for RACK1 in stabilizing vimentin-FAK interactions during sprouting.

In an independent study, we identified focal adhesion (FA) scaffold protein, hydrogen peroxide inducible clone 5 (Hic-5), as a critical regulator of angiogenesis. Hic-5 depletion interfered with endothelial invasion and lumen formation. S1P induced rapid Hic-5 translocation to FAs and Hic-5 silencing attenuated FAK expression and activation. S1P induced a novel interaction between Hic-5 and membrane type 1 matrix-metalloproteinase (MT1-MMP). In vitro binding experiments revealed that LIM2 domain of Hic-5 was required for MT1-MMP binding. Moreover, Hic-5 and MT1-MMP levels were up-regulated in detergent resistant membrane fractions of invading ECs, indicative of their crosstalk. Hic-5 silencing interfered with S1P- induced MT1-MMP membrane translocation, a critical event for successful angiogenesis. Since MT1-MMP and FAK interaction has been reported to be essential for matrix degradation at FA sites, we further tested if Hic-5 mediated this interaction. Our results indicated that presence of Hic-5 significantly enhanced FAK and MT1-MMP complex formation. In conclusion, we report that scaffold proteins RACK1 and Hic-5 regulate successful endothelial sprouting responses in 3D matrices.

DEDICATION

To my parents Dr. Mayank Dave, Mrs. Bina Dave and my loving brother, Pranav Dave, for their blessings, prayers, faith, love, support, and patience. I stand here today as a mere reflection of their values, teachings, strength and integrity.

ACKNOWLEDGEMENTS

First and foremost, I would like to express my sincere gratitude to my advisor, Dr. Kayla Bayless. It has been a privilege and a true learning experience to be her second Ph.D. student. Her undying passion for science and dedication inspired me immensely to work harder and will continue being a source of motivation for my future endeavors. This work would have never been possible without her contribution in time, intellect and funding. I would also like to acknowledge Dr. Steve Maxwell, Dr. Rajesh Miranda, and Dr. Veronica Sanchez for providing guidance and encouragement as my committee members. Thanks are due to Dr. Geoffrey Kapler for his instrumental support and help in directing me to Bayless Lab.

My appreciation is also extended to all current and former laboratory members. In particular, I would like to thank Dr. Hojin Kang for his co-operation during my initial years, Colette Abbey for technical support and Camille Duran as well as Robert Rogers for creating a cheerful working environment. I would further like to thank Dr. Po-Feng Lee and Dr. Heewon Seo for technical assistance. Thanks are extended to all my colleagues, faculty and staff at Health Science Center for making this journey a great experience. I would also like to acknowledge the Department of Biophysics and Biochemistry for support in funding through my first year of graduate school.

My time at Texas A&M University was made enjoyable and memorable in large part due to the many friends and associations, which have become a part of my life. In

particular, I sincerely thank Jayashre Ridhi for her invaluable moral support and unconditional friendship. Thanks are also due to Anuja Pasale, Gaurang Bastikar, Gaurav Bhiwandkar, Shreyas Erapalli, Aditya Maddali, Shreyas Sati, Nikita Ojha, Nandhini Krishnan, Yi Sun, Varun Chheda, Kunjan Majmudar, and Kathan Shah, for giving me lifetime worth of memories. My experience was enriched by Indian Association and Indian Graduate Student Association at Texas A&M University.

I am truly grateful to my family members for believing in me and encouraging me to pursue further studies. Thank you, Mayank Dave, for being my role model and inspiring me endlessly with your simplistic way of living life. Thank you, Bina Dave, for being a perfect example of successful and independent working woman. Pranav Dave, I thank you from the bottom of my heart, for being the wise little brother and teaching me to never give up on my dreams.

Finally I would like to thank Almighty for showering his blessings and looking over my family in my absence.

NOMENCLATURE

bFGF Basic fibroblast growth factor

EC Endothelial cell

ECM Extracellular matrix

EDG Endothelial differentiation gene

FA Focal adhesion

FAK Focal adhesion kinase

Hic-5 Hydrogen peroxide inducible clone 5

HUVEC Human umbilical vein endothelial cells

LD Asp and Leu rich

LIM Lin11, Isl-1 & Mec-3

MT1-MMP Membrane type 1 matrix-metalloproteinase

PTX Pertussis toxin

RACK1 Receptor for activated C kinase 1

S1P Sphingosine 1-phosphate

VEGF Vascular endothelial growth factor

VE-cadherin Vascular endothelial cadherin

VIM Vimentin

WD-repeat tryptophan-aspartate repeat

3D Three dimensional

TABLE OF CONTENTS

Page

ABSTRACT ii

DEDICATION iv

ACKNOWLEDGEMENTS v

NOMENCLATURE vii

TABLE OF CONTENTS viii

LIST OF FIGURES xi

LIST OF TABLES xiii

CHAPTER I INTRODUCTION AND LITERATURE REVIEW 1

CHAPTER II PROTEOMIC PROFILING OF ENDOTHELIAL INVASION REVEALED RECEPTOR FOR ACTIVATED C KINASE 1 (RACK1) COMPLEXED WITH VIMENTIN TO REGULATE FOCAL ADHESION KINASE (FAK) 15

- Introduction 15
- Experimental Procedures 17
  - Endothelial Cell Culture and Invasion 17
  - Proteomic Screen 1: Differential In-Gel Electrophoresis (DIGE) 17
  - Proteomic Screen 2: Two-Dimensional Gel Electrophoresis 21
  - In Gel Digestion 21
  - Protein Identification 21
  - Immunoblotting 23
  - Generation of Stable Cell Lines Using shRNA 23
  - mRNA Extraction and PCR Analysis 24
  - shRACK1 Rescue Experiments 25
  - Immunoprecipitation 26
  - Immunofluorescence and Colocalization Studies 27
  - Imaging and Quantification of Invasion Density and Distance 28

Cell Adhesion Assays 28
Results 29
Identification of RACK1 as a Regulator of S1P Induced Invasion in ECs 29
RACK1 Was Required for EC Invasion 36
RACK1 Depletion Decreased FAK Activation 42
FAK Activation Occurred during EC Invasion 43
Vimentin Regulated FAK Expression in ECs 45
RACK1 Complexed with Vimentin and GFs Enhanced this Interaction 48
Vimentin Association with FAK Required RACK1 52
Knockdown of Vimentin and RACK1 Decreased Cell Attachment and Focal Adhesion Formation 55
Discussion 58

CHAPTER III HIC-5 MEDIATED ENDOTHELIAL SPROUTING BY REGULATING FOCAL ADHESION KINASE AND A KEY SURFACE METALLOPROTEINASE 63

Introduction 63
Materials And Methods 67
Endothelial Cell Culture and Invasion 67
Hic-5 Cloning 67
293 Cell Culture and Transfection 69
Generation of Stable Cell Lines using shRNA 69
Immunoblotting 69
Immunoprecipitation 70
Immunofluorescence 71
Isolation of Detergent Resistant Membrane (DRM) Fraction from ECs 72
Isolation of Membrane Fraction from ECs by Subcellular Fractionation 73
Imaging and Quantification of Invasion Density, Distance, and Lumen Size 73
Quantification of Hic-5 Positive Aggregates 74
Results 74
Hic-5 was Required for S1P- and GF- Mediated Sprouting 74
S1P Promoted Hic-5 Colocalization with FAK 77
Hic-5 Depletion Resulted in Attenuated FAK Expression and Activation 80
Hic-5 was Required for Successful Lumen Formation during Endothelial Sprouting 82
Hic-5 Complexed with MT1-MMP in an S1P- Dependent Manner in ECs 83
LIM2 Domain of Hic-5 was Required for Binding to MT1-MMP 86
MT1-MMP and Hic-5 Were More Resistant to Detergent Extraction during Endothelial Invasion 90

Hic-5 Silencing Interfered with MT1-MMP Membrane Translocation 92
Hic-5 Enhanced Complex Formation Between FAK and MT1-MMP 97
Discussion 99

CHAPTER IV CONCLUSIONS AND FUTURE DIRECTIONS 104

Future Directions 107

REFERENCES 111

LIST OF FIGURES

Page

Figure 1: 3D *in vitro* angiogenic model 9

Figure 2. PTX dose response experiment..... 30

Figure 3. Effect of pertussis toxin (PTX) on S1P- and GF- induced EC invasion..... 31

Figure 4. Western blot analysis to verify upregulation of identified proteins..... 36

Figure 5. RACK1 knockdown decreased invasion responses in ECs. 38

Figure 6. RACK1 rescue partially restores sprouting responses and invasion distance reduced by RACK1 silencing. 41

Figure 7. Depletion of RACK1 reduced FAK activation.. 43

Figure 8. EC invasion required FAK activation. 45

Figure 9. Vimentin regulated FAK expression in ECs..... 47

Figure 10. Calpain inhibition does not affect FAK expression or activation.. 48

Figure 11. Growth factor stimulation enhanced RACK1-vimentin complex formation.. 50

Figure 12. RACK1, vimentin, and FAK complex formation is enhanced during EC invasion..... 54

Figure 13. Inhibition of FAK activity does not alter complex formation between RACK1, VIM and FAK. 55

Figure 14. Vimentin silencing reduced EC adhesion responses. 58

Figure 15. Hic-5 was required for S1P- and GF- mediated EC invasion. 76

Figure 16. S1P altered Hic-5 localization in ECs.. 78

Figure 17. S1P promoted Hic-5 co-localization with pFAK. 79

Figure 18. Hic-5 depletion decreased levels of pFAK and total FAK.. 81

Figure 19. Hic-5 was required for successful lumen formation during endothelial sprouting. 83

Figure 20. Hic-5 co-localized with activated MT1-MMP in an S1P- dependent manner. 85

Figure 21. Hic-5 complexed with MT1-MMP in an S1P- dependent manner. 86

Figure 22. The LIM2 domain of Hic-5 was required for MT1-MMP binding. 89

Figure 23. Hic-5 and MT1-MMP were more resistant to detergent extraction during endothelial invasion. 92

Figure 24. Hic-5 silencing attenuated pMT1-MMP membrane translocation. 95

Figure 25. Hic-5 depletion resulted in decreased levels of MT1-MMP at the endothelial membrane following S1P treatment. 96

Figure 26. Figure 13. Hic-5 mediated complex formation between FAK and MT1-MMP. 98

Figure 27. Roles of scaffold proteins RACK1 and Hic-5 during endothelial sprouting 106

LIST OF TABLES

Page

Table 1. Molecules known to stimulate angiogenesis 3

Table 2. List of up-regulated proteins from proteomic screen 1 33

Table 3. List of down-regulated proteins from proteomic screen 1 34

Table 4. List of up-regulated proteins from proteomic screen 2 35

Table 5. Primer sequences for Hic-5 cloning 68

Table 6. Summary of MT1-MMP and Hic-5 binding studies 88

CHAPTER I

INTRODUCTION AND LITERATURE REVIEW*

Angiogenesis is defined as the formation of new blood vessels that arise from pre-existing vasculature. Angiogenesis is also referred to as neovascularization and plays a key role in several physiological processes such as embryonic growth and development, pregnancy, ovulation, and wound healing, [1, 2]. Loss of angiogenic regulation results in uncontrolled angiogenesis, which is a common denominator in several human disorders, including but not limited to, cancer [3, 4], rheumatoid arthritis [4, 5], coronary artery disease [6, 7], Alzheimer's disease [8], stroke [9], diabetic [10, 11], atherosclerosis [12], age-related macular degeneration [13, 14], hypertension [15], chronic wounds [16] and ulcers [17]. Thus, understanding molecular signaling pathways that regulate angiogenesis becomes instrumental.

During angiogenesis, normally quiescent endothelial cells (ECs) lining blood vessels, are activated in response to external pro-angiogenic cues and undergo rapid morphogenic changes such as proliferation, basement membrane degradation, sprout initiation, migration, invasion, and lumen formation to extend new sprouts into the surrounding three-dimensional (3D) matrix [18-21].

Several pro-angiogenic factors have been reported that stimulate robust endothelial sprouting responses *in vitro* and *in vivo* (Table 1). Vascular endothelial growth factor (VEGF) has been identified as a key driver of physiological angiogenesis during embryogenesis, skeletal growth, and reproduction [22, 23]. Other growth factors such as basic fibroblast growth factor (bFGF) [24], platelet derived growth factor BB (PDGF-BB) [25], and stromal derived factor 1α (SDF-1α) [26] have also been reported to promote tube formation in ECs. Sphingosine 1- phosphate (S1P), a blood-borne lipid mediator which is known to play crucial role in barrier enhancement, vascular maturation and angiogenesis, stimulates endothelial sprouting *in vitro* [27, 28]. Wall shear stress and fluid forces have also emerged as regulators of endothelial morphogenesis and vessel remodeling [29, 30]. ECs lining blood vessels are exposed to mechanical forces tangential to the cell surface due to blood flow [30-32]. Importantly, ECs must integrate multiple biochemical and mechanical signals, which activate various intracellular signaling pathways that are well-described to regulate angiogenesis. A wide range of intracellular molecules have been identified to respond to exogenous pro-angiogenic stimuli and regulate endothelial sprouting responses. The extensive list includes actin binding proteins, microtubules, intermediate filaments, junctional proteins, integrins, kinases, ion channel proteins, small GTPases, proteases, surface receptors, and scaffold proteins (Table 1).

Table 1. Molecules known to stimulate angiogenesis

Category	Proteins	*In vitro* studies	*In vivo* studies
Exogeneous pro-angiogenic stimuli	Vascular endothelial growth factor (VEGF)	Senger *et al.*, 1983 [33] Pepper *et al.*, 1992 [34] Nicosia *et al.*, 1994 [35] Mandriota and Pepper; 1997 [36]	Leung *et al.*, 1989 [37] Plouet *et al.*, 1989 [38] Connolly *et al.*, 1989 [39] Phillips *et al.*, 1994 [40] Tolentino *et al.*, 1996 [41] Carmeliet *et al.*, 1996 [42] Ferrara *et al.*, 1996 [43]
	Basic fibroblast growth factor (bFGF)	Shing *et al.*, 1984 [44] Montesano *et al.*, 1986 [45] Pepper *et al.*, 1992 [34] Presta *et al.*, 2005 [46]	Shing *et al.*, 1985 [47] Presta *et al.*, 1986 [48] Gualandris *et al.*, [49]
	Platelet derived growth factor BB (PDGF-BB)	Battegay *et al.*, 1994 [25] Nicosia *et al.*, 1994 [35]	Brown *et al.*, 1995 [50] Xue *et al.*, 2011 [51]
	Stromal derived factor 1α (SDF-1α)	Saunders *et al.*, 2006 [26]	Mirshahi *et al.*, 2000 [52] Ara *et al.*, 2005 [53]
	Sphingosine 1-phosphate (S1P)	Lee *et al.*, 1999 [54] Wang *et al.*, 1999 [55] Garcia *et al.*, 2001 [28] Bayless and Davis; 2003 [27]	Oyama *et al.*, 2008 [56]
	Nitric oxide (NO)	Ziche *et al.*, 1994 [57]	Ziche *et al.*, 1994 [57] Lee *et al.*, 1999 [58] Fukumura *et al.*, 2001 [59] Amano et al., 2003 [60]
	Wall shear stress (WSS)	Kang *et al.*, 2008 [61] Kang *et al.*, 2011 [30] Jung *et al.*, 2012 [62]	Ichioka *et al.*, 1997 [63] Zhou *et al.*, 1998 [64] Lucitti *et al.*, 2007 [65] Jung *et al.*, 2012 [62]
	Interstitial flow	Song *et al.*, 2011 [66]	
	Mechano-transduction	Reviewed in: Egginton, 2011 [67] Kaunas *et al.*, 2011 [29] Roman *et al.*, 2012 [68]	Reviewed in: Egginton, 2011 [67] Kaunas *et al.*, 2011 [29] Roman *et al.*, 2012 [68]
Intermediate filaments	Vimentin	Kwak *et al.*, 2012 [69]	Eckes *et al.*, 2000 [70] Lundkvist *et al.*, 2004 [71] Neiminen *et al.*, 2006 [72]

Table 1. Continued

Category	Proteins	*In vitro* studies	*In vivo* studies
MTs (Microtubules)	MT tip complex proteins	Kim *et al.*, 2013 [73]	
	MT depolymerizing factors	Reviewed in Bayless and Johnson; 2011 [74]	Reviewed in Bayless and Johnson; 2011 [74]
Actin binding proteins	Filamin A		Feng *et al.*, 2006 [75]
Proteases	Calpains	Su *et al.*, 2006 [76] Kang *et al.*, 2011 [30] Kwak *et al.*, 2012 [69]	Su *et al.*, 2006 [76] Hoang *et al.*, 2010 [77] Hoang *et al.*, 2011 [78]
	MT1-MMP	Hiraoka *et al.*, 1998 [79] Hotary *et al.*, 2000 [80] Bayless and Davis, 2003 [27] Chun *et al.*, 2004 [81] Saunders *et al.*, 2006 [26] Kang *et al.*, 2008 [61]	Holmbeck *et al.*, 1999 [82] Zhou *et al.*, 2000 [83] Chun *et al.*, 2004 [81]
Small GTPases	Rac1	Bayless and Davis; 2002 [84] Koh *et al.*, 2008[85]	Kamei *et al.*, 2006 [86] Hoang *et al.*, 2011 [87]
	Cdc42	Bayless and Davis; 2002 [84] Koh *et al.*, 2008 [85] Sacharidou *et al.*, 2010 [88]	Kamei *et al.*, 2006 [86] Hoang *et al.*, 2011 [89]
	Rap1	Yan *et al.*, 2008 [90] Carmona *et al.*, 2009 [91]	
	Rho	Hoang *et al.*, 2004 [92] Liu and Senger; 2004 [93]	Hoang *et al.*, 2004 [92] Garnaas *et al.*, 2008 [94]
Integrins	$\alpha_2\beta_1$	Davis and Camarillo, 1996 [20]	Senger *et al.*, 1997 [95] Senger *et al.*, 2002 [96] San Antonio *et al.*, 2009 [97]
	$\alpha_1\beta_1$		Senger *et al.*, 1997 [95] Senger *et al.*, 2002 [96]
	$\alpha_4\beta_1$		Garmy-Susini *et al.*, 2005 [98]

Table 1. Continued

Category	Proteins	*In vitro* studies	*In vivo* studies
Integrins	$\alpha_5\beta_1$	Bayless *et al.*, 2000 [99]	Kim *et al.*, 2000 [100]
	$\alpha_v\beta_3$	Bayless *et al.*, 2000 [99]	Brooks *et al.*, 1994 [101] Drake *et al.*, 1995 [102] Friedlander *et al.*, 1995 [103] Hammes *et al.*, 1996 [104] Bader *et al.*, 1998 [105]
	$\alpha_v\beta_5$		Friedlander *et al.*, 1995 [103]
Kinases	Focal adhesion kinase (FAK)	Cabrita *et al.*, 2011 [106] Dave *et al.*, 2013 [107]	Shen *et al.*, 2005 [108] Braren *et al.*, 2006 [109] Tavora *et al.*, 2010 [110]
	PKCε	Koh *et al.*, 2008 [85]	
	GSK-3β		Hoang *et al.*, [89]
	Pak	Koh *et al.*, 2008 [85] Koh *et al.*, 2009 [111]	Kiosses *et al.*, 2002 [112]
	Src	Koh *et al.*, 2009 [111] Liu and Senger; 2004 [93]	Reviewed in Rak *et al.*, 1995 [113]
	Raf kinase	Koh *et al.*, 2009 [111]	Reviewed in Rak *et al.*, 1995 [113] Hamden *et al.*, 2005 [114]
	Akt	Dimmeler *et al.*, 1998 [31] Igarashi *et al.*, 2001[115] Morales-Ruiz *et al.*, 2001 [116] Kang *et al.*, 2008 [61]	Dimmeler *et al.*, 1998 [31] Ackah *et al.*, 2005 [117]
Junctions	VE-cadherin	Yang *et al.*, 1999 [118]	Carmeliet *et al.*, 1999 [119] Gory-Faure *et al.*, 1999 [120] Montero-balaguer *et al.*, 2009 [121] Wang *et al.*, 2010 [122]
	PECAM-1	DeLisser *et al.*, 1997 [123] Yang *et al.*, 1999 [118] Cao *et al.*, 2002 [124]	Cao *et al.*, 2009 [125] Duncan *et al.*, 1999 [126]

Table 1. Continued

Category	Proteins	*In vitro* studies	*In vivo* studies
Ion channel proteins	Clic4	Ulmasov *et al.*, 2009 [127] Tung *et al.*, 2009 [128]	Ulmasov *et al.*, 2009 [127]
	Clic1	Tung *et al.*, 2010 [129]	
Scaffold proteins	Receptor for Activated C Kinase 1 (RACK1)	Dave *et al.*, 2013 [107]	Berns *et al.*, 2000 [130]
	Annexin 2 (ANXA2)	Su *et al.*, 2010 [131]	Heyraud *et al.*, 2008 [132]
	Moesin		Wang *et al.*, 2010 [122]
Hypoxia	HIF pathway	Tang *et al.*, 2004 [133] Skuli *et al.*, 2012 [134]	Skuli *et al.*, 2012 [134]
Cell surface receptor	Par3	Koh *et al.*, 2008 [85] Dejana and Vestweber?	Nakayama *et al.*, 2013 [135]Dejana and Vestweber?
	Robo1	Sheldon *et al.*, 2009 [136]	
	Robo4	Sheldon *et al.*, 2009 [136]	Huminiecki *et al.*, 2002 [137] Park *et al.*, 2003 [138] Suchting *et al.*, 2005 [139] Koch *et al.*, 2011 [140]
	Notch	Taylor *et al.*, 2002 [141] Sainson *et al.*, 2005 [142]	Seikmann *et al.*, 2007 [143] Suchting *et al.*, 2007 [144] Hellstrom *et al.*, 2007 [145] Dufraine *et al.*, 2008 [146]
	Delta like 4 (Dll4)	Su *et al.*, 2009 [147]	Lobov *et al.*, 2007 [148] Al Haj Zen *et al.*, 2010 [149]
	UNC5B/ Netrin-1	Larrivee *et al.*, 2007 [150]	Lu et al., 2004[151] Park *et al.*, 2004 [152] Navankasattusas *et al.*, 2008 [153] Koch *et al.*, 2011 [140]

Several *in vivo* and *in vitro* models have been employed to study this dynamic process, since standard two dimensional (2D) cell culture techniques fail to replicate individual steps of angiogenesis such as sprout initiation, invasion, and lumen formation. Tumor angiogenic studies gained momentum when Judah Folkman first proposed that tumor growth required angiogenesis [33]. Chorioallantoic membrane (CAM) assays are another method to test angiogenic cytokines that can be placed directly onto a 7-9 day old embryo to visualize vascularization [34]. Another elegant model to study angiogenesis *in vivo* is the corneal assay which monitors penetration of new blood vessels into the normally avascular cornea in response to tumor fragments or angiogenic factors [35]. For studies of physiological angiogenesis, development and pregnancy provide ideal model systems and have been used extensively [36]. More recently, the zebrafish has emerged as a viable whole animal model to study angiogenesis, which has an advantage of allowing detailed live imaging of vessel formation in a vertebrate embryo that can be genetically manipulated with relative ease [37, 38].

The ability to isolate and culture ECs has facilitated the development of several *in vitro* techniques to study angiogenesis. Early independent studies by Sage and Montesano cultured ECs with growth factors and phorbol esters in 3D collagen or fibrin matrices [39, 40]. Nicosia and colleagues demonstrated that rat aortic rings reproducibly generated microvessel outgrowths in fibrin or collagen matrices, and provide a sensitive *ex vivo* assay to screen pro- and anti-angiogenic substances [41]. A variety of *in vitro* assays have subsequently been developed that mimic different stages of angiogenesis.

These include (i) bead assays, in which ECs coated on microcarrier beads are embedded in 3D matrices [42]; (ii) vasculogenesis assay; where ECs suspended in collagen or fibrin matrices undergo tubulogenesis [43]; (iii) microvessel fragment assay which involves embedding microvascular fragments isolated from adipose tissue into 3D matrices [44]; (iv) EC monolayer invasion assay, in which ECs seeded as a monolayer on collagen or fibrin matrices undergo sprouting perpendicular to the monolayer [27, 45, 46]; and (v) a sandwich method, where an EC monolayer is placed between two collagen matrices to initiate tube formation [46].

In this study, we have used a 3D *in vitro* angiogenic model where the synergistic effects of sphingosine- 1- phosphate (S1P) and angiogenic growth factors (GFs), vascular endothelial growth factor (VEGF) and basic fibroblast growth factor (bFGF), induce robust and rapid endothelial sprouting responses in 3D collagen matrices (Figure 1) [45]. This model mimics wound environment wherein, platelets deposit S1P and VEGF at the wound site, whereas bFGF is secreted by fibroblasts and other cells to induce angiogenesis [47-51].

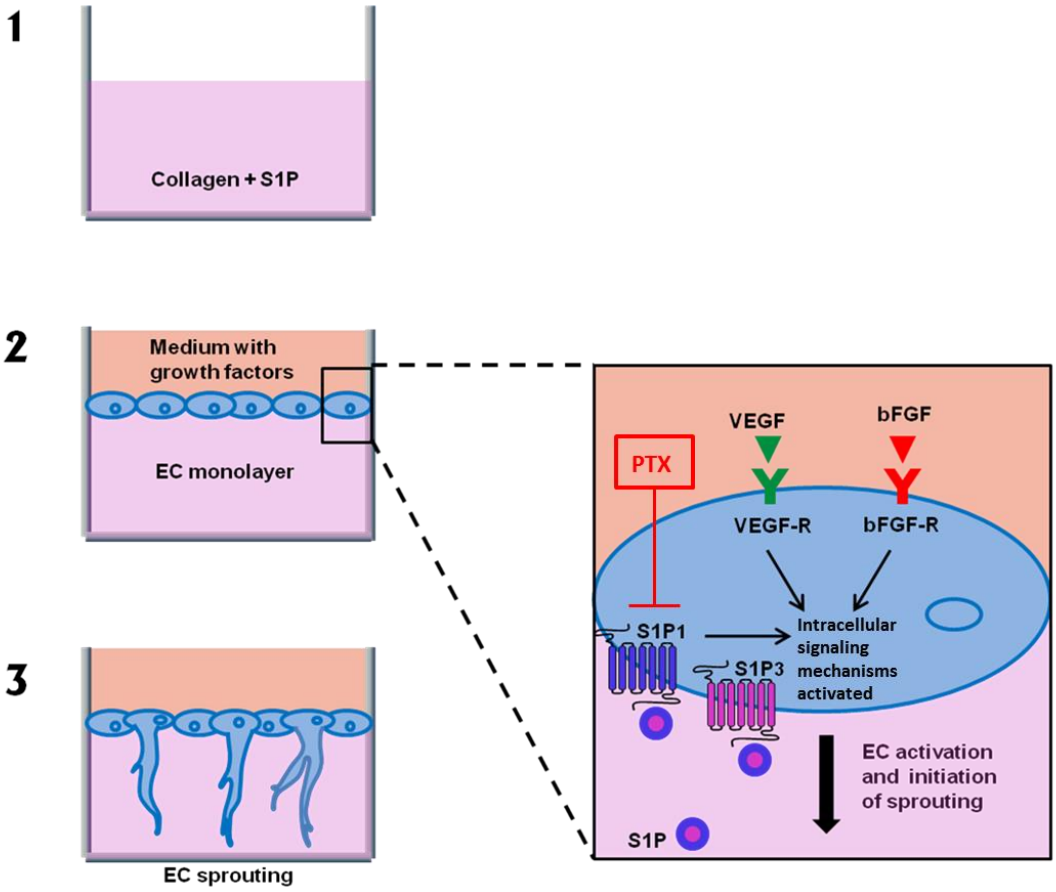

Figure 1: 3D *in vitro* angiogenic model

Sphingosine- 1-phosphate (S1P) is a blood borne lipid mediator that has been widely reported to induce angiogenesis [52-54]. S1P is released from ceramide by enzyme ceramidase. Sphingosine kinase phosphorylates sphingosine to produce S1P [55]. S1P is known to function primarily as a regulator of vascular and immune systems. S1P stimulates growth, suppresses apoptosis, increases thermo tolerance and regulates motility, cytoskeletal rearrangement and cellular Ca^{2+} levels [55]. S1P acts through one

or more of its five known G protein- coupled receptors (GPCRs), S1P1–S1P5 [55, 56], which were originally named Endothelial Differentiation Gene (EDG receptors). ECs express receptors, EDG-1 (S1P1) and EDG-3 (S1P3) [56]. Both S1P1 and S1P3 are Gi coupled receptors, and can be inactivated by pertussis toxin (PTX). PTX blocks S1P receptor activity by catalyzing ADP-ribosylation of α subunits of heteromeric G proteins (G0, Gi, and Gt) thus preventing G proteins from interacting with their receptors and interfering with intracellular communication [57]. Thus, PTX can be used as an effective tool to dissect downstream S1P signaling.

S1P1 null mice exhibit vascular defects, and impaired mural cell (smooth muscle cells and pericytes) association with developing vasculature [58]. In ECs, S1P plays a significant role in adherens junction assembly, chemotaxis, cell spreading, membrane ruffling, morphogenesis into capillary like networks and cord formation on matrigel [59-62]. S1P- mediated endothelial functions have been shown to be dependent on small GTPases Rho and Rac [63, 64]. S1P is also known to play critical role in FA (focal adhesion) assembly. S1P treatment directs translocation of several focal proteins to and FA sites, thus regulating FA growth and turnover [65]. In addition, S1P was shown to induce membrane translocation of MT1-MMP, a critical step towards successful angiogenesis [54, 66]. Previous studies from our laboratory have also shown that S1P induced membrane translocation of annexin 2, a scaffold protein required to maintain VE-cadherin based junctional integrity in sprouting ECs [67]. Moreover, results from our laboratory have also indicated that S1P in combination with wall shear stress (WSS)

is sufficient for endothelial sprouting [30, 68]. Thus, S1P acts through several downstream effector molecules in ECs to induce EC activation and sprouting.

The VEGF family consists of seven members including VEGF-A through -E, placental growth factor (PlGF) and T.f. svVEGF (derived from snake venom of *Trimeresurus flavoviridis*) [69]. VEGF-A or VEGF was first isolated in 1983 by Senger *et al.*, which had strong vascular permeability activity and was named vascular permeability factor (VPF) [70]. Extensive studies have revealed that VEGF-A is not only important in vasculogenesis and growth of new blood vessel formation from endothelial progenitor cells (EPCs), but also for angiogenesis, growth of new blood vessels from pre-existing ones and tumor angiogenesis [71]. VEGF ligands induce intracellular changes by binding to specific VEGF receptors (VEGFRs) [72]. VEGFR is a subfamily of the large protein tyrosine kinase receptors (PTKRs) family and comprises of three members VEGFR-1, -2 and -3. PTKR family comprises of 20 subfamilies which include FGFR, PDGFR, EGFR, and insulin receptors among others. VEGF ligands show specificity in binding to VEGFRs [72]. VEGF-A binds only VEGFR1 and R2 whereas VEGF-C and –D, which are involved in regulation of lymphangiogenesis, bind VEGFR2 and R3 [73, 74].

VEGF-A is a disulfide linked homodimer of 40 kDa. In adults, VEGF-A is stimulated during wound healing and female menstrual cycle. Pathologically, increased VEGF-A levels have been reported in various cancers and autoimmune diseases such as rheumatoid arthritis, multiple sclerosis diabetic retinopathy, age-related macular

degeneration and arthrosclerosis [75-78]. Many studies have shown increased levels of VEGF mRNA in tumor lines [79-81]. Also, many tumors secrete VEGF-A *in vitro* [82, 83]. VEGF-A promotes differentiation of EPCs in the early embryo, and stimulates vascular EC growth, survival, tube formation, and migration [84]. VEGF-A knockout in mice is embryonic lethal even in heterozygotes, strongly suggesting a critical role for VEGF-A during development. Lethality arises from multiple defects in angiogenesis such as disconnection of heart with aorta and poor development of dorsal aorta [85]. VEGF-A is alternatively spliced to generate nine isoforms of from 121 to 109 aa in length. VEGF-A is the most common form (165 aa) and, owing to its mild affinity for heparin, it exists as bound as well as soluble forms [86]. The signaling mechanism of VEGF/VEGFR is similar to that of many PTKRs [87]. The major pathways activated by VEGF are the phospholipase Cγ (PLCγ) pathway, phosphoinositol 3-kinase (PI3K) and Ras/MEK/MAPK pathway [88, 89].

Basic fibroblast growth factor (bFGF) or FGF2 is a heparin binding growth factor, which was first discovered by Judah Folkman in 1984 [90]. This 18.8 kDa protein stimulated potent angiogenic activity *in vitro* and *in vivo* [91]. In ECs, bFGF stimulated cell proliferation, capillary morphogenesis, DNA synthesis. motility and protease up-regulation (MMPs and uPA) [92-94]. bFGF also regulates expression of cadherins and integrins to direct vessel maturation and cell adhesion to ECM [92]. bFGF has been shown to promote robust neovascularization in several models like CAM assay, cornea assay and matrigel plug assay [92]. Four isoforms are known to be co-expressed by *fgf2*

gene in humans, out of which the 24 and 18 kDa isoforms induce maximal neovascularization [95, 96]. Interestingly, *fgf2* knockout mice do not display any defects in neovascularization following hypoxia [97] or injury [98], suggesting redundancy of FGF family members [99, 100].

bFGF exerts most of its effects by interacting with its cognate tyrosine kinase receptors expressed on the EC surface. Four bFGF receptors have been identified (FGFR1-FGFR4), which display structural variability and different binding affinity for bFGF isoforms [101, 102]. FGFR1 [103] and FGFR2 [104] are expressed of in ECs. Interaction of bFGF with FGFR results in receptor dimerization and autophosphorylation of specific Tyr residues and activation [105-108]. Some of the key molecules known to be activated by bFGF are FAK [109], Src [109], PLCγ [110], PI3K [111, 112] and Ras/MEK/MAPK pathway [109, 113-115].

In this study, we have identified two scaffold proteins that are essential for angiogenesis by using the S1P, VEGF and bFGF driven 3D *in vitro* angiogenic model (Figure 1). Our results indicated that scaffold protein Receptor for Receptor for Activated C Kinase 1 (RACK1) was upregulated during S1P- and GF- induced invasion and was required for successful sprouting responses. Moreover, GFs induced complex formation between RACK1 and intermediate filament protein vimentin, to regulate cell attachment, migration and focal adhesion kinase (FAK) activation and expression. In another study, we identify FA scaffold protein, Hic-5, to be required for successful endothelial sprouting and lumen formation. Our data indicated that Hic-5 was required

for membrane type 1 matrix-metalloproteinase (MT1-MMP) regulation and FAK expression and activation in ECs. In conclusion, these two studies show for the first time a direct requirement for RACK1 and Hic-5 in successful endothelial sprouting in 3D matrices. These enclosed studies also explore how RACK1 and Hic-5 regulate downstream effector proteins that are known to be important for angiogenesis.

CHAPTER II

PROTEOMIC PROFILING OF ENDOTHELIAL INVASION REVEALED RECEPTOR FOR ACTIVATED C KINASE 1 (RACK1) COMPLEXED WITH VIMENTIN TO REGULATE FOCAL ADHESION KINASE (FAK)*

INTRODUCTION

In this study, we report that Receptor for Activated C Kinase 1 (RACK1) was differentially expressed in two independent proteomic screens designed to dissect the downstream targets of S1P-induced endothelial invasion. RACK1 is a member of the tryptophan-aspartate repeat (WD-repeat) family of proteins and was originally named for associating with Protein kinase C beta type III. However, it is now well known that RACK1 interacts with several proteins and plays roles in shuttling and anchoring them to specific subcellular locations and stabilizing their activity [116, 117]. RACK1 is critical for development [118-120], cell proliferation and migration [121-124], and circadian rhythms [125].

---

*Part of this research was originally published in the *Journal of Biological Chemistry*. Dave JM, Kang H, Abbey CA, Maxwell SA, Bayless KJ. "Proteomic profiling of endothelial invasion revealed receptor for activated C kinase 1 (RACK1) complexed with vimentin to regulate focal adhesion kinase (FAK)." *J Biol Chem*. 2013; 288(42): 30720-33.

RACK1 mediates effects on cell migration mostly through regulation of FA assembly by promoting FAK activation downstream of integrin clustering and adhesion [122, 123, 126, 127]. Studies in RACK1 null mice have not been reported, however, Berns *et al.* demonstrated that RACK1 was up-regulated during cord formation in bovine aortic ECs *in vitro* and in angiogenically active tissues such as corpora lutea, ovarian follicles, and human carcinomas *in vivo* [128]. Although these reports suggest a relevant role for RACK1 during angiogenesis, the molecular events directed by RACK1 remain unclear.

The major intermediate filament protein, vimentin, was also identified in a proteomic screen as a downstream target of S1P-induced EC invasion. Our laboratory has shown vimentin depletion in ECs resulted in poor invasion responses [66]. Recent studies in mouse fibroblasts suggest that vimentin may stabilize FA assembly [129] and regulate FA contact size in response to shear stress [130]. Focal adhesions (FAs) are dynamic macromolecular assemblies that link cells to the extracellular matrix (ECM) [131-135]. FAK is a major tyrosine kinase protein concentrated at FAs. ECM engagement and integrin assembly promote FAK phosphorylation which further recruits and phosphorylates other proteins at FAs, to promote cytoskeletal rearrangement and cell migration [136-138]. FAK has been extensively studied in cell migration, angiogenesis, and cardiac morphogenesis [139-142].

In this study, we show for the first time a trimolecular complex between RACK1, vimentin, and FAK in three-dimensional invading cultures. Knockdown of RACK1

resulted in poor invasion responses and attenuated FAK activation, whereas vimentin depletion resulted in decreased FAK expression in ECs. Furthermore, RACK1 was needed to stabilize the complex between vimentin and FAK.

EXPERIMENTAL PROCEDURES

Endothelial Cell Culture and Invasion

Human umbilical vein endothelial cells (HUVECs; Lonza, Allendale, NJ), passages 3-6, were cultured as previously described [45]. Three dimensional (3D) invasion experiments were established using 40 ng/mL VEGF and bFGF growth factors alone (GF) or S1P and GFs (S1P+GF) or S1P and GF plus 0.1 μg/mL pertussis toxin (S1P+GF+PTX). Collagen matrices (2.5 mg/mL) containing 0 or 1 μM S1P (Avanti Polar Lipids, Alabaster, AL) were prepared as described previously, and invasion responses where indicated, were quantified for invasion density as previously described in detail [45].

Proteomic Screen 1: Differential In-Gel Electrophoresis (DIGE)

Collagen gels from 12.5 h invading cultures (S1P+GF or S1P+GF+PTX) were collected and incubated in M199 containing 10 μg/mL collagenase (Sigma), and HALT Phosphatase Inhibitor Cocktail (Thermo Scientific, Ashville, NC) at 37°C for 10 minutes. For each condition, 240 gels were prepared. Cells were pelleted at 500xg for 5 minutes and washed once in ice-cold PBS. Cell pellets were flash-frozen in liquid

nitrogen and stored at -80°C. Frozen cell pellets were lysed by thawing and pipetting on ice in 1 mL of lysis solution I (0.3% SDS; 200 mM dithiothreitol; 50 mM Tris, pH 7.5; broad range protease inhibitors (GE Healthcare, Waukesha, WI); HALT Phosphatase Inhibitor Cocktail (Thermo Scientific). Proteins were further solubilized by heating at 100°C for 10 minutes followed by incubating on ice for 5 minutes. Lysates were sonicated with a 15 seconds burst (amplitude setting 60) on ice using a Sonics Vibracell sonicator to further fragment DNA and cytoskeletal structures. Nucleic acids were digested by adding DNase/RNase mix (GE Healthcare) and rotating the lysates at 4°C for 45 minutes. Lysates were delipidated in chloroform-methanol by adding 4 mL of methanol and vortexing for 30 seconds, followed by adding 1 mL of chloroform and vortexing for 30 seconds, and finally by adding 3 mL of Millipore-purified water and vortexing for 60 seconds. Samples were rotated at room temperature for 15 minutes, transferred to corex glass tubes, and centrifuged at 5500xg in a Sorvall JA20 rotor for 20 minutes at room temperature. The interphase contained the proteins, which was transferred to a microfuge tube and mixed with 0.5 mL of methanol. After spinning for 10 minutes in a microfuge, the pellets were resuspended in 0.6 mL of water and proteins re-precipitated by adding a 0.8 volume of ice-cold acetone and incubating on ice for 15 minutes. Proteins were pelleted out of the acetone solution by spinning in a microfuge for 15 minutes and re-solubilized in 100 mL of a 2D gel proteomic solubilization buffer (9.9 M urea; 4% CHAPS; 14% thiourea; 4.8% SDS; 10 mM Tris, pH 7.5; 40 mM DTT). Proteins were allowed to solubilize for 1 h by rotating at room temperature and then

desalted through microspin desalting columns (Pierce Protein Biology, Rockford, IL) into desalting solution (9.9 M urea; 4% CHAPS). Protein concentrations were determined by the BCA protein assay after pre-treating and re-precipitating an aliquot of each sample with BCA compatibility reagent and Compat-Able protein assay preparation set (Pierce cat. #23250 and #23215, respectively) to eliminate interference from BCA protein reagent with thiourea. After determining protein concentration, the samples were adjusted to 50 mg protein/10 mL desalt buffer I and subjected to a second spin through a desalting microspin column into DIGE labeling buffer (9.9 M urea; 4% CHAPS; 30 mM Tris-HCl, pH 8).

Protein samples were prepared for differential gel electrophoresis (DIGE), which is based on pre-labeling of different protein fractions with cyanine-based fluors (CyDye DIGE Fluor minimal dyes) and their subsequent co-electrophoresis in a single 2D gel. The DIGE technology has the advantage of allowing elimination of inconsistencies based on gel to gel variations and the exact quantification of proteins spots separated by gel electrophoresis. Proteins in DIGE labeling buffer (150 mg in 30 mL volume) were covalently-attached to CyDyes (Cy5, Cy3, Cy2) using the manufacturer's protocol (GE Healthcare). A 500 mg aliquot (75 mL volume) of a pooled total protein preparation consisting of unlabeled CHOP-sensitive and -resistant cells was then added to each CyDye-labeled protein sample. This allowed each gel to be a preparative gel for picking spots for mass spectrometry. The CyDye-labeled preparative protein samples were then passed through a desalting microspin column equilibrated with desalting solution to

remove free CyDye reagents and buffer. Desalted CyDye-labeled protein lysates (~100 mL) were mixed with 400 mL of Destreak Rehydration sample buffer (GE Healthcare Life Sciences) containing 0.077 mg of DTT. Protein samples were solubilized by rotating for 1 h at room temperature. After adding another 0.077 mg DTT and ampholytes (100X Bio-Lyte pI 3-10 ampholytes, Bio-Rad, Hercules, CA), samples were rotated for 30 minutes at room temperature and then allowed to rehydrate pH 3-10 Immobiline dry-strip gel strips (GE Healthcare Life Sciences) for 18 h. Rehydrated Immobiline dry strips were subjected to step-wise isoelectric focusing at 150 V for 6 h, 500 V for 1 h, 1000 V for 1 h, and 8000 V for 6 h in an Ettan IPGphorII unit. Proteins were then separated in the second dimension on large format (27 x 21 cm) 8-16% gradient SDS polyacrylamide gels at 5 W/gel for 9.5 h. CyDye-labeled proteins in the 2D gels were imaged with a Typhoon 9200 laser scanner. A gel selected for spot-picking was counter-stained with Sypro Red for 6 h in 7.5% acetic acid, destained for 1 h in 7.5% acetic acid, and re-imaged in a Typhoon 9200 laser scanner. Image analysis was performed using the Biological Variation Analysis (BVA) modules of the DeCyder software version 5.0 (GE Healthcare), which first normalizes each sample to its respective in-gel Cy2 internal standard, and then matches all controls and samples between different gels. Comparing each group in the BVA module generated average expression ratios and Student's t-tests of individual protein spots.

Proteomic Screen 2: Two-Dimensional Gel Electrophoresis

Two-dimensional gel electrophoresis was performed as previously described [143].

In Gel Digestion

Spot-picking and in-gel digestion were carried out robotically at the Protein Analysis Laboratory, Texas A&M University, on selected Sypro Red-stained preparative gels using the Ettan Spot Picker and the Ettan Digester (GE Healthcare). For in-gel digestion, protein spots of interest (1.4 expression ratio or greater) were excised, and the gel plugs washed twice for 15 minutes in 50% Acetonitrile (ACN)/50mM Ammonium Bicarbonate (ABC). The plugs were washed once more with 100% ACN for 15 minutes and then dried by centrifugal lyophilization for 30 minutes. In-gel digestion was conducted by adding 20 mL of trypsin (20 ng/mL) and incubating for 15 minutes. After adding 100 μL of 25 mM ABC, the gel plugs were incubated at 37°C overnight. The supernatants were removed and saved. A solution of 80% ACN/0.1% trifluoracetic acid was added to the gel plug for 30 minutes. The supernatant was then removed and pooled with the first supernatant. The peptide volume was reduced down to 10 μL by centrifugal lyophilization and then subjected to LCMS.

Protein Identification

LCMS was carried out on a ThermoFinnagan (Thermo Electron, Asheville, NC) LCQDecaXP (ESI-TRAP model). Samples were run using an in-house packed C18

reverse phase nanospray needle. Mass spectra were used to interrogate human sequences in the NCBInr database (5/2009; 478,579 entries human database). The automatic data analysis and database searching were fulfilled by the TurboSEQUEST software in the Bioworks Browser (version 3.3.1 SP1). Searches with TurboSEQUEST were performed to allow for a maximum of two missed trypsin cleavages. Additional TurboSEQUEST search parameters were as follows: mass typesetting was monoisotopic precursor and fragments; threshold tolerance was 50,000; peptide tolerance, precursor ion tolerance, and fragment ion tolerance were 2.5000, 1.4000 and 0.0001 AMU, respectively. Ions and ion series calculated were B and Y ions. Searches were also conducted using the MASCOT search engine (www.matrixscience.com). The database searched by MASCOT was NCBInr 20070216 (4626804 sequences; 1596079197 residues) and the taxonomy was Homo sapiens (human) (191437 sequences). MASCOT search parameters were as follows: fixed modifications, carboxymethyl; variable modifications, oxidation (M); mass values, monoisotopic; protein mass, unrestricted; peptide mass tolerance, ± 1.8 Da; fragment mass tolerance: ± 0.8 Da. The search identification had a statistically significant $p<0.05$ (based on mass/mass spectra). Redundancy of proteins that appeared in the database under different names and accession numbers was eliminated. If more than one protein was identified in one spot, the single protein member with the highest protein score (top rank) was singled out from the multiprotein family.

Immunoblotting

Total cell lysates were prepared by solubilizing collagen matrices in boiling 1.5X Laemmli sample buffer at 95°C for 10 min. Protein samples were resolved by using 8.5-14% SDS-PAGE, transferred onto Immobilon PVDF membranes (Millipore), blocked with 5% nonfat dry milk or 5% BSA, washed, and probed with primary antibodies overnight at 4°C. Membranes were incubated with HRP conjugated secondary antibodies, washed, and developed using Immobilon Western Chemiluminescent HRP Substrate (Millipore) using HyBlot CL autoradiography film (Denville Scientific, South Plainfield, NJ). The antibodies used are: vimentin (sc-5565 and sc-6260, Santa Cruz Biotechnology, Temecula, CA), ANXA2 (AF3928, BD Transduction Laboratories, San Jose, CA), RACK1 (sc-17754, Santa Cruz Biotechnology) (ab119442, Abcam, Cambridge, MA), α-tubulin (T6199, Sigma-Aldrich), FAK (3285, Cell Signaling, Danvers, MA) (05-537, Millipore), pFAK (Tyr397, 8556, Cell Signaling), β2M (M8523, Sigma), α-actinin (A-2543, Sigma), GAPDH (ab8245, Abcam), VE-cadherin (sc-52751, Santa Cruz Biotechnology), filamin A (MCA464ST, BioRad) and HRP conjugated secondary antibodies (Dako, Carpinteria, CA).

Generation of Stable Cell Lines Using shRNA

Lentiviral vectors specific for RACK1 (#SHCLNG-NM006098), vimentin (#SHCLNG-NM011701), and β2M (#SHCLNG-NM004048) were purchased from Sigma-Aldrich. Lentiviral particles were generated by transfecting 1.25 μg of backbone shRNA lentiviral plasmid with 3.75 μg of VIRAPOWER packaging mix (Invitrogen)

into confluent 293FT cells (Invitrogen), using Lipofectamine 2000 (Invitrogen) in T25 flasks. Viral supernatants were harvested at 60 h, centrifuged at 1500xg for 5 minutes and filtered through a 0.45 μm filter (Millipore, Rockland, MA). 25-30% confluent T25 flasks of HUVECs were infected with 2 mL viral supernatant, 3 mL endothelial growth medium, and Polybrene (12 μg/mL; Sigma) for 4 h. HUVECs were allowed to grow for four days prior to use in experiments.

mRNA Extraction and PCR Analysis

HUVEC were treated with shRNAs to RACK1 (shRACK1 -1: TRCN 0000273167; shRACK1 -2: TRCN 0000006472; and shRACK1 -3: TRCN 0000006471) and β2M (shβ2M -1: TRCN 0000057254; shβ2M -2: TRCN 0000057255). RNA was extracted from HUVEC expressing shRNA as well as an untreated control, using an RNeasy MiniKit (Qiagen). Eluted RNA was treated with RNase Free DNase (Qiagen) for 10 minutes at RT and inactivated at 65°C for 15 minutes. RNA quality was assessed with an agarose gel. cDNA was generated by SuperScript III First-Strand Synthesis System (Invitrogen) using 1 ug of RNA and Oligo(dT)20 as per manufacturer's instructions. Amplicons were run on 2% agarose gels in 1X TAE buffer at 120V for 20 minutes with a 100 bp DNA ladder (Invitrogen) and stained with GelRed (Phenix Research Products, Candler, North Carolina). The primers used for this study were: ANXA2 (NM_001002858.2; 262 bp 5'-CAGAGGAT-GCTCTGTCATTG-3' and 5'-GGCTTGT- TCTGAATGCACTG-3'); PECAM1 (NM_000442.4; 172 bp 5'-ATGATGCCCAGTTT- GAGGTC-3' and 5'-ACGTCTTCAGTGGGGTTGTC-3');

FAK (NM_153831.3; 217 bp 5'-CTGGCTACCCTG-GTTCACAT-3' and 5'-TGTTGCTGTCGGAT-TAGACG-3'); Vimentin (NM_003380.3; 177 bp 5'-GGGACCTCTACGAGGAGGAG-3' and 5'-AA- GATTGCAGGGTGTTTTCG-3'); RACK1 (NM_006098.4, 1000 bp 5'-CCACCATGA- CTGAGC-3' and 5'-GCGTGTGCCAATGGT-3'); VE-Cadherin (NM_001795.3, 182 bp 5'-C-CAGGTATGAGATCGTGGTG-3' and 5'-AA-ACAGAGAGCCCACAGAGG3'); β2M, (NM_ 004048.2, 158 bp 5'-TTTCATCCATCCGAC-ATTGAAG-3' and 5'-ACACGGCAGGCATAC-TCATC-3'); Filamin-A, (NM_001456.3, 243 bp 5'-TCCAGCAGAAC-ACTTTCACG-3' and 5'-CGATGGACACCAG-TTTGATG-3') and GAPDH (NM_002046.4, 228 bp 5'-CGACCA-CTTTGTCAAGCTCA-3' and 5'-AGGGGTCTA-CATGGCAACTG-3').

shRACK1 Rescue Experiments

HUVEC cDNA was used to amplify RACK1 insert using primers 5'-GCAAGCTTGCCACCATGACTGAGCAC-3' and 5'-GCGGTACCGCGTGTGCCAA-TGGTCAG-3'. RACK1 inserts were inserted into the pEGFP-C2 vector in the HindIII and Kpn1 sites. The resulting EGFP-RACK1 fusion construct was amplified using 5'-AGGATATCCTAGCGTGTGCCAATGGT-3'and 5'- AGGTCGACGCCACCATGGT-GAGCAA-3' primers. EGFP-RACK1 fusion was inserted into pENTR4 vector using SalI and EcoRV restriction sites. Inserts were validated by sequencing and recombined with pLenti6/V5-DEST (Invitrogen) in Stbl3 cells (Invitrogen). After confirming expression, EGFP-RACK1 in pLenti6/V5 was mutated at shRACK1-1 target site using

Quickchange Lightning site-directed mutagenesis kit (Stratagene, Invitrogen) according to manufacturer's instructions. The rescue construct was designated as R3 because primers incorporated three base pair changes (5'- GGAAACTGACCCGGGACGAGAC-CAACTACGGAATTCCACAG-3' and 5'-CCTTTGACTGGGCCCTGCTCTGGTTG-ATGCCTTAAGGTGTC-3'). In rescue experiments, HUVEC infected with shRNA directed against β2M (shβ2M) or RACK1 (shRACK1-1) were cultured for 48 h before infecting with lentiviruses R3 or GFP control rescue constructs. Lentiviruses (5 mL) were generated by transfecting 2 μg of backbone plasmids into confluent 293FT cells (Invitrogen) with 6 μg VIRAPOWER packaging vectors (Invitrogen) using Lipofectamine 2000 (Invitrogen). Viral particles were harvested at 60 h, centrifuged at 500xg for 5 minutes and filtered through a 0.45 μm filter (Millipore). T25 flasks of HUVECs at 25-30% confluence were infected with 4.5 mL viral supernatant and Polybrene (12 μg/mL; Sigma) overnight. Another 4.5 mL of viral supernatant and Polybrene (Sigma) were added to HUVECs and infected for 48 h. HUVECs were allowed to grow for three days prior to use in invasion experiments.

Immunoprecipitation

In 2D experiments, confluent ECs ($3x10^6$) cultured in T75 flasks were treated for 1 h with or without 1 μM S1P or 40 ng/mLVEGF and bFGF. Cells were placed on ice and washed twice with 10 mL cold PBS. Cell pellets were lysed in 1 mL cold lysis buffer (50 mM Tris-HCl, pH 7.5, 150 mM NaCl, 1% NP40, 0.5% sodium deoxycholate, 1X protease inhibitor cocktail (Roche Diagnostics) and 1mM PMSF) and incubated for

10 minutes on ice with occasional mixing. Cell lysates were centrifuged at 16,000xg for 15 minutes at 4°C. Five microliters of protein G-magnetic beads (Invitrogen) were added for 1 h at 4°C with agitation to pre-clear cell lysates. Supernatants (1 mL) were incubated with 2 μg antisera directed to vimentin, RACK1, or FAK for 18 h at 4°C with agitation. Protein G-magnetic beads (10 μL) were added for 2 h at 4°C. Beads were washed 6 times with 1 mL lysis buffer without protease inhibitors, eluted in 1% SDS and analyzed by Western blotting. For 3D experiments, 30 gels with 30,000 ECs each were collected in 600 μL of cold lysis buffer (50 mM Tris-HCl, pH 7.5, 150 mM NaCl, 1% NP40, 0.5% sodium deoxycholate, 1X protease inhibitor cocktail (Roche Diagnostics) and 1mM PMSF). Mixtures were incubated for 30 minutes at 4°C with gentle agitation. Cell lysates were centrifuged at 16,000xg for 20 minutes at 4°C. Supernatants were collected and incubated with protein G-magnetic beads (5 μL) for 1 h at 4°C with agitation for preclearing the cell lysates. The remaining steps were performed as above.

Immunofluorescence and Colocalization Studies

Cells were seeded on collagen or fibronectin coated coverslips (20 μg/mL) and allowed to grow overnight. In wound assays, cells were wounded with a pipette tip and washed twice with M199. Cells were treated with 1 μM S1P or 40 ng/mL growth factors (or both) for 1 h, fixed in 4% paraformaldehyde, and rinsed three times in Tris-Glycine buffer (0.3% Tris, 1.5% Glycine), permeabilized with 0.5% Triton X-100 for 20 minutes with gentle agitation before blocking in buffer containing 0.5% TX-100, 1% BSA and 1% serum overnight at 4°C. Primary antibodies were added in blocking buffer (1:50) for

3 h at room temperature, washed, and incubated with Alexa-488- or -594-conjugated secondary antibodies (Molecular Probes, Grand Island, NY) (1:300) in blocking buffer for 1 h. After washing, coverslips were mounted and imaged using a Nikon TI A1R inverted confocal microscope. For quantification of colocalization, intensity profiles of RACK1 (red) and vimentin (green) along randomly-selected lines in the image were plotted using NIS-Elements software. Average Pearson's correlation coefficient from 'n' number of cells for each treatment group was statistically analyzed.

Imaging and Quantification of Invasion Density and Distance

Top and side views of invading ECs were captured using an Olympus CKX41 microscope equipped with Q color 3 Olympus camera and 10 X objective. Invasion densities were quantified by counting fixed cultures under transmitted light using an inverted microscope equipped with eyepieces with a 10 X 10 ocular grid. For each condition, atleast three random fields were selected and the number of invading cells per high power field (HPF) was counted manually. Data are reported as mean numbers of invading cells per HPF (±SD). Invasion length was measured using digital images taken from a side view of cultures at 10X magnification using Image-Pro Analyzer 7.0. Data are reported as average invasion distance in microns (±SEM).

Cell Adhesion Assays

High binding EIA/RIA 96 well plates (Corning-Costar) were precoated overnight with various doses of fibronectin and blocked with 10 mg/mL BSA for 45 minutes. ECs

expressing shRNAs directed to β2M, RACK1 and vimentin (30,000 cells per well) were incubated at 37°C for 15 minutes before removing unbound cells. Plates were fixed in 3% formalin for 3 h before staining with 0.1% amido black in 10% acetic acid and 30% methanol for 15 minutes. Plates were thoroughly washed and dried before adding 50 μL of 2N NaOH per well. The absorbance (595 nm) was read using Victor X3 plate reader (Perkin Elmer, Waltham, Massachusetts).

RESULTS

Identification of RACK1 as a Regulator of S1P Induced Invasion in ECs

The EC invasion assay utilized in this study is a defined 3D model of endothelial invasion where robust and rapid invasion responses are triggered by S1P, bFGF, and VEGF [45, 143]. To identify intracellular targets of S1P that regulate EC invasion, ECs were treated with growth factors only (GF), S1P and growth factors (S1P+GF), or S1P and growth factors plus pertussis toxin (S1P+GF+PTX) to inhibit sprouting responses. PTX blocks S1P receptor activity by catalyzing ADP-ribosylation of α subunits of heteromeric G proteins (G_0, Gi, and Gt) thus preventing G proteins from interacting with their receptors and interfering with intracellular communication [57]. Dose response experiments determined 0.1 ng/mL PTX blocked S1P- and GF- induced invasion (Fig. 2). Treatment with PTX effectively blocked invasion in ECs to control levels with GF alone (Fig. 3A). Quantification of invasion density showed significantly more sprouting with S1P+GF treatment compared to GF alone or S1P+GF+PTX treatment (Fig. 3B).

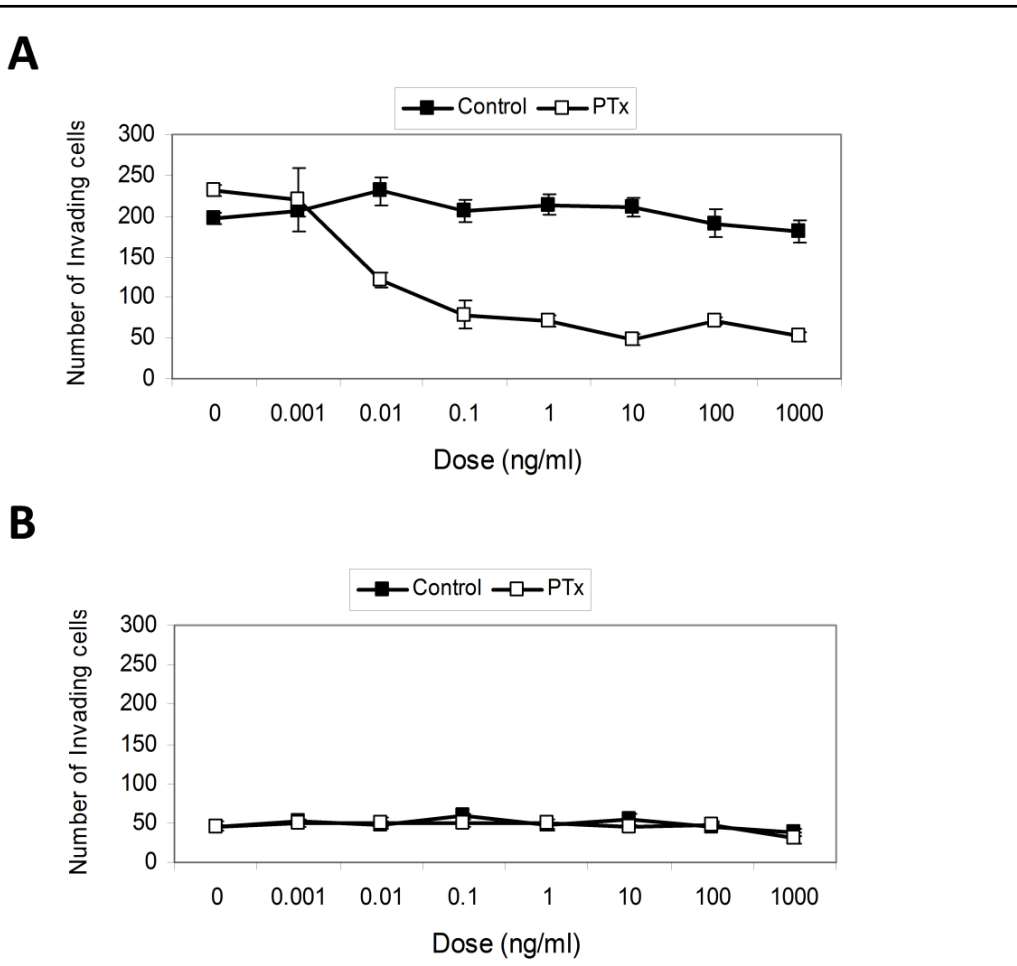

Figure 2. PTX dose response experiment. Invasion experiments were established by pre-incubating cells without (Control) or with indicated doses of pertussis toxin (PTX) for 20 minutes at 37°C prior to seeding on collagen matrices with **(B)** 0 μM S1P or **(A)** 1 μM S1P and 40 ng/mL VEGF and bFGF (GF). Cultures were fixed in 3% glutaraldehyde and stained with toluidine blue prior to quantification. Data represents average number of invading cells per standardized field (n=3 fields).

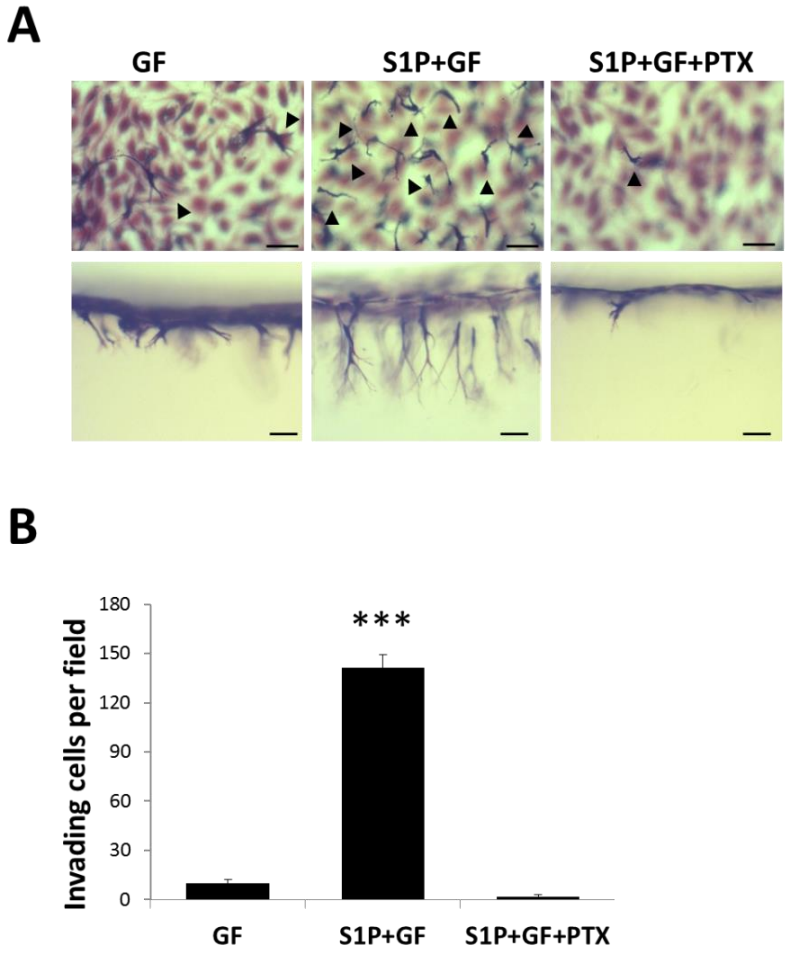

Figure 3. Effect of pertussis toxin (PTX) on S1P- and GF- induced EC invasion. (A) Photographs illustrating invasion responses (upper panels, top-view; lower panels, side-view). ECs were treated with 40 ng/mL VEGF and bFGF alone (GF), or 1 μM S1P + GF (S1P+GF), or S1P, GF, and 0.1 ng/mL pertussis toxin (S1P+GF+PTX). Cultures were fixed in 3% glutaraldehyde at 12.5 h, stained with toluidine blue, and photographed. Black arrowheads indicate invading cells. Scale bar=50 μm. **(B)** Quantification of EC invasion density in response to various treatments at 12.5 h invasion. Data represents average number of invading cells per 1 mm2 field ± SD (n=5 fields, Student's t-test, *** $p<0.001$, compared to other treatments).

Protein lysates from 12.5 h invading EC cultures shown in figure 2A were analyzed in two independent proteomic screens designed to dissect downstream regulators of S1P signaling in ECs. Protein identification was carried out using two search engines; TurboSEQUEST (TQ) and Mascot (M) and the identified target proteins were ranked according to their XCorr values (XC scores), where a score above 2.0 is indicative of a good correlation. Differential in-gel electrophoresis (proteomic screen 1) revealed annexinA2 (ANXA2), RACK1, and vimentin were upregulated with S1P+GF treatment compared to S1P+GF+PTX (Table 2). In addition, several proteins were found to be downregulated in S1P-induced invasion compared to non-invading ECs (Table 3). An independent screen using a distinct approach (Proteomic screen 2) confirmed ANXA2 and RACK1 were upregulated with S1P and GF treatment compared to S1P+GF+PTX (Table 4).

Table 2. List of up-regulated proteins from proteomic screen 1

Spot #	Predicted protein match	TQ or M	Calculated pI value	Nominal mass (Daltons)	Expression change	Score XC	Sequence coverage (%)
760	Annexin A2 chain A, structure in presence of Ca^{2+} ions	TQ, M	8.32	36631	1.27	TQ 260.28, M 115	60
790	Annexin A2	TQ, M	7.57	38780	1.23	TQ 170.25, M 176	55
744		M			1.22	M 184	48
870	Receptor for activated protein kinase C (RACK1)	TQ	7.54	35054	1.26	TQ 30.21	11.99
	Actin related protein 2/3 complex, subunit 2 (ARPC2)	TQ, M	6.84	34427		TQ 18.16, M 60	14
602	Vimentin	TQ	5.06	53619	1.20	TQ 128.22	18

Table 3. List of down-regulated proteins from proteomic screen 1

Spot #	Protein match	TQ or M	Calculated pI value	Nominal mass (Daltons)	Expression change	Score XC	Sequence coverage (%)
236	HSP70 protein 8, isoform 1	TQ	5.37	70854	-1.22	TQ 20	50
	HSP70 protein 8, isoform 2	TQ	5.37	53484		TQ 160	37.73
	HSP70 protein 8, isoform 1 variant	M	5.28	71083		M 124	50
	HSP70 protein 1A	TQ, M	5.37	69995		TQ 48, M 146	6.24
955	Lamin A/C	TQ	8.54	70619	-1.22	TQ 60	9
	HSP 27	TQ	5.97	22768		TQ 40	23.14
824	Annexin A5	TQ	4.5	35915	-1.25	TQ 70.3	35
808	Otubain 1	TQ	4.7	31264	-1.26	TQ 50.25	24.35
672	Vimentin fragment	TQ	4.91	53619	-1.30	TQ 124	25.11
668		TQ, M			-1.40	TQ 140, M 134	18.24
705		TQ			-1.53	TQ 100	9
446	ATP synthase, mitochondrial F1 complex β subunit	TQ	ND	56524	-1.36	TQ 130	39
89	Tumor rejection antigen	TQ, M	4.76	92696	-1.49	TQ 280	18
	HSP 94B	M	5.14	46343		M 46	18
1090	Stimulator of TAR RNA binding	M	7.52	58316	-1.85	M 74	18
	Chaperonin containing TCP1, δ subunit	TQ	7.75	57887		TQ 70.22	15.03

Table 4. List of up-regulated proteins from proteomic screen 2

Predicted protein match	Score XC	Sequence coverage (%)	Accession number
Annexin A2	100.24	27.14	119574085.0
Receptor for activated C kinase 1 (RACK1)	50.23	12	30584373.0
Lamin B2	60.19	11.33	119589784.0
Peroxiredoxin 1	40.19	19.59	55959887.0

Upregulation of ANXA2, RACK1, and vimentin were confirmed in separate experiments using western blotting (Fig. 4A). Although we observed upregulation of ARPC2 (Table 2), a requirement for ARPC2 in S1P- and GF-induced EC invasion was not confirmed (data not shown), thus ARPC2 was not investigated further. ANXA2, RACK1 and vimentin protein expression levels observed with PTX treatment were consistent with GFs alone (Fig. 4). Quantification of the data revealed significant upregulation of ANXA2, RACK1, and vimentin with S1P+GF treatment compared to GF alone or S1P+GF+PTX treatment (Fig. 4B). No change in β2M levels were observed in all treatment groups. Our laboratory has investigated the role of ANXA2 in separate studies and found that ANXA2 complexed with VE-cadherin, upstream of Akt activation, to regulate EC sprouting [67], and thus ANXA2 was not investigated in this study. Because RACK1 has been implicated in cell migration and blood vessel formation [128], and we have previously identified a requirement for vimentin [66], we focused

our investigation on better understanding the interplay between RACK1 and vimentin in EC invasion responses.

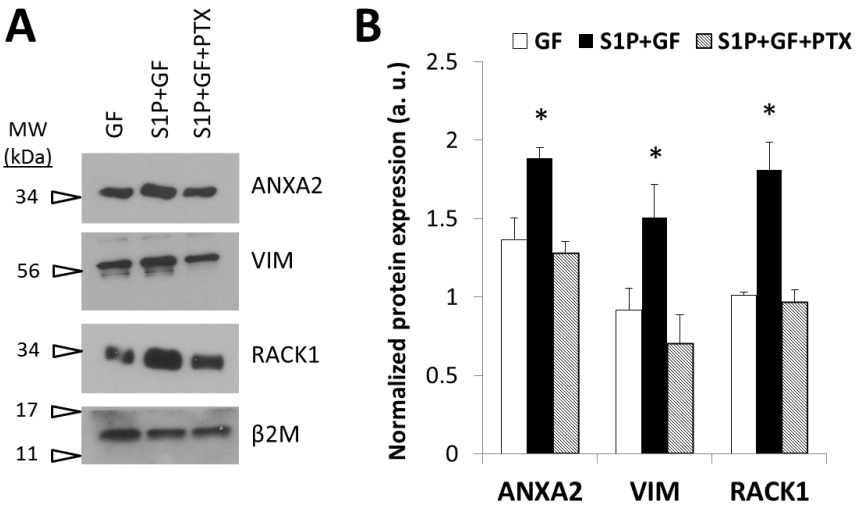

Figure 4. Western blot analysis to verify upregulation of identified proteins. (A) Verification of annexin A2 (ANXA2), vimentin (VIM) and receptor for activated C kinase (RACK1) protein upregulation. ECs treated with GF, S1P+GF or S1P+GF+PTX were allowed to invade for 12.5 h prior to preparing cell extracts. Antisera specific to ANXA2, VIM, RACK1 and β2M were used for Western blot analyses. **(B)** Quantification of protein expression from Western blots using Image J software and normalized to β2M. The results represent average values normalized to β2M ± SD in arbitrary units (a.u.) from three independent experiments (Students t-test, * $p<0.05$, compared to all other treatments).

RACK1 Was Required for EC Invasion

Recombinant lentiviruses from three individual shRNA sequences targeted against RACK1 (shRACK1-1, -2 and -3) and two shRNA sequences specific to β2-microglobulin (β2M, shβ2M-1 and -2) were utilized to transduce ECs. To test knockdown efficiency at the mRNA and protein level, PCR analysis using primers

specific to RACK1, β2M and GAPDH revealed efficient silencing of RACK1 mRNA with shRACK1-1 and shRACK1-2 treatment (Fig. 5A). Western blot analyses of cell lysates revealed knockdown of RACK1 protein that were consistent with mRNA levels (Fig. 5A and B). β2M control also showed efficient knockdown with shβ2M-1 and -2 treatment of β2M mRNA (Fig. 5A) and protein (Fig. 4B). To test specificity of shRNA mediated knockdown of RACK1 and β2M, expression levels of other molecules known to regulate EC sprouting such as vimentin, VE-cadherin, filamin A (FLNA) and FAK, were analyzed (Figure 5A and B). No significant changes in mRNA or protein levels of GAPDH, ANXA2, FAK, VE-cadherin, FLNA or vimentin were seen with shβ2M and shRACK1 treatment (Fig. 5A and B). To test the effect of RACK1 silencing on S1P- and GF- mediated endothelial invasion, ECs were transduced separately with recombinant lentiviruses shRACK1-1 and -2, non-transfected ECs (WT), ECs transfected with packaging vectors only (MOCK), or shRNA sequences directed against β2-microglobulin (shβ2M) were used as controls. Photographs of invading cultures illustrated that knockdown of RACK1 interfered with endothelial invasion responses stimulated by S1P and GF (Fig. 5C). Western blot analyses of extracts collected from invading cultures showed selective knockdown of RACK1 and β2M with respective shRNAs (Fig. 5D). Quantification of invasion density revealed a significantly decreased number of invading cells with RACK1 depletion as compared to shβ2M, WT and MOCK controls (Fig. 5E). These results demonstrated that RACK1 was required for S1P- and GF- stimulated EC invasion in 3D collagen matrices.

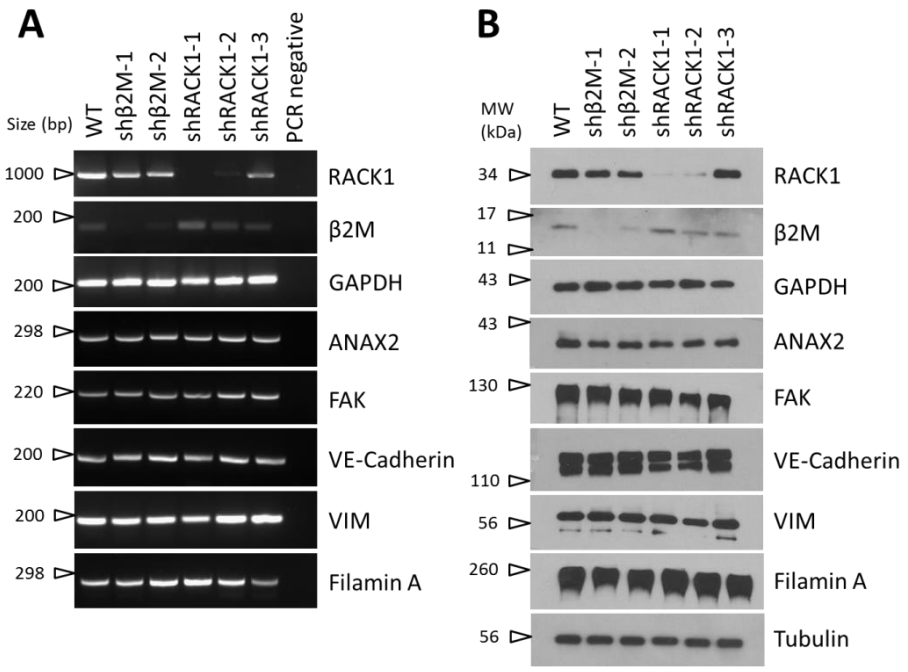

Figure 5. RACK1 knockdown decreased invasion responses in ECs. (A) Non-transduced ECs (WT), or ECs transduced with lentiviruses delivering shRNA directed to β2-microglobulin (shβ2M-1 and -2) or RACK1 (shRACK1-1, -2 and -3) were utilized to generate RNA, cDNA, and RT-PCR reactions using RACK1-, β2M-, GAPDH-, ANXA2-, FAK-, VE-Cadherin-, VIM-, and Filamin A- specific primer sets. **(B)** Cell lysates from treatment groups as in A were analyzed by Western blotting using RACK1, β2M-, GAPDH-, ANXA2-, FAK-, VE-cadherin-, VIM-, filamin A-, and tubulin-specific antisera. **(C)** Non-transduced ECs (WT), or ECs transduced with lentiviruses delivering shRNA directed to β2-microglobulin (shβ2M-1) or RACK1 (shRACK1-1 and -2) were tested in 3D invasion assays using S1P+GF. Photographs to illustrate the invasion responses (top-view, upper panel; side-view, lower panel). Scale bar=50 μm. **(D)** Western blot analyses of whole cell lysates to verify β2M and RACK1 protein suppression using RACK1-, β2M-, and tubulin- specific antisera. Quantification of **(E)** invasion density and **(F)** invasion distance at 20 h of invasion. Data in (E) represent average number of invading cells per 1 mm2 field ± SD (n=3 fields, Students t-test, **p<0.01, compared to shβ2M). Data in (F) represent average length of structures ±SEM (n>80 cells; Students t-test, **p<0.01, ***p<0.001 compared to shβ2M). Representative experiment shown (n=4).

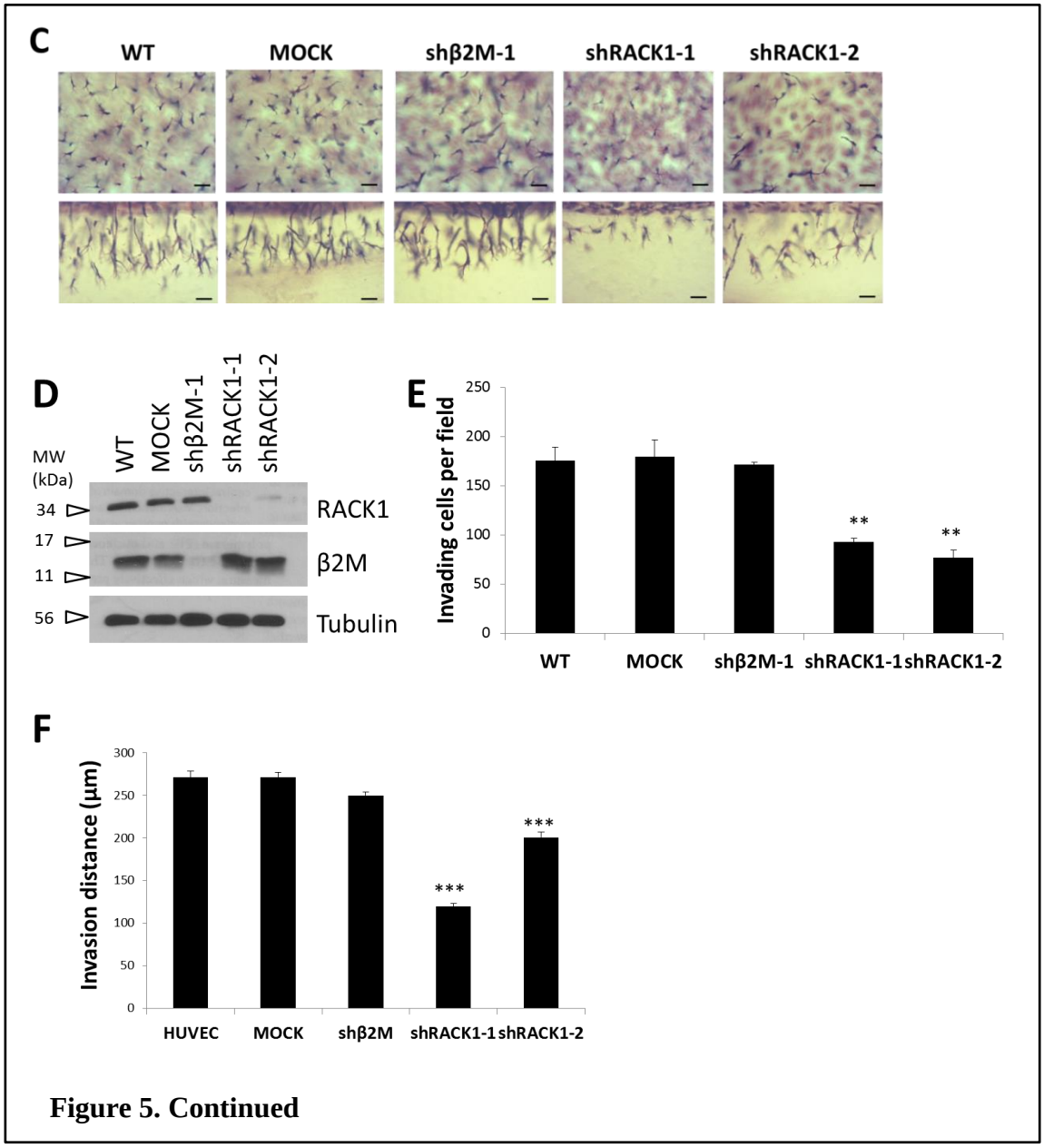

Figure 5. Continued

To test whether RACK1 rescue would restore invasion responses decreased by RACK1 silencing, GFP-RACK1 constructs were mutated using site-directed mutagenesis to alter the shRACK1-1 target site (R3). GFP and R3 constructs were

overexpressed in ECs treated with lentiviruses delivering shRNA targeted to β2M and RACK1 and utilized in invasion experiments along with non-transfected ECs (WT) (Fig 6A). Western blot analyses of cell lysates showed successful knockdown of RACK1 and β2M (Fig. 6B). Also, expression of R3 rescue construct (~65 kDa) was successfully detected in shRACK1+R3 treatment group with GFP antisera (Fig. 6B). Quantification of invasion density revealed no significant impairments in invasion responses compared to WT when transducing with shβ2M+GFP, indicating multiple transductions had no negative effects. A significant decrease in sprouting was seen with shRACK1+GFP compared to shβ2M+GFP or WT control (Fig. 6C). Furthermore, expression of R3 rescue construct with RACK1-specific shRNA (shRACK1+R3) resulted in a slight but significant increase of invasion density (Fig. 6C) and invasion distance (Fig. 6D) compared to shRACK1+GFP. Thus, rescuing with the RACK1 expression with R3 GFP-RACK1 in shRACK1-1 expressing ECs increased the number and length of sprouting ECs compared to GFP control, supporting a requirement for RACK1 in mediating endothelial sprouting responses.

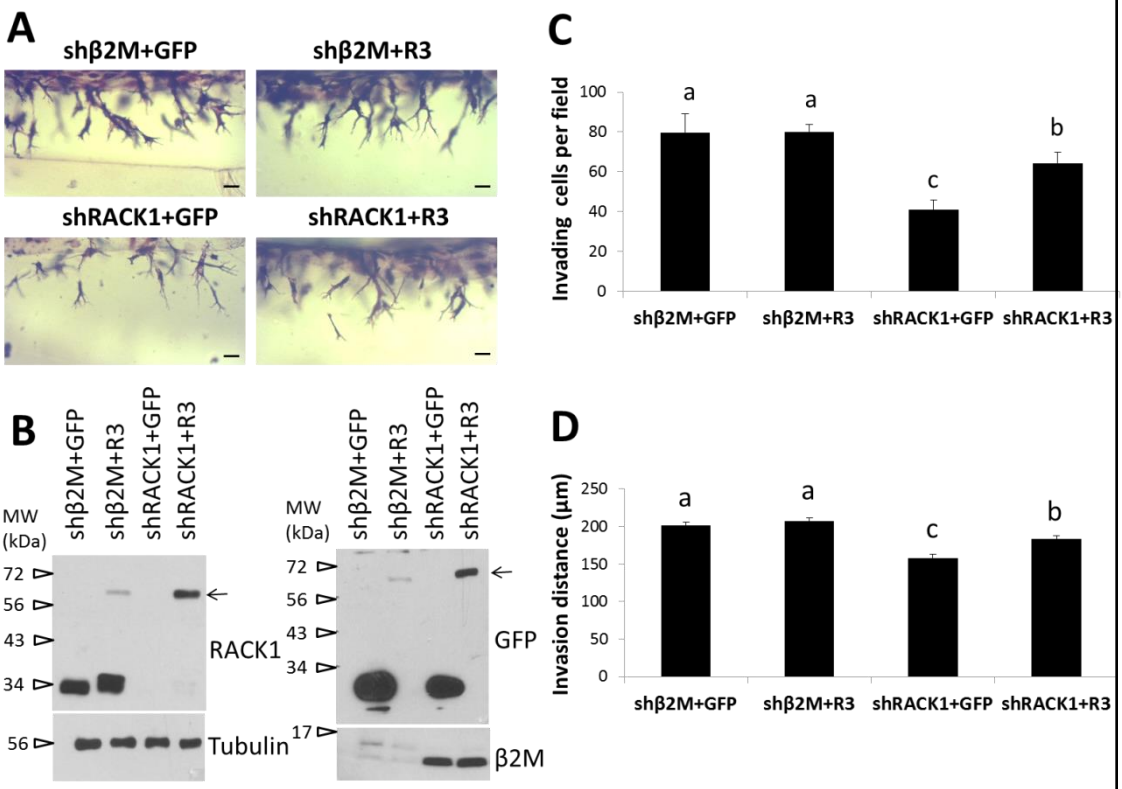

Figure 6. RACK1 rescue partially restores sprouting responses and invasion distance reduced by RACK1 silencing. ECs were transduced with lentiviruses delivering shRNA directed to β2M (shβ2M) or RACK1 (shRACK1) before being transduced with lentiviruses delivering enhanced green fluorescent protein (GFP) control or R3 (GFP-RACK1 rescue construct). **(A)** Photographs of a side view illustrating invasion responses. Scale bar=50 μm. **(B)** Western blot analyses of whole cell lysates probed with RACK1-, GFP-, β2M- and tubulin-specific antisera. Arrow indicates expression of R3 (65kDa) construct. **(C)** Quantification of invasion density at 22 h. Data represents average number of invading cells per 1mm2 field ± SD (n=4 fields, one-way ANOVA). **(D)** Quantification of invasion distance from EC monolayer to the tip of invading structures. The results represent average values ± SEM (n>100 sprouts, one-way ANOVA). (C and D) Means with the same letter are not significantly different.

RACK1 Depletion Decreased FAK Activation

RACK1 is proposed to act as a scaffold protein and plays a role in various cellular processes including cell migration [121, 123, 144]. Most functions of RACK1 associated with cell adhesion, spreading and migration are linked to its ability to associate with FA proteins such as FAK and regulate its activity [123, 126, 145, 146]. These studies guided us to investigate whether RACK1 affected FAK activity during EC sprouting in collagen matrices. ECs were transduced with recombinant lentiviruses expressing shRACK1 or shβ2M and utilized in invasion assays. Whole cell extracts were collected from invading cultures at 0, 2, and 3 h and analyzed by western blotting. We observed that RACK1 and β2M were successfully silenced (Fig 7A). In addition, FAK activation, indicated by an autophosphorylation event at tyrosine residue 397 (Y397), was decreased at 2 h in RACK1 depleted ECs compared to shβ2M controls. However, overall expression of total FAK was not affected. Tubulin and GAPDH loading controls remained constant (Fig. 7A). FAK phosphorylation significantly decreased in ECs expressing shRACK1 compared to shβ2M at 2 h of invasion (Fig. 7B). These results suggested that RACK1 was required for FAK activation in ECs.

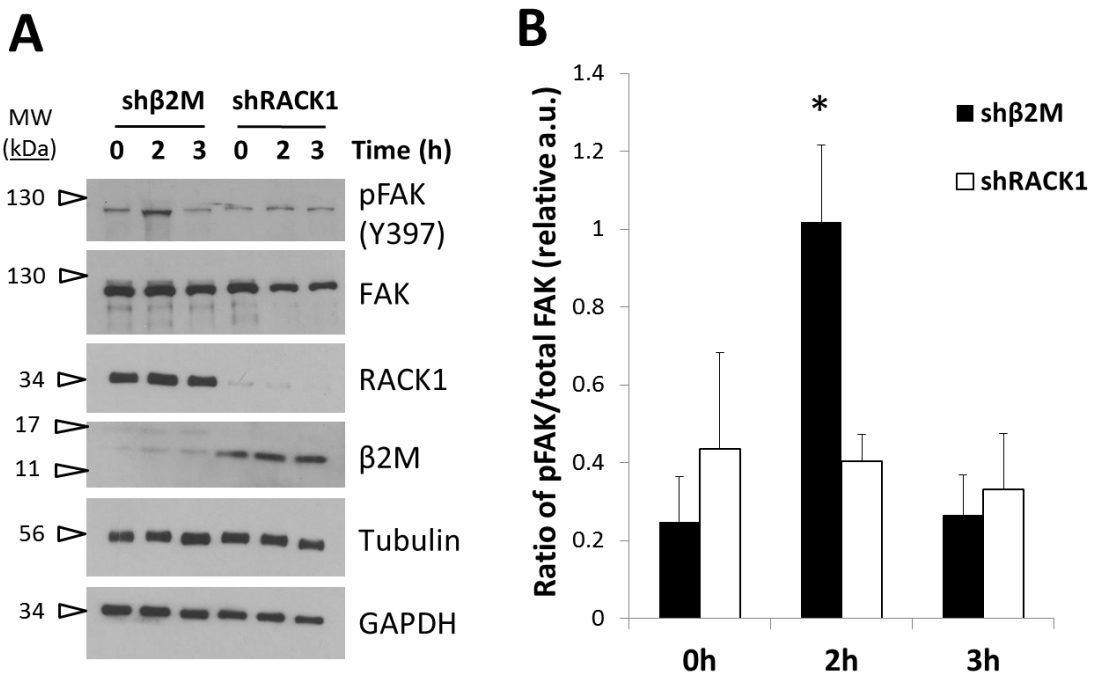

Figure 7. Depletion of RACK1 reduced FAK activation. (A) ECs expressing shRNA directed to β2M (shβ2M) or RACK1 (shRACK1) were allowed to invade for the time points indicated. Whole cell lysates were prepared and analyzed by Western blot analysis using polyclonal antisera directed to phosphorylated FAK (pFAK) (Y397) and β2M, and monoclonal antibodies directed to total FAK, RACK1, and tubulin. **(B)** Intensity levels for pFAK (Y397) and total FAK were normalized to tubulin using Image J software. Ratios of normalized pFAK and FAK were plotted ± SD in arbitrary units (a.u.) from three independent experiments (Student's t-test, * $p<0.05$, compared to shβ2M control).

FAK Activation Occurred during EC Invasion

Because RACK1 knockdown decreased FAK activation, we investigated whether FAK activity was required for endothelial sprouting. ECs treated with FAK inhibitor (FI), which selectively blocks FAK phosphorylation at Y397, were allowed to invade

collagen matrices overnight. Quantification of invasion responses indicated FI treatment dose-dependently inhibited invasion, indicating FAK activation was required for endothelial invasion (Fig 8A). No adverse effects on cell monolayers or cell viability were observed with blocking FAK activity (data not shown). Western blot analysis confirmed a dose-dependent decrease in Y397 phosphorylation (Fig. 8B) with FI treatment, correlating with a decrease in EC sprouting (Fig 8A). Representative side-view images of sprouting EC cultures treated with 0, 5 and 10 μM FI illustrated partial and complete inhibition of sprouting at 5 and 10 μM dose of FI, respectively (Fig. 8C). These results demonstrated a requirement for FAK activation during S1P- and GF-stimulated endothelial sprouting.

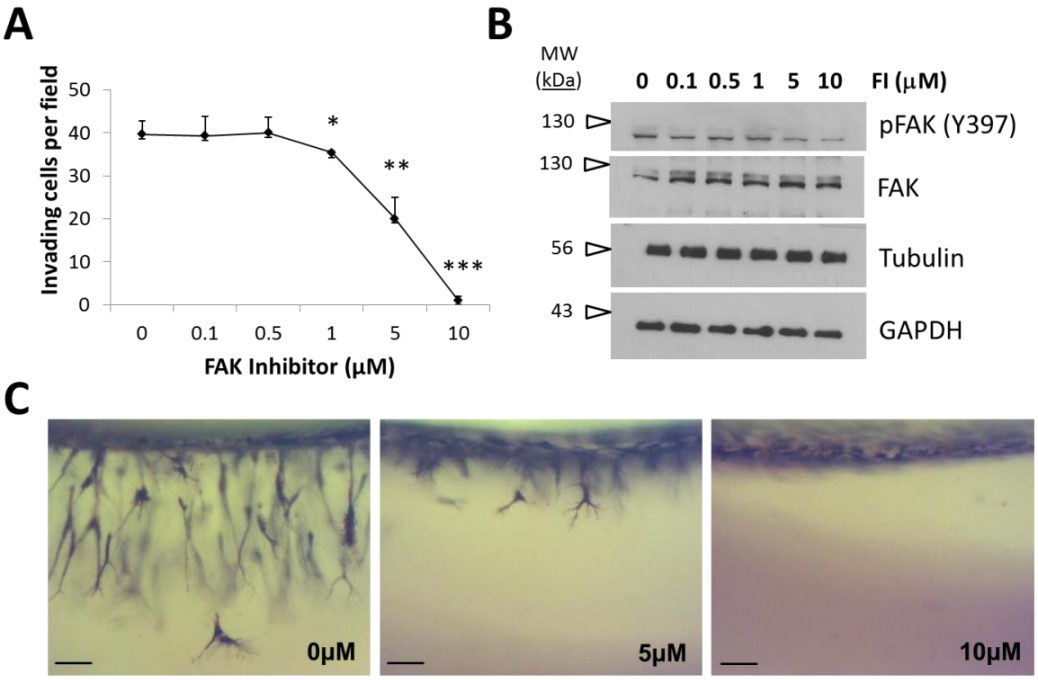

Figure 8. EC invasion required FAK activation. (A) ECs were pre-incubated with FAK inhibitor (FI) at the concentrations indicated for 20 minutes at 37°C prior to seeding on collagen matrices. ECs were allowed to invade for 20 h with S1P+GFs. Samples were fixed in 3% glutaraldehyde and stained with toluidine blue. Data represents average numbers of invading cells per 0.25 mm2 field ± SD (n=3, Student's t-test, * $p<0.05$, ** $p<0.01$, *** $p<0.001$, as compared to 0 μM FI treatment). **(B)** Whole cell extracts from invading cultures from (A) at 2 h with indicated FI concentration were immunoblotted with antisera directed against pFAK (Y397), FAK, tubulin, and GAPDH. **(C)** Representative photographs of a side view of invasion (24 h) with 0, 5 and 10 μM FI treatment. Scale bar=50 μm.

Vimentin Regulated FAK Expression in ECs

Proteomic studies demonstrated that full length 60 kDa vimentin was upregulated in invading versus non-invading ECs (Table 2), and Burgstaller *et al.* have suggested that networking and anchorage of vimentin intermediate filaments at FAs resulted in cell shape changes, polarization and prolonged lifespan of FAs in mouse fibroblasts [129].

We have previously shown that vimentin was required for endothelial sprouting [66]. Because of the link between vimentin and FA regulation [129] and a known requirement for vimentin in EC sprouting [66], we tested whether vimentin regulated FAK in S1P- and GF-stimulated invasion. ECs transduced with recombinant lentiviruses expressing short hairpin RNAs directed against vimentin (shVIM) or β2M (shβ2M) were allowed to invade collagen matrices. Whole cell extracts collected from invading cultures at 0, 2, and 3 h were analyzed by western blotting. We observed a decrease in total and phosphorylated FAK levels with vimentin knockdown compared to shβ2M controls (Fig. 9A). Quantification of western blots revealed a significant difference in the expression of total FAK at all time-points between shVIM and shβ2M expressing ECs (Fig. 9B). These data suggested that vimentin regulated FAK expression. We reported calpain-dependent vimentin cleavage occurred predominantly in response to GF stimulation and that vimentin solubility was altered during EC invasion [66]. To determine whether vimentin solubility affected FAK expression, we analyzed invading cultures treated with a calpain inhibitor. A decrease in FAK expression was not observed when ECs were treated with calpain inhibitor-III, which specifically blocked calpain dependent vimentin cleavage (Fig. 10), suggesting that the solubility state of vimentin did not affect FAK expression during endothelial sprouting.

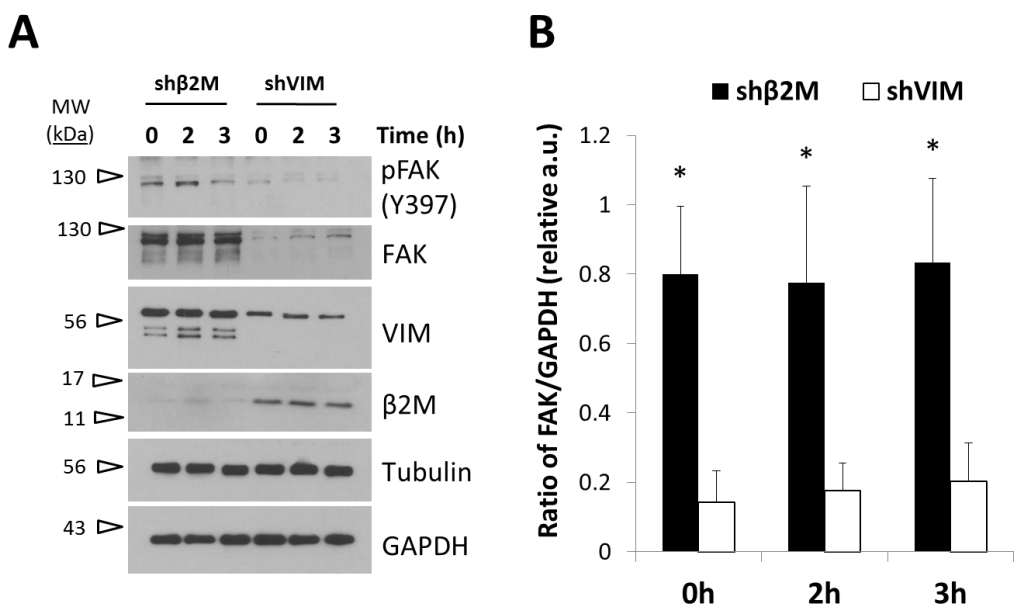

Figure 9. Vimentin regulated FAK expression in ECs. (A) ECs were transduced with shRNA directed to β2M (shβ2M) and vimentin (shVIM) and placed in invasion assays in the presence of S1P+GF. Whole cell lysates were prepared at indicated time points. Western blot analyses were conducted using polyclonal antisera directed to phospho-FAK (Y397) and β2M, as well as monoclonal antisera directed to total FAK, tubulin, GAPDH and vimentin. **(B)** Quantification of FAK protein expression using Image J software and normalized to GAPDH. The results represent average values ± SD in arbitrary units (a.u.) from three independent experiments (Students t-test, * $p<0.05$, compared with shβ2M expression).

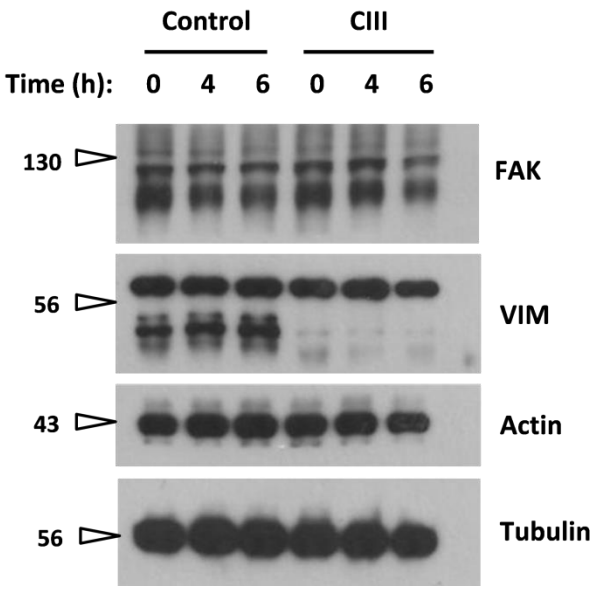

Figure 10. Calpain inhibition does not affect FAK expression or activation. ECs pre-incubated with or without 100 μM CI-III were allowed to invade collagen matrices for 6 h. Whole cell extracts were prepared at indicated time-points and immunoblotted with antisera directed against FAK, vimentin, actin and tubulin.

RACK1 Complexed with Vimentin and GFs Enhanced this Interaction

The above data show RACK1 and vimentin regulate FAK activation and expression. Immunoprecipitation experiments revealed vimentin complexed with RACK1 (Fig. 11A). RACK1 also immunoprecipitated with vimentin antisera (Fig. 11B), indicating that a complex containing RACK1 and vimentin was formed in EC monolayers stimulated with S1P and GFs. To test whether this association was stimulated by individual pro-angiogenic stimuli, EC monolayers were untreated (control), treated with 1 μM S1P, or treated with a combination of 40 ng/mL VEGF and

bFGF (GF) for 1 h. Immunoprecipitations were performed by incubating lysates with RACK1 specific antisera, and eluates were probed for vimentin and RACK1. Interestingly, we observed an increase in RACK1-vimentin association with GF (but not S1P) stimulation, while equivalent amounts of RACK1 were immunoprecipitated in all conditions (Fig. 11C). Data quantified from three independent experiments indicated a significant increase in immunoprecipitated vimentin with GF treatment, as compared to the starting material (Fig. 11D). To confirm GF-mediated increase in co-localization, ECs seeded on collagen coated glass coverslips were serum starved for 1 h and not treated (Control) or treated with S1P or GF and stained with RACK1- and vimentin-specific antisera (Fig. 11E). Quantification of colocalization in each treatment group confirmed that GFs significantly increased overlap when compared to control or S1P treatment (Fig. 11F). These results support that GFs enhanced complex formation between RACK1 and vimentin.

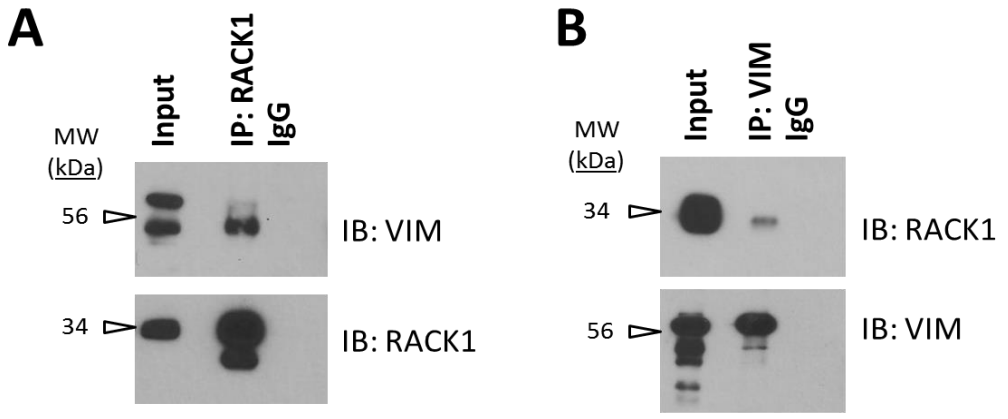

Figure 11. Growth factor stimulation enhanced RACK1-vimentin complex formation. (A) ECs were cultured in T75 flasks for 3 days without replenishing growth media and stimulated with S1P+GF for 1 h. Immunoprecipitations were performed using monoclonal RACK1 antibodies or isotype controls (IgG) and probed for vimentin and RACK1 using Western blot analyses. **(B)** Reverse immunoprecipitations were performed using a polyclonal vimentin antibodies or isotype controls (IgG) and probed for RACK1 and vimentin using Western blot analyses. **(C)** ECs cultured in T75 flasks for 3 days and stimulated with nothing (control), 1 μM S1P (S1P), or 40 ng/mL GF (GF) for 1 h. Immunoprecipitations were performed using monoclonal RACK1 antibodies or isotype controls (IgG). Eluates were probed with vimentin- and RACK1- specific antisera using Western blotting. **(D)** Quantification of co-precipitated vimentin normalized to starting material from Western blots using Image J software. The results represent average values ± SD in arbitrary units (a.u.) from three independent experiments (Student's t-test, **$p<0.01$, compared to control). **(E)** ECs seeded on glass coverslips were serum-starved for 1 h and treated without (Control), with 1 μM S1P (S1P), or with 40 ng/ml GFs (GF) for 1 h. Following paraformaldehyde fixation, cells were stained with monoclonal anti-RACK1 or polyclonal anti-vimentin antibodies and detected with species-specific secondary antibodies conjugated to Alexa Fluor 594 and Alexa Fluor 488. Images were collected using Nikon A1 confocal laser microscopy. Scale bar=5 μm. **(F)** Quantification of RACK1 (red) and vimentin (green) co-localization using Pearson's correlation coefficient. The results represent average values ± SD from each treatment group. n = number of cells per treatment group (one-way ANOVA with Bonferroni's multiple comparison post-hoc test, * $p<0.05$, compared to control).

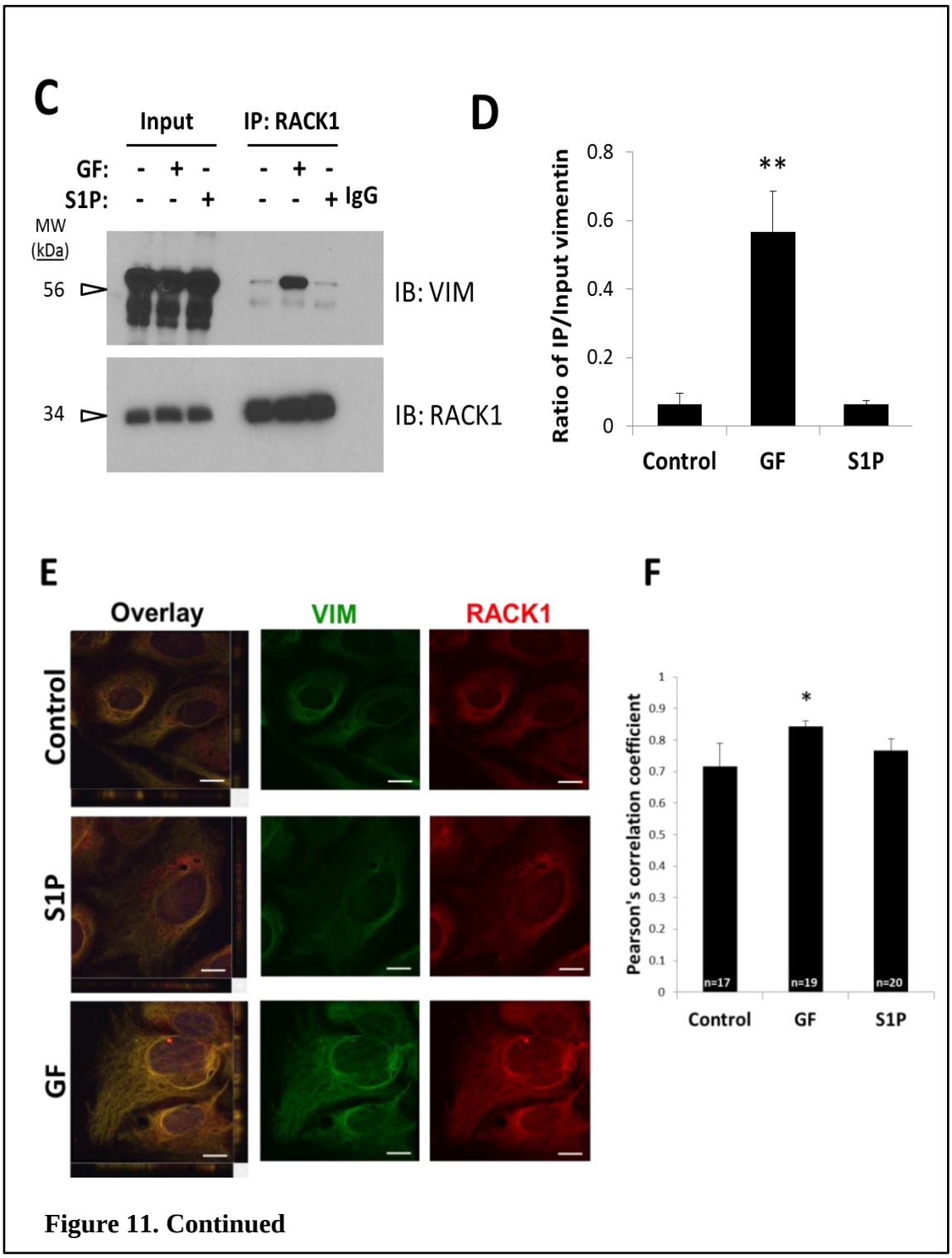

Figure 11. Continued

Vimentin Association with FAK Required RACK1

Thus far our data showed that downstream of pro-angiogenic signals, RACK1 and vimentin complexed to regulate FAK expression and activation. To test whether FAK was a part of this complex, as well as whether S1P and GF stimulation enhanced formation of the complex, lysates from ECs invading 3D collagen matrices treated without (-) or with (+) S1P and GF were collected for immunoprecipitation experiments. We observed that increased RACK1 and FAK co-immunoprecipitated with vimentin with S1P and GF stimulation (Fig. 12A). Reverse immunoprecipitations using RACK1- (Fig. 12B) and FAK-specific antisera (Fig. 12C) were performed to confirm these interactions were enhanced by S1P and GF treatment. Thus, conditions that stimulate EC invasion enhanced the formation of a RACK1, vimentin, and FAK complex in 3D cultures. Based on these data, we next tested whether FAK activation was needed to stabilize the complex. Interestingly, FAK inhibition (FI) did not alter complex formation between vimentin, RACK1, and FAK (Fig. 13). Vimentin binding to FAK remained unaltered with FI, and FAK and vimentin similarly bound RACK1 (Fig 13), which suggested that association of RACK1 and vimentin with FAK was independent of FAK activation. To further investigate the role of RACK1, we tested whether RACK1 silencing altered complex formation. Knockdown of RACK1 and β2M protein levels were confirmed using western blot analyses (Fig. 12D). RACK1 knockdown resulted in decreased complex formation between full length vimentin (60 kDa) and FAK compared to β2M knockdown (Fig. 12E). Quantification of data from three independent

experiments indicated a significant decrease in vimentin and FAK complex formation with RACK1 knockdown (Fig. 12F). Taken together, these results indicated that the scaffold protein RACK1 was needed to maintain complex formation between vimentin and FAK.

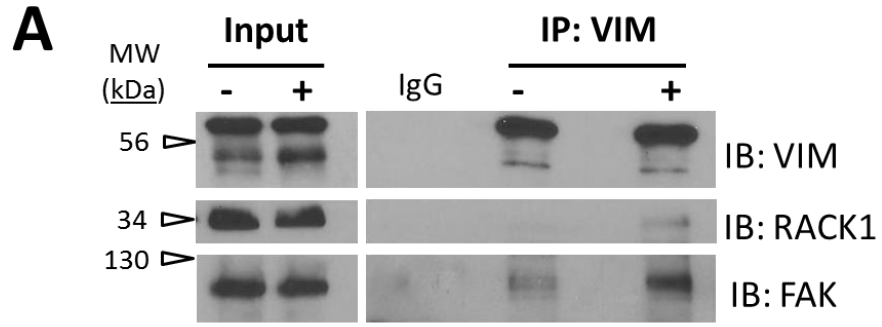

Figure 12. RACK1, vimentin, and FAK complex formation is enhanced during EC invasion. Confluent flasks (75cm^2) of ECs were serum starved for 2 h, trypsinized and placed in invasion assays in the absence (-) or presence of S1P+GF (+) for 3 h prior to lysate preparation. Immunoprecipitations were performed using polyclonal antisera directed to **(A)** vimentin, **(B)** RACK1 and **(C)** FAK, along with matched isotype controls (IgG). Eluates **(A-C)** were probed for vimentin (VIM), FAK, and RACK1 using Western blot analyses and are from one representative experiment (n=3). **(D-F)** ECs were transduced with lentiviruses delivering shRNAs directed to RACK1 (shRACK1) or β2M (shβ2M) and allowed to invade collagen matrices for 3 h prior to cell lysis and immunoprecipitation. **(D)** Western blot analyses of starting material to verify successful silencing of β2M and RACK1 proteins. **(E)** Immunoprecipitations were performed using a monoclonal FAK antibody or isotype control (IgG) and probed for FAK and vimentin (VIM) using Western blot analyses. **(F)** Quantification of co-precipitated vimentin normalized to input material from Western blots using Image J software. The results represent average values ± SD in arbitrary units (a.u.) from three independent experiments (Student's t-test, *$p<0.05$, compared with shβ2M control).

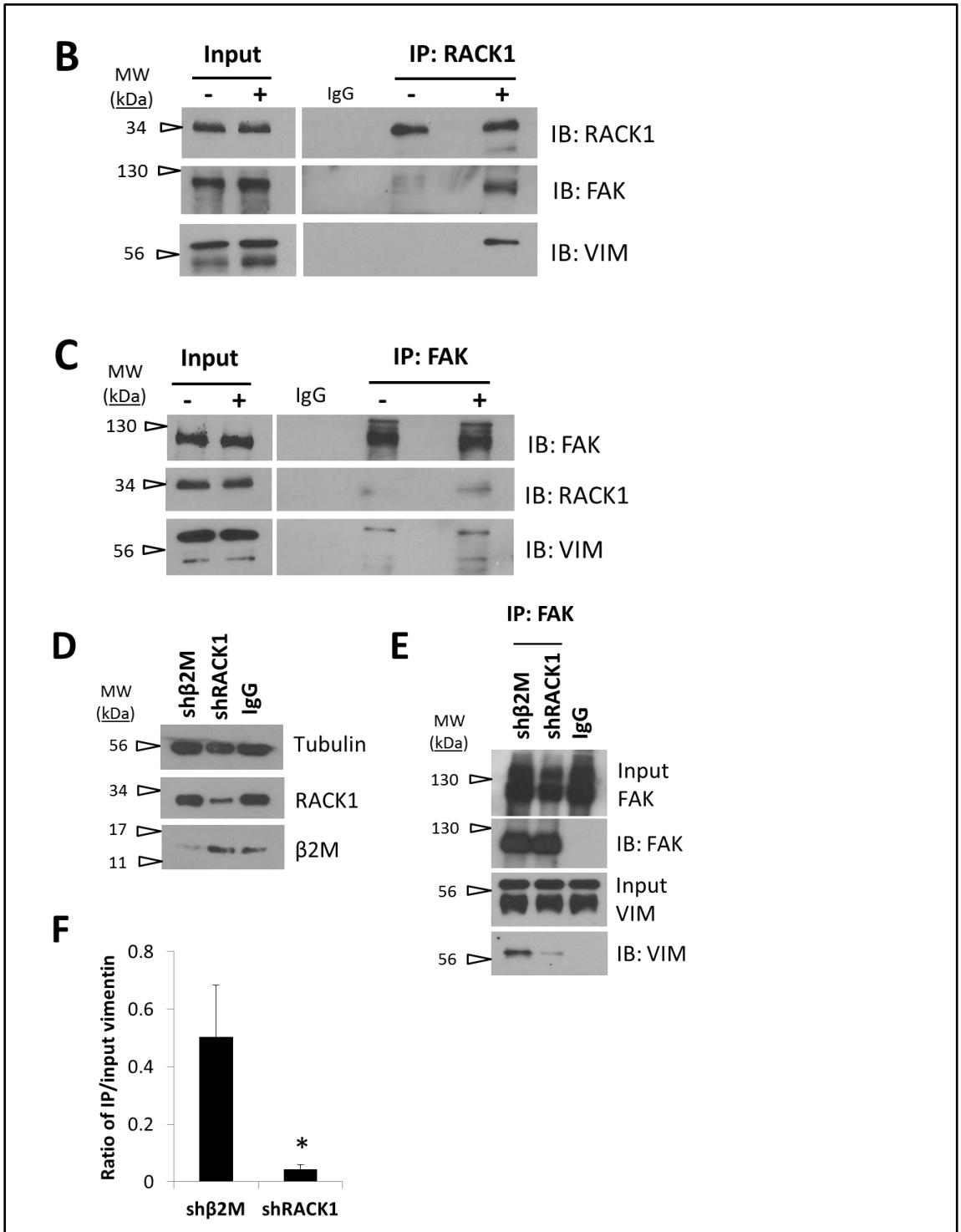

Figure 12. Continued

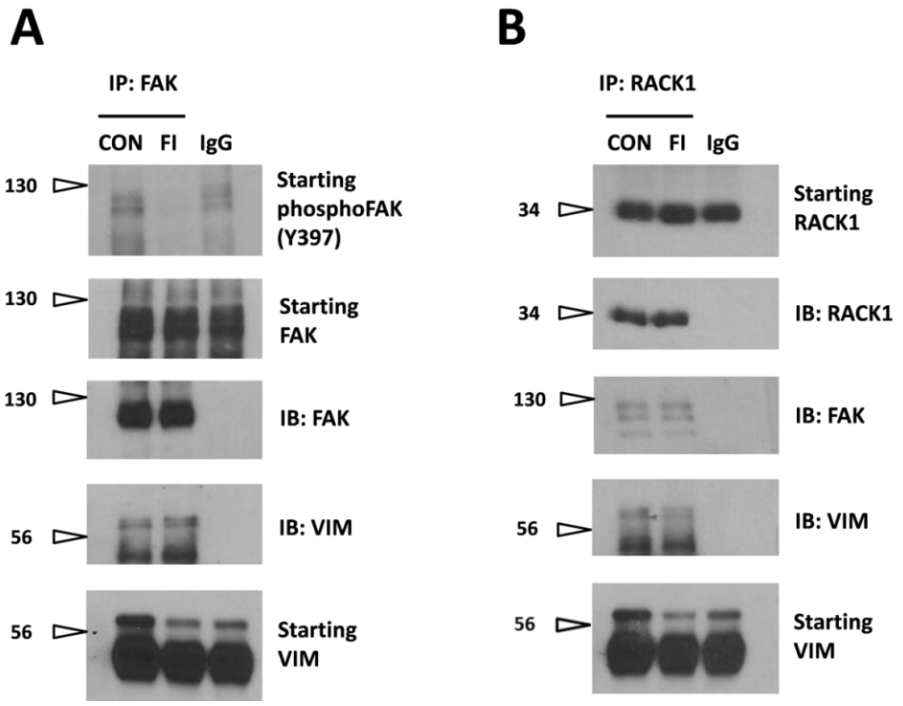

Figure 13. Inhibition of FAK activity does not alter complex formation between RACK1, VIM and FAK. Invasion experiments were established by pre-incubating cells with 0 (CON) or 10 μM FI (FI) for 20 minutes at 37°C prior to seeding on collagen matrices. ECs were allowed to attach the collagen matrices and invade for 3 h, prior to cell lysis and immunoprecipitations. ECs used for immunoprecipitation with IgG control were treated with 0 μM FI. **(A)** Immunoprecipitations were performed using a monoclonal FAK antibody or isotype control (IgG) and probed for pFAK (Y397), FAK and vimentin (VIM) using Western blot analyses. **(B)** Immunoprecipitations were performed using a monoclonal RACK1 antibody or isotype control (IgG). Eluates were probed for RACK1, FAK and vimentin (VIM) using Western blot analyses.

Knockdown of Vimentin and RACK1 Decreased Cell Attachment and Focal Adhesion Formation

We next tested the consequences of vimentin knockdown on cell adhesion, which has been linked to focal adhesion formation [147]. Endothelial cells expressing shRNA

directed to β2M or vimentin were allowed to attach to wells coated with increasing doses of fibronectin. These experiments were conducted rapidly (15 minutes) to determine whether vimentin silencing altered cell attachment using an established method [148]. Endothelial cell attachment to fibronectin occurred rapidly and was dose-dependent. However, cells expressing shRNA directed to vimentin (shVIM) exhibited decreased attachment compared to shβ2M controls (Fig. 14A). Western blot analyses confirmed successful knockdown of both vimentin and β2M (Fig. 14B). These data demonstrate that decreasing vimentin levels in ECs reduced cell attachment (Fig. 14A), which coincides with decreased FAK expression (Fig. 9). Similar experiments conducted with ECs expressing shRNA directed to RACK1 showed decreased attachment to fibronectin compared to shβ2M controls (Fig. 14C). Western blot analyses confirmed successful knockdown of both RACK1 and β2M (Fig. 14D). In addition to cell attachment, focal adhesion formation (visualized through pFAK Y397 and vinculin staining) was also decreased in ECs expressing shVIM and shRACK1 compared to shβ2M controls. While large, organized focal adhesions were observed in shβ2M controls, as indicated by vinculin and pFAK co-staining (Fig. 14E), smaller and less distinct structures were seen with shVIM and shRACK1 expression.

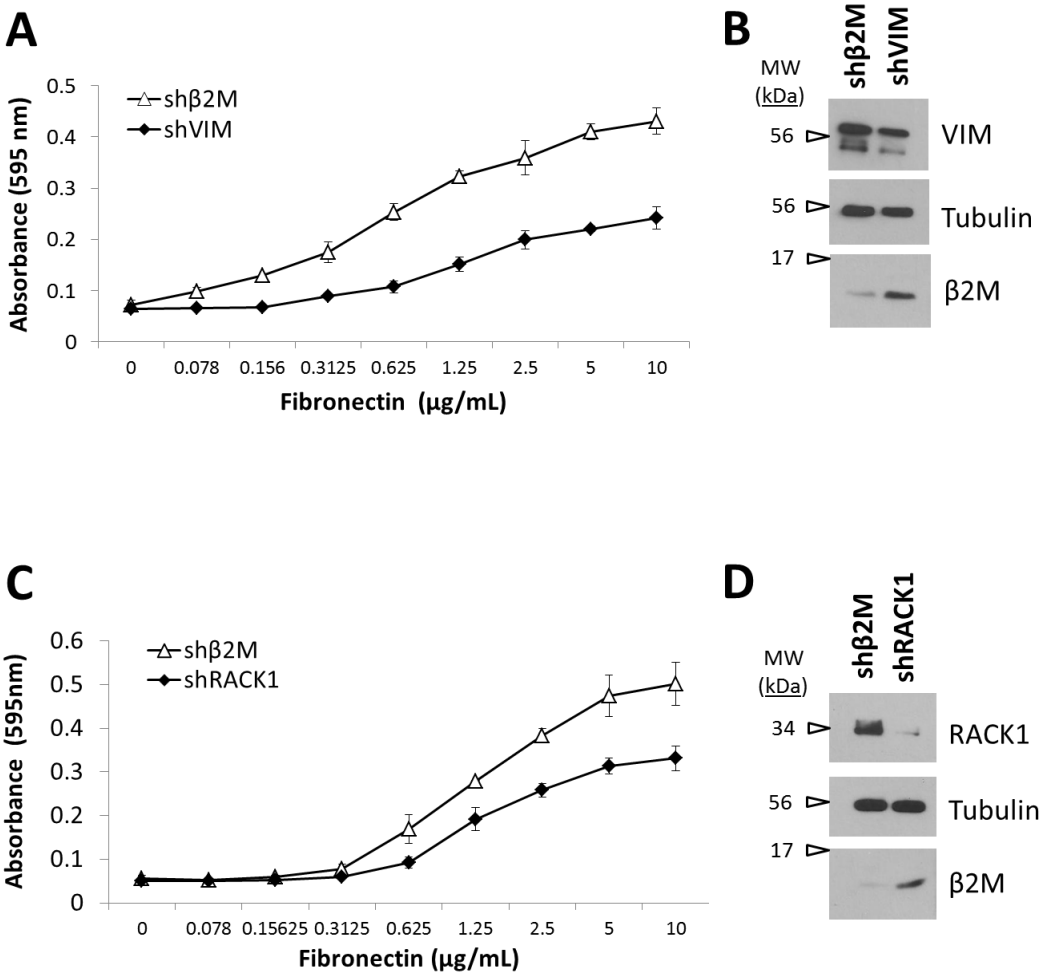

Figure 14. Vimentin silencing reduced EC adhesion responses. ECs were transduced with shRNA directed to **(A)** β2M (shβ2M) and vimentin (shVIM) or **(C)** shβ2M and shRACK1 for 4 days before being plated on wells coated with increasing amounts of fibronectin at the doses indicated for 15 min. Absorbance values (595 nm) represent relative levels of cell attachment. Experiments are representative of 4 independent experiments. **(B)** Western blot of cell extracts probed with antisera directed to β2M, α-tubulin and vimentin from experiment in panel **A**. **(D)** Western blot of cell extracts probed with antisera directed to β2M, α-tubulin and RACK1 from experiment in panel **C**. **(E)** Indirect immunofluorescent staining of ECs expressing shβ2M, shVIM, and shRACK1 using monoclonal antibody directed against pFAK (Y397) and vinculin. Scale bar=10 µm

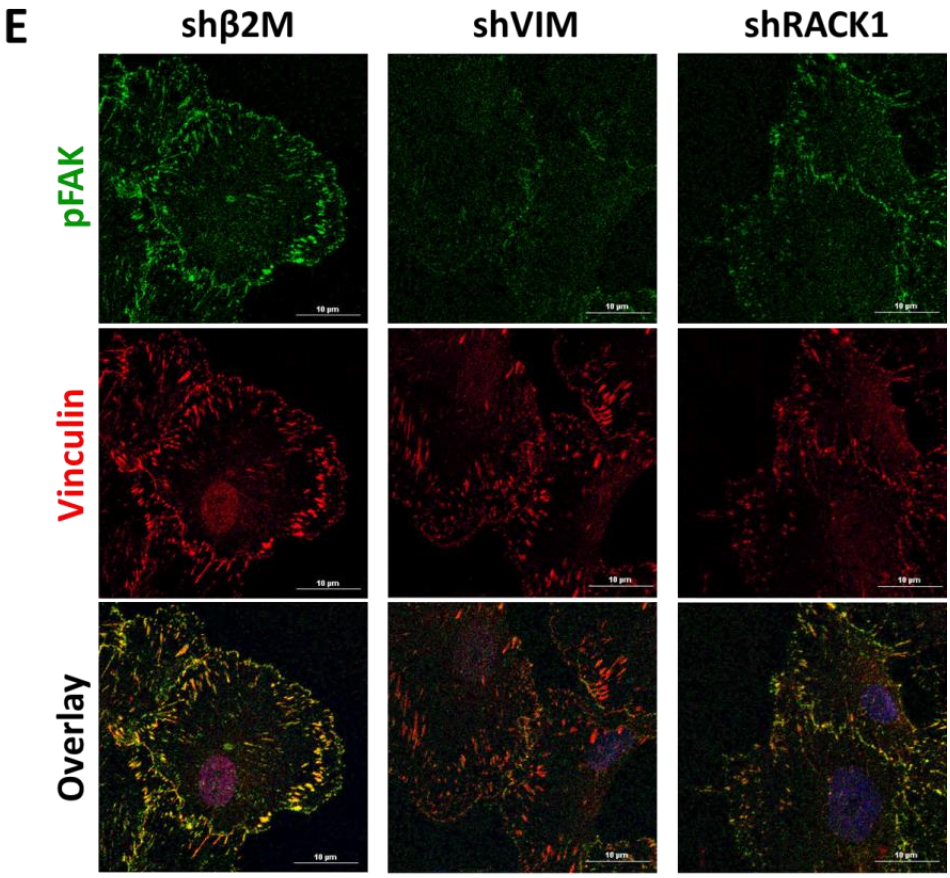

Figure 14. Continued

DISCUSSION

In this study, we performed a proteomic analysis to determine changes in protein expression associated with sprouting angiogenesis. The 3D model used in this study incorporated S1P with angiogenic growth factors VEGF and bFGF to stimulate robust EC sprouting [45]. The assay system mimicked a wound environment where S1P combined with VEGF and bFGF stimulated new blood vessel formation [16]. In this

study, we report a novel mechanism to control sprouting angiogenesis in 3D collagen matrices. Proteomic analyses from two independent screens showed upregulation of receptor for activated C kinase 1 (RACK1) in invading ECs, suggesting a crucial role for RACK1 downstream of S1P and GF signaling. Our findings suggest that RACK1 regulated sprouting through association with the major intermediate filament (IF) protein, vimentin and consequent regulation of FAK.

Our results are the first to demonstrate a complex formation between RACK1 and vimentin during endothelial sprouting. The WD-repeat protein, RACK1, is a highly conserved cellular adaptor protein with a seven-bladed β-propeller structure. This unique structure facilitates binding with a variety of proteins either directly or as a part of a larger complex [149-156]. RACK1 also shuttles proteins to specific cellular sites, modulating enzymatic activity of its binding partners and stabilizing protein interactions. We find here that GF stimulation increased RACK1 complex formation with full length vimentin during EC sprouting. The intermediate filament protein vimentin is involved in many important physiological functions such as distribution of organelles, signal transduction, cell polarity and gene regulation [157-159]. Previous work from our laboratory demonstrated a direct requirement of vimentin during angiogenic sprouting. Soluble vimentin, resulting from calpain mediated cleavage downstream of GF stimulation facilitated MT1-MMP membrane translocation and successful endothelial sprout formation [66]. We find here full length vimentin (60 kDa) regulated EC invasion through a unique pathway involving RACK1 and FAK.

The major focal kinase protein FAK has been established as a key mediator in cell migration and endothelial morphogenesis. FAK conditional knockout mice exhibited severe cardiac defects, ventricular hypertrophy and significantly attenuated chemotaxis in isolated cardiomyocytes resulting in embryonic lethal phenotype [140, 141]. Deletion of FAK specifically in ECs resulted in defective angiogenesis in embryos, yolk sacs and placenta, impaired vasculature and associated hemorrhage, edema and developmental delay [142]. Similar studies by Braren *et al.* revealed that FAK depletion in ECs resulted in distinctive and irregular embryonic vasculature with reduced vessel growth and vessel regression resulting in lethality between days E10.5 and E11.5. ECs derived from mutants exhibited aberrant lamellipodial extensions, altered actin cytoskeleton, and non-polarized cell movement [139]. These data supported a crucial role for FAK in cardiac and vascular morphogenesis and in regulation of EC survival and morphology. In agreement with these data, we observed that blocking FAK activation completely inhibited sprouting in ECs.

Our data also further investigated a connection between vimentin filaments and FAK, and to the best of our knowledge are the first to show that vimentin complexed with FAK. Numerous studies have established that vimentin intermediate filaments terminate at focal contacts [160, 161]. In fibroblasts, tethering of vimentin filaments to FAs decreased turnover rate and increased stabilization [129]. Further, vimentin regulated focal contact assembly and helped stabilize cell-matrix adhesions in ECs subjected to shear stress [130]. FAK is an integral component of FAs and functions to

assemble focal contacts in response to integrin clustering by ECM engagement [136, 137], as well as regulate focal adhesion turnover [162]. Our data showed that vimentin was required to maintain FAK expression and activity, which is consistent with data showing loss of vimentin correlated with decreased focal contact size and stability [129, 130]. Fitting with these data, loss of vimentin in endothelial cells and mouse dermal fibroblasts attenuated cell adhesion responses.

Vimentin depletion resulted in attenuation of phosphorylated and total FAK levels in ECs. Interestingly, we did not observe attenuated levels of FAK when blocking vimentin cleavage with a calpain inhibitor suggesting that the cleavage state of vimentin had no bearing on FAK expression levels. To our knowledge this is the first report to show that vimentin controlled FAK expression in ECs. These data have important implications in control of cell-matrix interactions during EC sprouting, and these findings help explain the ability of vimentin to control FA size and stability.

We show here that RACK1 and vimentin complexed with FAK. Furthermore, we found that blocking FAK activation did not change the dynamics of this complex indicating that formation of the complex did not require FAK activation. Our results indicated that vimentin and RACK1 were required to maintain expression and activation of FAK, which was crucial for successful sprouting. Since RACK1 is proposed as a scaffold protein, its functions are commonly ascribed to its ability to associate and stabilize multiple protein interactions. We therefore tested the effect of RACK1 depletion on vimentin-FAK interaction. We showed here for the first time that binding

between vimentin and FAK was RACK1-dependent. We found significantly decreased association between full length vimentin filaments and FAK with RACK1 knockdown. These findings reveal a novel scaffold function of RACK1 in stabilizing complex formation between vimentin and FAK, and suggest that RACK1 may assist in tethering of vimentin filaments to FA complexes [129, 161].

In conclusion, we have demonstrated that RACK1 and vimentin are upregulated in sprouting versus quiescent ECs. RACK1, vimentin, and FAK form a complex during endothelial sprout formation in 3D collagen matrices, and all of these molecules are present in caveolin-enriched microdomains in endothelial cells [163]. FAK [164, 165], RACK1 [128, 166, 167], and vimentin [168, 169] are upregulated during tumor formation and progression. Since expression of all these molecules is altered during malignant disease, this pathway may regulate invasive, metastatic cell behavior. Our data provide novel insights into the role of RACK1 during endothelial invasion in 3D collagen matrices downstream of S1P signaling.

CHAPTER III

HIC-5 MEDIATED ENDOTHELIAL SPROUTING BY REGULATING FOCAL ADHESION KINASE AND A KEY SURFACE METALLOPROTEINASE

INTRODUCTION

Hic-5 (55 kDa) belongs to the paxillin family of focal adhesion adaptor proteins which also includes paxillin and leupaxin [170]. Hic-5 was originally discovered as a cDNA clone induced by hydrogen peroxide (H_2O_2) or transforming growth factor β (TGFβ) and thus named hydrogen peroxide inducible clone 5 (Hic-5) [171]. The structure of Hic5, which shares significant homology with paxillin, consists of four LD (Asp and Leu rich) domains at the N-terminus and four LIM (**L**in11, **I**sl-1 & **M**ec-3) domains at the C-terminus. Both LD and LIM are protein-protein interacting domains, thus Hic-5 and its family members provide multiple proteins with interfaces to mediate interaction and co-operation, downstream of extracellular matrix (ECM) engagement [172, 173]. Hic-5 is known to interact with FAK [174], vinculin [175], paxillin [175], c-src kinase (Csk) [176], protein tyrosine kinase 2 β (PYK2) [170], and Arf GAP1 (GIT) [177] via its N terminal LD domains. The LIM domains at the C-terminus of Hic-5 mediate binding to PTP-PEST [178] and Hsp27 [179]. Oxidative stress induces translocation of Hic-5 into the nucleus wherein it acts as a transcriptional co-activator [180-182]. Thus, Hic-5 is a mobile scaffold protein that interacts with several proteins at FA sites as well as within the nucleus.

Hic-5 is expressed in ECs [183] and although Hic-5 knockout mice appeared normal and were fertile, subsequent studies revealed defective recovery following vascular injury of the femoral artery [184]. Studies in bovine pulmonary aortic ECs (BPAECs) revealed that Hic-5 was recruited to focal adhesion sites and pseudopodia upon lysophosphatidic acid (LPA) stimulation [185]. Similar observations were reported in breast cancer cells, where Hic-5 localized to invadopodia in response to TGFβ [186]. Accumulating evidence from recent studies has established a link between Hic-5 and cell migration. siRNA-mediated Hic-5 silencing reduced VEGF-mediated migration responses in ECs [187] and fibronectin-mediated migration of mouse kidney epithelial cells [188]. Hic-5 depletion or expression of Hic-5 mutants that failed to localize to FAs, decreased BPAEC migration in the presence of LPA [185]. Studies in breast cancer cells by Deakin and Turner showed that Hic-5 silencing induced an amoeboid morphology in tumor cells and attenuated integrin-mediated adhesions, migration, invasion, and tumor cell metastasis [175]. In addition, recent findings by Pignatelli and colleagues demonstrated that Hic-5 depleted tumor cells displayed reduced invasion and matrix degradation that was rescued by GFP-Hic-5 expression [186]. Altogether, these studies suggest that Hic-5 may be important for endothelial cell migration as well as tumor cell invasion, adhesion formation and matrix degradation. However, the role for Hic-5 in regulating sprouting responses during angiogenesis remains undetermined. Whether or not the role of Hic-5 is distinct in ECs is also unclear.

Membrane-type matrix metalloproteinases (MT-MMPs) are widely known to mediate ECM breakdown to facilitate cell migration and invasion in 3D matrices [189-192]. Several studies have reported that MT1-MMP (or MMP14) is required for angiogenic sprouting and lumen formation in ECs [192-196]. During tumor cell migration, MT1-MMP is enriched in invadopodia, which are defined as dot-shaped actin-rich membrane protrusions that extend into the 3D ECM surroundings [189, 197]. Although tumor cell invasion and endothelial sprouting are known to be MT1-MMP-dependent, the precise molecular mechanisms that regulate its membrane translocation and activity remain poorly understood. Focal adhesion kinase (FAK) is a major kinase protein associated with focal adhesions. FAK is tyrosine phosphorylated upon ECM engagement and integrin assembly. Activated FAK recruits and phosphorylates several other proteins at focal adhesions to promote focal adhesion growth, maturity, turnover, cytoskeletal rearrangement, and cell migration [136-138]. FAK has been extensively studied in angiogenesis and cardiac morphogenesis [139-142, 198, 199]. Although FAK is present in FAs [200], it has also been implicated in regulating invadopodia [201-203]. FAs have been implicated as potential sites for MT1-MMP-dependent matrix degradation [204, 205]. Crosstalk between FAK and MT1-MMP has been reported in tumor cells, where ECM degradation by MT1-MMP promoted FA stability and cell-matrix adhesion turnover to direct cell migration [204, 206]. Additional studies demonstrated that FAK promotes cell-surface localization of MT1-MMP by disrupting endophilin A2- dependent endocytosis [207]. In addition, recent data have indicated that

successful association between MT1-MMP and FAK is required for optimal MT1-MMP activity and successful matrix degradation at these sites [205]. Taken together, these data demonstrate that interplay between MT1-MMP and FAK is critical for tumor cell migration and invasion.

In this study, we identify Hic-5 as a critical regulator of MT1-MMP and FAK during sprouting angiogenesis. Hic-5 was required for successful endothelial sprouting responses and lumen formation in 3D matrices. Hic-5 silencing attenuated FAK expression and activation as well as MT1-MMP membrane translocation, both events known to be indispensable for successful angiogenesis. We show here for the first time a complex formed between Hic-5 and MT1-MMP that is enhanced by pro-angiogenic sphingolipid, S1P, and requires the LIM2 domain of Hic-5. FAK, Hic-5, and MT1-MMP co-localized in 3D endothelial sprouting structures, and levels of Hic-5 and MT1-MMP were increased in detergent resistant membrane fractions of invading ECs. Furthermore, complex formation between FAK and MT1-MMP was enhanced by nearly four folds in presence of Hic-5. Altogether, these data indicate that Hic-5 is required for endothelial sprouting and formed a complex with MT1-MMP in response to S1P. Hic-5 appears to act as a scaffold and mediates MT1-MMP and FAK interactions. In conclusion, our data provide new evidence about endothelial-specific role for Hic-5 in directing angiogenic events.

MATERIALS AND METHODS

Endothelial Cell Culture and Invasion

Human umbilical vein ECs (HUVECs; Lonza, Allendale, NJ), passages 3-6, and were cultured as previously described. 3D invasion experiments were established using 1 μM S1P (Avanti Polar Lipids, Alabaster, AL) and 40 ng/mL VEGF and bFGF (GF). Collagen matrices (2.5 mg/mL) containing S1P were prepared as described previously, and invasion responses were quantified for invasion density and distance as previously described in detail [45].

Hic-5 Cloning

FLAG-tagged Hic-5 constructs were generated in the pFLAG-CMV2 vector (Sigma). HUVEC RNA was isolated using Qiagen's RNeasy MiniKit as per manufacturer's protocol. cDNA was generated with Invitrogen's SuperScript III First-Strand Synthesis System using 1 ug of RNA. A PCR reaction was performed using 3μl of cDNA template with AccuPrime Taq HIFI Polymerase (Invitrogen), 10 μM of forward and reverse primers in a 50 μl reaction volume (Table 1). The Hic-5 amplicons were cleaned with Qiagen's QIAquick PCR Purification Kit, digested with HindIII (NEB) and Xba1 (NEB) as was the pFLAG-CMV2 vector at 37°C overnight, gel purified with Qiagen's QIAquick Gel Extraction Kit, and ligated overnight at 14°C. For deletion constructs, a PCR reaction was performed using FLAG-FL-Hic-5 template with

AccuPrime Taq HIFI Polymerase (Invitrogen), 10 μM of forward and reverse primers containing a Pac1 (NEB) restriction site in a 50μl reaction volume (Table 1). PCR products were treated with 1 μL Dpn1 (NEB) for 1 h at 37°C, cleaned with Qiagen's QIAquick PCR Purification Kit, digested with Pac1, gel purified using Qiagen's QIAquick Gel Extraction Kit, and ligated overnight at 14°C. Positive clones were verified by sequencing before being transfected into 293 cells for binding studies.

Table 5. Primer sequences for Hic-5 cloning

Construct	**Primer sets**	**Restr. sites**
FLAG-FL-Hic-5	5'AGCAAAGCTTGAGGACCTGGATGCCCTG3' 5'AGCATCTAGATCAGCCGAAGAGCTTCAGG3'	HindIII Xba1
FLAG-N-Hic-5	5'AGCAAAGCTTGAGGACCTGGATGCCCTG3' 5'AGCATCTAGACCGGCGGCTGAGGTCGGAC3'	HindIII Xba1
FLAG-C-Hic-5	5'AGCAAAGCTTGGTGTTCCCACCCAGGCC3' 5'AGCATCTAGATCAGCCGAAGAGCTTCAGG3'	HindIII Xba1
FLAG-LIM1-2-3	5'AGCAAAGCTTGAGGACCTGGATGCCCTG3' 5'AGCATCTAGATCAGTGGAAGTGGTTCTCGCAC3'	HindIII Xba1
FLAG-LIM1-2	5'AGCAAAGCTTGAGGACCTGGATGCCCTG3' 5'AGCATCTAGATCAGAAGTCCCGGCGGCAGTAG3'	HindIII Xba1
FLAG-LIM1	5'AGCAAAGCTTGAGGACCTGGATGCCCTG3' 5'AGCATCTAGATCAAAAGTAGCACTCGGGGCAG3'	HindIII Xba1
FLAG-ΔLIM2	5'CGCTTCTCGCCAAGATTAATTAAGTGTGGCTTCTGCAAC3' 5'GGCGAACAGCTGCAGTTAATTAAGAAGTCCCGGCGGCAG3'	Pac1
FLAG-ΔLIM3	5'CTGTTCGCCCCGCGCTTAATTAAGTGCCAGGGCTGCCAG3' 5'CGAGCCGCGTCGTGCTTAATTAAGTGGAAGTGGTTCTC3'	Pac1

293 Cell Culture and Transfection

293 cells (Invitrogen), passages 3-12, were cultured in DMEM and 10% FBS. Transfection experiments were established by transfecting 0.4 μg of of each plasmid into $1x10^6$ cells using Lipofectamine 2000 (Invitrogen) in 6-well plates. Cells were cultured for 18 h prior to making extracts for immunoprecipitation experiments.

Generation of Stable Cell Lines using shRNA

Lentiviral vectors specific for Hic-5 (#SHCLNG-NM015927) and β2M (#SHCLNG-NM004048) were purchased from Sigma-Aldrich. Lentiviral particles were generated by transfecting 1.25 μg of backbone shRNA lentiviral plasmid with 3.75 μg of VIRAPOWER packaging mix (Invitrogen) into confluent 293 cells (Invitrogen) using Lipofectamine 2000 (Invitrogen) in T25 flasks. Viral supernatants were harvested at 60 h, centrifuged at 1000xg for 10 minutes and filtered through a 0.45 μm filter (Millipore, Rockland, MA). 25-30% confluent T25 flasks of HUVECs were infected with 2 mL viral supernatant, 3 mL endothelial growth medium, and polybrene (12 μg/mL; Sigma) for 5 h. HUVECs were cultured for four days prior to use in experiments.

Immunoblotting

Collagen matrices were solubilized in boiling 1.5X Laemmli sample buffer at 95°C for 5 min to prepare cell lysates. Protein samples were resolved using 8.5-14% SDS-PAGE, transferred onto Immobilon PVDF membranes (Millipore), blocked with 5% nonfat dry milk or 5% BSA, washed, and probed with primary antibodies overnight

at 4°C. Membranes were incubated with HRP conjugated secondary antibodies, washed, and developed with Immobilon Western Chemiluminescent HRP Substrate (Millipore) and HyBlot CL autoradiography film (Denville Scientific, South Plainfield, NJ). The antibodies used were directed to: Hic-5 (611164, BD Transduction Laboratories), MT1-MMP (MAB3328, Millipore), pFAK (ab4803, Abcam), FAK (05-537, Millipore), β2M (M8523, Sigma), actin (CP01, Calbiochem), α-tubulin (T6199, Sigma), GAPDH (ab8245, Abcam), GFP [64], Flag (ab18230, Abcam), integrin β1 (610467, BD Transduction Laboratories), integrin αV (611012, BD Transduction Laboratories), vinculin (V9131, Sigma), PECAM-1 (sc1505), and VE-cadherin (sc52751, Santa Cruz).

Immunoprecipitation

ECs ($3x10^6$ cells) cultured in T75 flasks were serum starved for 4 h and treated with 1 μM S1P for 30 min. Cells were placed on ice, washed twice with 10 mL cold PBS with cations (0.9 mM Mg^{2+} and Ca^{2+}), lysed in 700 μL cold lysis buffer (0.5% NP40 in PBS with cations, 1X protease inhibitor cocktail (Roche Diagnostics) and 100X HALT phosphatase inhibitor), and incubated for 10 min on ice with occasional mixing. Lysates were centrifuged at 16,000xg for 15 minutes at 4°C. Supernatants were collected and incubated with protein G-magnetic beads (5 μL) for 1 h at 4°C with agitation for preclearing. Supernatants were incubated with 2 μg antisera directed to MT1-MMP (ab38971, Abcam) or species- specific IgG control for 18 h at 4°C with agitation. Protein G-magnetic beads (10 μL) were added for 2 h at 4°C. Beads were washed 5 times with 1

mL lysis buffer without protease inhibitors, eluted in 1% SDS and analyzed by Western blotting. For IPs with 293 cells, $1x10^6$ cells, cultured in a 6 well plate, were washed twice with 1 mL cold PBS with cations, lysed in 700 mL cold lysis buffer (50 mM Tris-HCl, pH 7.5, 150 mM NaCl, 1% NP40, 0.5% sodium deoxycholate, 1X protease inhibitor cocktail (Roche Diagnostics) and 100X HALT phosphatase inhibitor), and incubated on ice for 20 min with mixing every 5 min. To test if Hic-5 enhanced MT1-MMP complex formation with FAK, pre-cleared 293 cell lysates co-transfected with MT1-MMP and FLAG-tagged Hic-5 constructs or GFP were allowed to mix with equal amounts of pre-cleared 293 cell lysate co-transfected with constitutively active FAK (CD2FAK, Addgene) for 2 h at 4°C with gentle agitation. Mixtures were incubated with 2 μg antisera directed to FAK (ab40794, Abcam) or species-specific IgG control for 18 h at 4°C with agitation. The remaining steps were performed as described above.

Immunofluorescence

ECs were seeded on collagen coated coverslips (50 μg/mL) and allowed to grow overnight. Cells were serum starved for 2 h, wounded with a pipette tip and washed twice with M199. Cells were treated for times indicated with 1 μM S1P or 40 ng/mL growth factors (or both), fixed in 4% paraformaldehyde, and rinsed three times in Tris-Glycine buffer (0.3% Tris, 1.5% Glycine), and permeabilized with 0.5% Triton X-100 (TX-100) for 20 minutes with gentle agitation before being blocked in buffer containing 0.5% TX-100, 1% BSA, and 1% serum overnight at 4°C. Primary antibodies were added in blocking buffer (1:100) for 3 h at room temperature, washed, and incubated with

Alexa-488- or 594-conjugated secondary antibodies (Molecular Probes, Grand Island, NY) (1:300) in blocking buffer for 1 h. After washing, coverslips were mounted and imaged using a Nikon TI A1R inverted confocal microscope. Primary antibodies used for staining were directed to Hic-5 (611164, BD Transduction Laboratories), pFAK (Tyr397, ab4803, Abcam), and VE-cadherin (sc9989, Santa Cruz). Antibodies recognizing phosphorylated MT1-MMP (Y397) and pre-immune serum were obtained from 21st Century Biochemicals, as previously described [54].

Isolation of Detergent Resistant Membrane (DRM) Fraction from ECs

ECs supplemented with 0 or 40 ng/mL GFs were seeded at a density of 30,000 cells/well on 2.5 mg/mL collagen matrices containing 0 or 1 μM S1P. At 6 h of invasion, collagen matrices were washed three times with 200 μL cold PBS with cations. Starting material was collected by solubilizing collagen matrices from each treatment group into boiling 1.5X sample buffer (50 μL/gel). 100 μL of CSK buffer (10 mM HEPES, 250 mM sucrose, 150 mM KCl, 3 mM $MgCl_2$, 1 mM EGTA, 1X protease inhibitor cocktail, 100X HALT phosphatase inhibitor) containing 0.05%, 0.1% or 0.5% TX-100 was added consecutively to each collagen matrix and allowed to incubate on ice for 10 min with continuous, gentle agitation. Soluble fractions were collected after each CSK wash, and after the last wash with 0.5% TX-100 CSK buffer, detergent resistant membrane fractions were collected by placing remaining material in 1.5X boiling sample buffer (30 μL/gel). Starting material, detergent soluble fractions, and detergent resistant membrane fractions were analyzed by Western blotting.

Isolation of Membrane Fraction from ECs by Subcellular Fractionation

On day four of lentiviral transfection, shβ2M and shHic-5 ECs cultured in 10 cm dishes were serum starved for 2 h prior to treatment with 0 or 1 μM S1P for 1 h. Cells were collected in 1.5 mL homogenization buffer (20 mM HEPES (pH 7.4), 1 mM EDTA, 250 mM sucrose, 20 mM NaCl, 1.5 mM $MgCl_2$, protease inhibitor cocktail (Roche), phenylmethylsulfonyl fluoride (2 mM), 1 mmol/L mercaptoethanol). Cells were disrupted by 10 strokes through a 25 gauge needle and homogenates were centrifuged at 1000xg for 5 min at 4°C to remove unbroken cells. Protein content of supernatants was determined by BCA assay (Thermo Scientific) to ensure equal amounts of starting material were centrifuged at 150,000xg for 30 min at 4°C. Cytoplasmic proteins in the supernatant were removed and membrane pellets were reconstituted in 600 μL 1.5X boiling sample buffer, and analyzed by western blotting.

Imaging and Quantification of Invasion Density, Distance, and Lumen Size

Top and side views of invading ECs were captured using an Olympus CKX41 microscope equipped with Q color 3 camera. Invasion densities were quantified by counting fixed cultures under transmitted light using an eyepiece equipped with a reticle displaying a 10x10 ocular grid. For each condition, at least three random fields were selected and the number of invading cells per field was counted manually. Data are reported as mean numbers of invading cells per field (±SD). Invasion length was measured using digital images taken from a side view of cultures at 10X magnification

using Image-Pro Analyzer 7.0. Data are reported as average invasion distance in micrometers (±SEM). Approximately 100 cells per treatment group were included in analyses. For quantification of lumen size, side view images of cultures at 20X magnification were analyzed using Image-Pro Analyzer 7.0. Data are reported as percentage of lumens formed in invading structures and average lumen diameter in micrometers (±SEM). At least 100 structures per treatment group were included in analyses.

Quantification of Hic-5 Positive Aggregates

The automated fuzzy thresholding algorithm [208, 209] created with MATLAB code was applied to 8-bit TIFF-format immunofluorescence image taken with confocal microscopy. This MATLAB algorithm consisted of steps for increasing dynamic range with intensity transformation, smoothing images with fuzzy transformation and was able to create binary image co-registered with focal adhesion based on histograms of smoothed images. The binary image highlighted with focal adhesion locations was further used to quantify number or size of focal adhesion per image.

RESULTS

Hic-5 was Required for S1P- and GF- Mediated Sprouting

Recombinant lentiviruses from two individual shRNA sequences targeted against Hic-5 (shHic-5-1 and -2) and and shRNA sequence specific to β2-microglobulin (shβ2M) were utilized to transduce ECs. To test the effect of Hic-5 depletion on S1P-

and GF- mediated invasion, non-transduced ECs (WT), or ECs transduced with recombinant lentiviruses directed against β2-microglobulin (shβ2M) or Hic-5 (shHic-5-1 and -2) were utilized in invasion experiments. Photographs of invading cultures illustrated that knockdown of Hic-5 interfered with EC invasion responses stimulated by S1P+GF (Fig. 15A). Western blot analyses of extracts collected from invading cultures showed selective knockdown of Hic-5 and β2M proteins by their respective shRNAs (Fig. 15B). Quantification of invasion density revealed a significantly decreased number of invading cells with Hic-5 silencing compared to shβ2M controls (Fig. 15C). In addition, the length of invading structures was significantly decreased with Hic-5 silencing compared to shβ2M controls (Fig. 15D). These results demonstrated that Hic-5 was required for S1P- and GF- stimulated EC invasion in 3D collagen matrices.

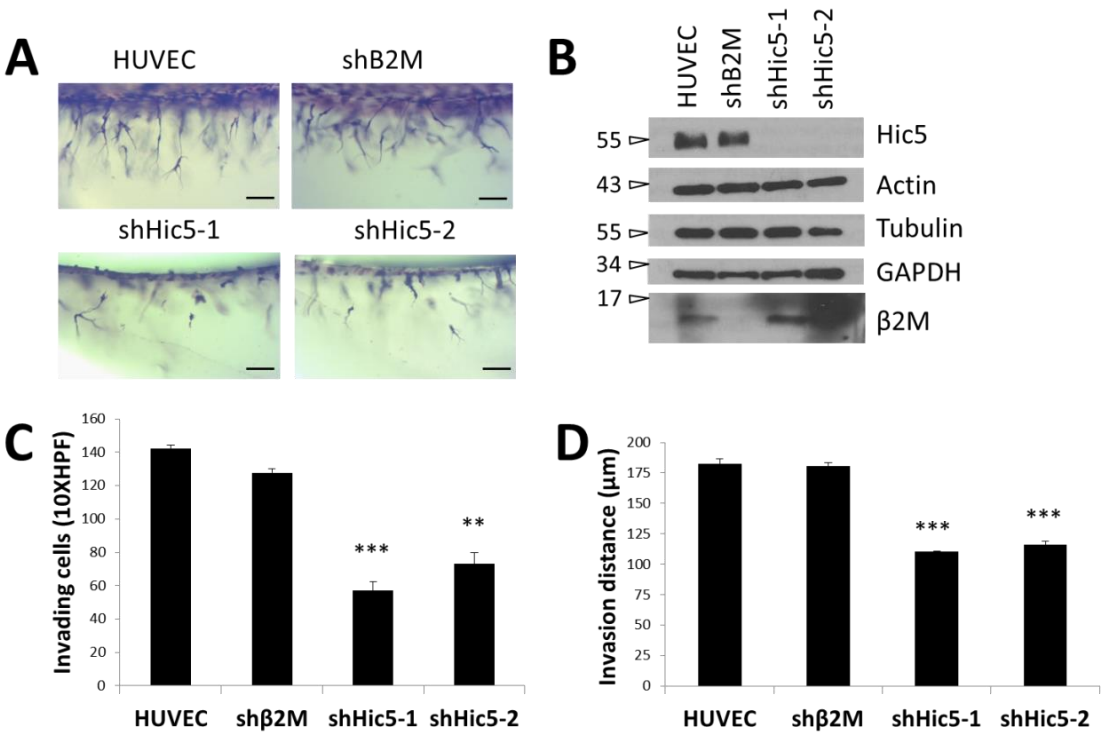

Figure 15. Hic-5 was required for S1P- and GF- mediated EC invasion. (A) Non-transduced ECs (WT), or ECs transduced with lentiviruses delivering shRNA directed to β2-microglobulin (shβ2M-1 and -2) or Hic-5 (shHic-5-1, and -2) were tested in 3D invasion assays using S1P+GF. Invasion cultures were fixed at 20h with 3% glutaraldehyde, stained with toluidine blue and photographed to illustrate side view of invasion responses. Scale bar=50 µm. **(B)** Cell lysates from treatment groups as in **(A)** were analyzed by Western blotting using Hic-5-, β2M-, GAPDH-, actin-, and tubulin-specific antisera to verify β2M and Hic-5 protein suppression. Quantification of **(C)** invasion density and **(D)** invasion distance at 20 h of invasion. Data in **(C)** represent average number of invading cells per 1 mm2 field ± SD (n=3 fields, Students t-test, ***p<0.001, **p<0.01, compared to shβ2M). Data in **(D)** represent average length of structures ±SEM (n>100 cells; Students t-test, ***p<0.001 compared to shβ2M). Representative experiment shown (n=4).

S1P Promoted Hic-5 Colocalization with FAK

Hic-5 silencing interfered with endothelial invasion responses that were stimulated by S1P and GFs. To determine the effect of either S1P or GF on Hic-5 localization, ECs seeded onto collagen-coated coverslips were serum starved and not treated (control) or treated with 1 μM S1P or 40 ng/mL GF (VEGF + bFGF) or both and stained with Hic-5 specific antisera. We observed that S1P treatment increased Hic-5 positive aggregates at the cell periphery (Fig. 16A). Quantification of size of Hic-5 positive structures revealed that S1P and S1P+GF treatment had significantly larger Hic-5 positive aggregates (Fig. 16B). To determine if S1P upregulated Hic-5 expression, whole cell lysates from ECs serum starved for 2 h were treated with 1 μM S1P for 0, 15, 30, or 60 min. Western blot analyses revealed that S1P treatment did not increase total levels of Hic-5 (Fig. 16C), demonstrating that S1P mediated a translocation but not upregulation of Hic-5. Since Hic-5 is described as a focal adhesion scaffold protein, and S1P is known to mediate translocation of focal proteins to adhesion sites, we further investigated if Hic-5 positive aggregates were focal adhesions. ECs seeded on collagen coated coverslips were serum starved, treated with S1P for the indicated times, and stained with Hic-5- and pFAK (Y397)-specific antisera (Fig. 17). Hic-5 (red) and pFAK (green) overlap indicated that S1P mediated Hic-5 translocation to focal adhesion sites. Taken together, these data suggested that Hic-5 localized to focal adhesion sites in response to S1P treatment.

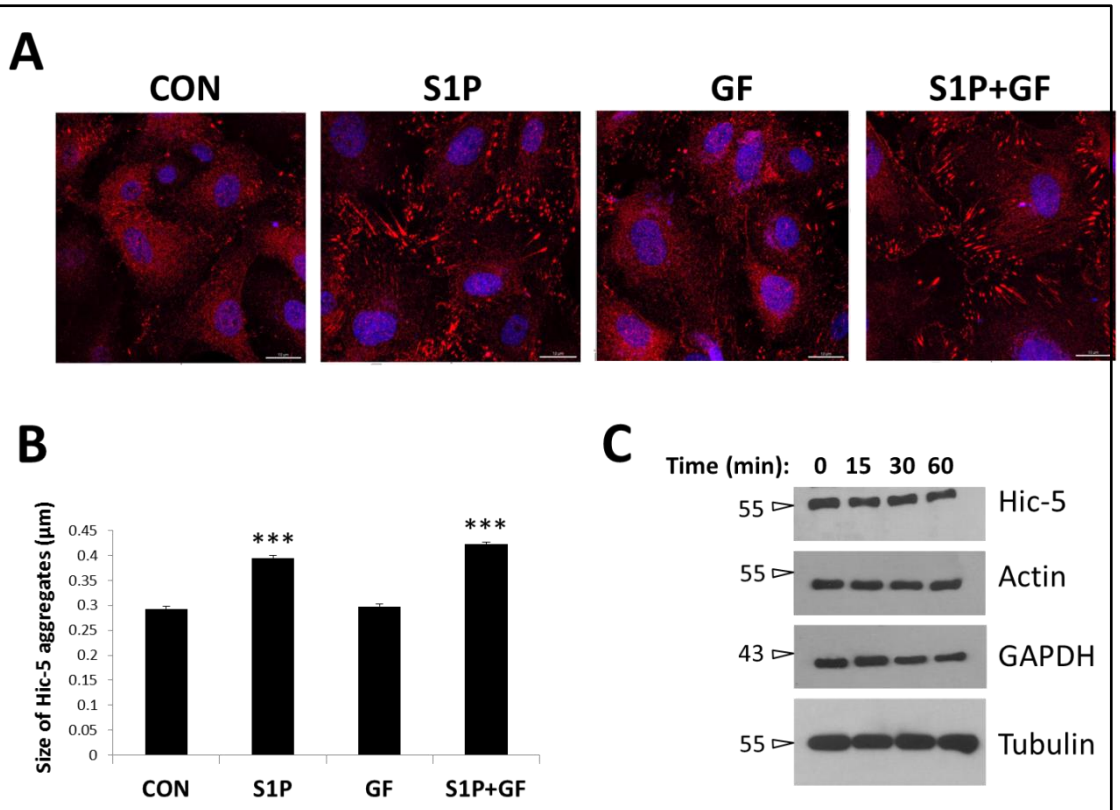

Figure 16. S1P altered Hic-5 localization in ECs. (A) ECs seeded on collagen (50 µg/mL) coated coverslips were serum starved for 2h and left untreated (CON) or treated with 1 µM S1P (S1P), or 40 ng/mL VEGF and bFGF (GF) or both (S1P+GF) for 1h. Following paraformaldehyde fixation, cells were stained with anti-Hic-5 detected with species-specific secondary antibodies conjugated to Alexa Fluor 594. Images were collected using Nikon A1 confocal laser microscopy. Scale bar=10 µm. **(B)** Quantification of average size (in microns) of Hic-5 positive aggregates as observed in **(A)** using MATLAB code created to quantify focal adhesion size. Data are representative of three independent experiments. (Students t-test, ***$p<0.001$, as compared to CON). **(C)** ECs seeded in 12-well plates were serum starved for 2h and treated with 1 µM S1P for indicated time prior to making whole cell lysates. Western blot analyses of cell lysates were performed using Hic-5-, actin-, GAPDH-, and tubulin- specific antisera.

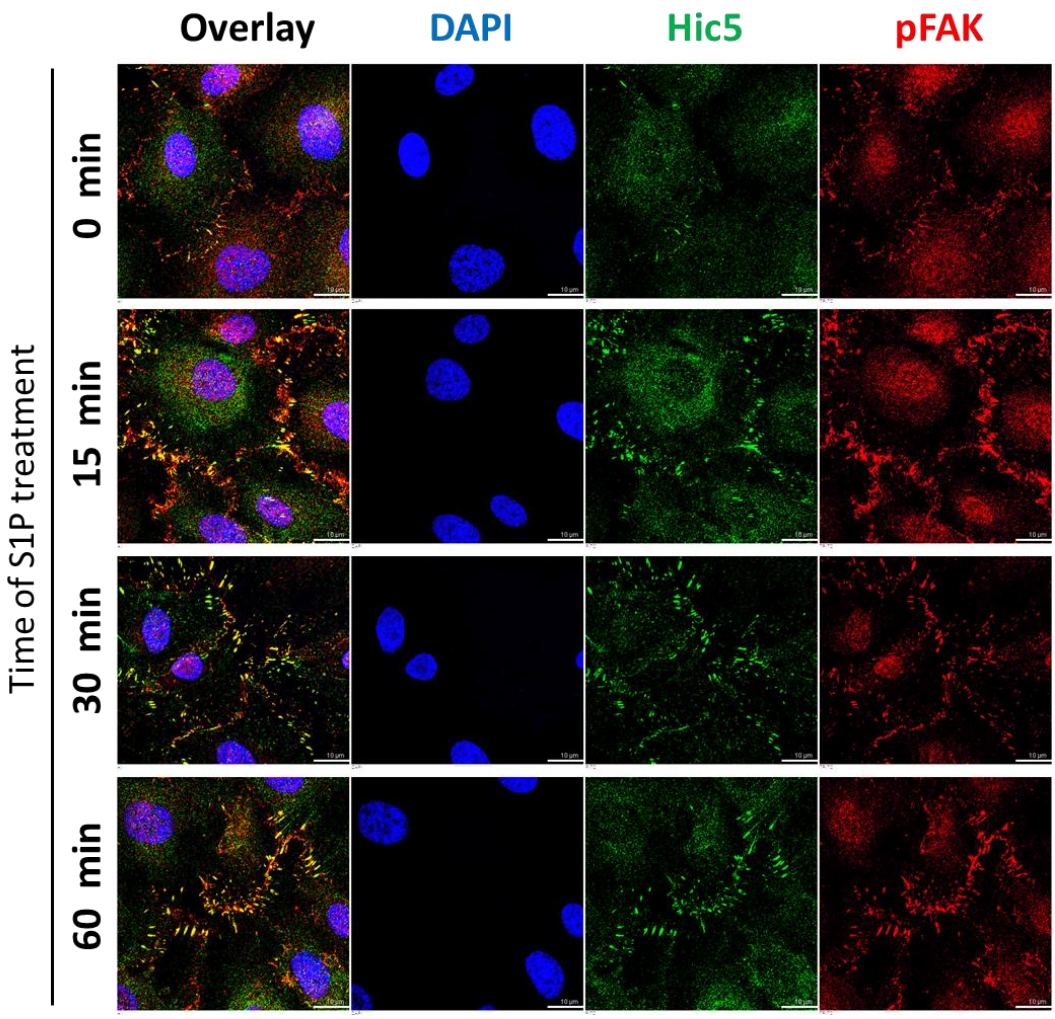

Figure 17. S1P promoted Hic-5 co-localization with pFAK. ECs seeded overnight on collagen coated coverslips were serum starved for 2h and treated with 1 μM S1P for indicated times. Cells were fixed in 4% paraformaldehyde, stained with anti-Hic-5 and anti-pFAK antibodies and detected with species-specific secondary antibodies conjugated to Alexa Fluor 488 and Alexa Fluor 594, respectively. Images were collected using confocal microscopy. Scale bar=10 μm.

Hic-5 Depletion Resulted in Attenuated FAK Expression and Activation

We and others have shown that FAK activation and expression is crucial for successful endothelial sprouting [139, 142, 210]. Recent studies in breast cancer cells demonstrate a requirement for Hic-5 during robust focal adhesion formation in 3D cell-derived matrix (CDM) [211]. To determine if Hic-5 regulated expression or activation of FAK in S1P- and GF-stimulated endothelial invasion, ECs transduced with recombinant lentiviruses expressing short hairpin RNAs directed against Hic-5 (shHic-5) or β2M (shβ2M) were allowed to invade collagen matrices. Whole cell extracts collected from invading cultures at 0, 0.5, and 1 h were analyzed by Western blotting. We observed a decrease in total and phosphorylated (Y397) FAK levels with Hic-5 knockdown compared to shβ2M controls (Fig. 18A). Quantification of Western blots revealed a significant decrease in the expression of phosphorylated (Y397) and total FAK at all time-points in shHic-5 versus shβ2M expressing ECs (Fig. 18B and 18C). These data suggested that Hic-5 was required for FAK expression and activation to direct successful endothelial sprouting.

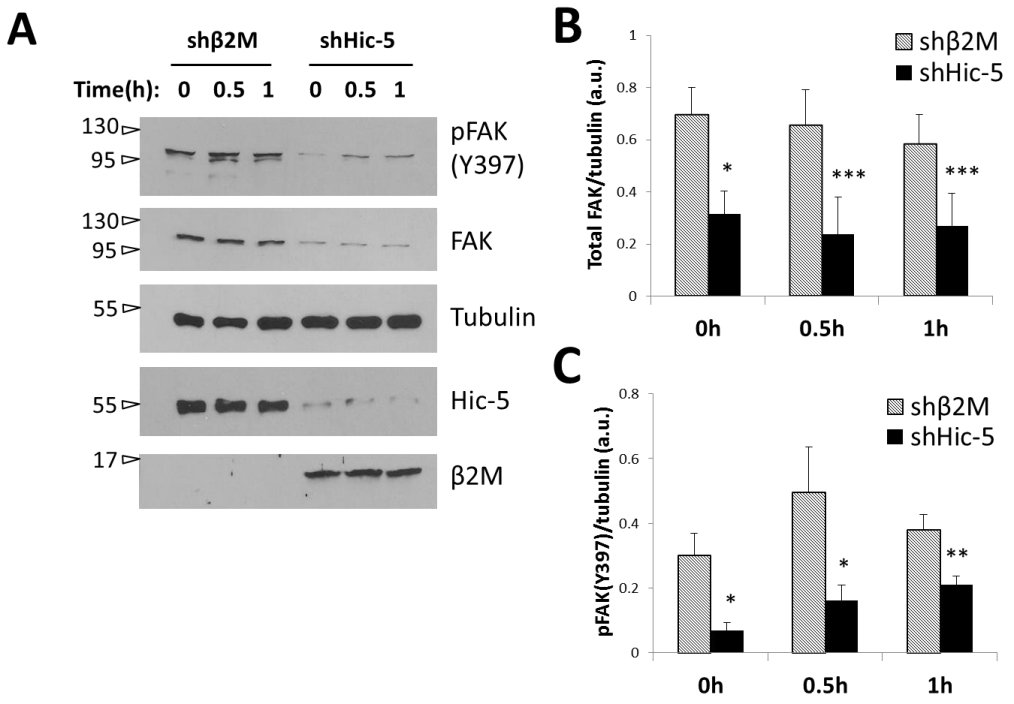

Figure 18. Hic-5 depletion decreased levels of pFAK and total FAK. (A) ECs were transduced with shRNA directed to β2M (shβ2M) and Hic-5 (shHic-5) and placed in invasion assays in the presence of S1P+GF. Whole cell lysates were prepared at the indicated time points. Western blot analyses were conducted using polyclonal antisera directed to phospho-FAK (Y397) and β2M, as well as monoclonal antisera directed to total FAK, tubulin, and Hic-5. **(B)** Quantification of FAK protein expression was performed using Image J software and normalized to tubulin. The results represent average values ± SD in arbitrary units (a.u.) from three independent experiments (Students t-test, ***$p<0.001$, * $p<0.05$, compared with shβ2M). **(C)** Quantification of pFAK protein expression using Image J software and normalized to tubulin. The results represent average values ± SD in arbitrary units (a.u.) from three independent experiments (Students t-test, **$p<0.01$, * $p<0.05$, as compared with shβ2M).

Hic-5 was Required for Successful Lumen Formation during Endothelial Sprouting

To test the effect of Hic-5 depletion on endothelial lumen formation, non-transduced or ECs transduced with recombinant lentiviruses directed against β2-microglobulin (shβ2M) or shHic-5-1 and -2 were utilized in S1P- and GF-mediated sprouting assay. Side view photographs of invading cultures illustrated that knockdown of Hic-5 resulted in smaller lumens compared to WT or shβ2M controls (Fig. 19A). Quantification of lumen size from three independent experiments revealed a significant decrease in lumen diameter with Hic-5 knockdown (Fig. 19B). Also, the number of invading cells forming lumens was lesser with Hic-5 silencing compared to WT and shβ2M controls (Fig. 19C). These results demonstrated that Hic-5 was required for successful lumen formation during endothelial morphogenesis in 3D collagen matrices.

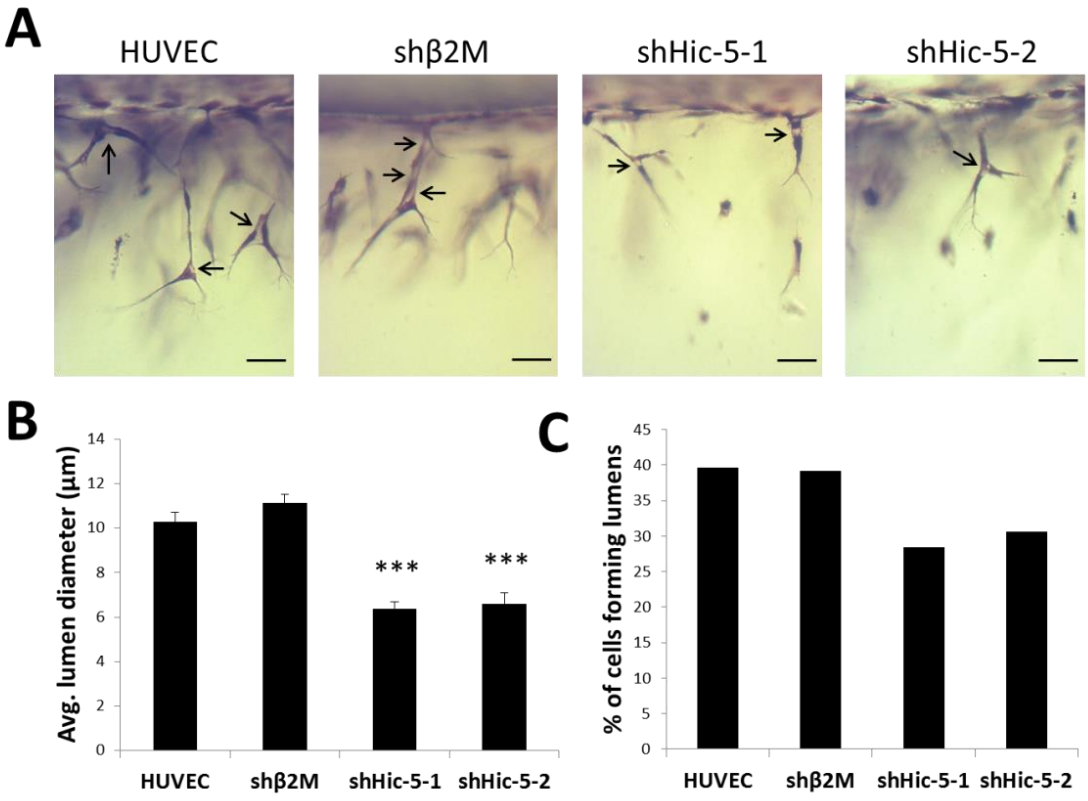

Figure 19. Hic-5 was required for successful lumen formation during endothelial sprouting. (A) Representative photographs of a side view of invading structures from non-transduced ECs (HUVEC) or ECs transduced with lentiviruses delivering shRNA directed to β2M (shβ2M) or Hic-5 (shHic-5-1, and -2). Black arrows indicate lumens. Quantification of **(B)** average lumen diameter (in microns) and **(C)** percentage of cells forming lumens from invading cultures in **(A)** (n>100 cells). Results are representative of three independent experiments. (Students t-test, ***p<0.001, as compared with shβ2M).

Hic-5 Complexed with MT1-MMP in an S1P- Dependent Manner in ECs

Endothelial lumenogenesis is a critical step needed for successful morphogenesis and assembly of ECs into new vessels [43]. Several studies have demonstrated that

proper MT1-MMP signaling is required for successful lumen formation during angiogenesis [26, 212, 213]. Our data suggested that Hic-5 silencing interfered with lumen formation during S1P- and GF-dependent sprouting responses. Moreover, both MT1-MMP [214, 215] and Hic-5 [185] are known to be enriched in invadopodia of migrating cells. Also, MT1-MMP is recruited to focal adhesion sites and regulated FA-type matrix degradation in tumor cells [205]. Therefore, we next asked whether Hic-5 co-localized with MT1-MMP in ECs. ECs seeded on collagen coated coverslips were serum starved for 2h, treated with nothing (CON), 1 μM S1P (S1P), 40 ng/mL GF (GF) or S1P and GF (S1P+GF) for 1h and stained with Hic-5 (red) or pMT1-MMP (Y573, green). Overlay photographs indicated successful colocalization between Hic-5 and pMT1-MMP in ECs treated with S1P or S1P+GF (Fig 20). These data suggested enhanced interactions between Hic-5 and MT1-MMP may occur with S1P treatment. To confirm this, ECs were treated with 0 or 1 μM S1P for 30 min, and lysates were immunoprecipitated using MT1-MMP- or species-specific IgG antisera. While equal amounts of MT1-MMP were immunoprecipitated in both treatment groups (Fig 21A), we observed an increase in complex formation between Hic-5 and MT1-MMP with S1P stimulation. Quantification of western blots from three independent experiments revealed that S1P treatment significantly increased Hic-5 and MT1-MMP complex formation (Fig 21B). Taken together, these data revealed a novel complex formation between focal adhesion scaffold protein Hic-5 and MT1-MMP formed following S1P stimulation in ECs.

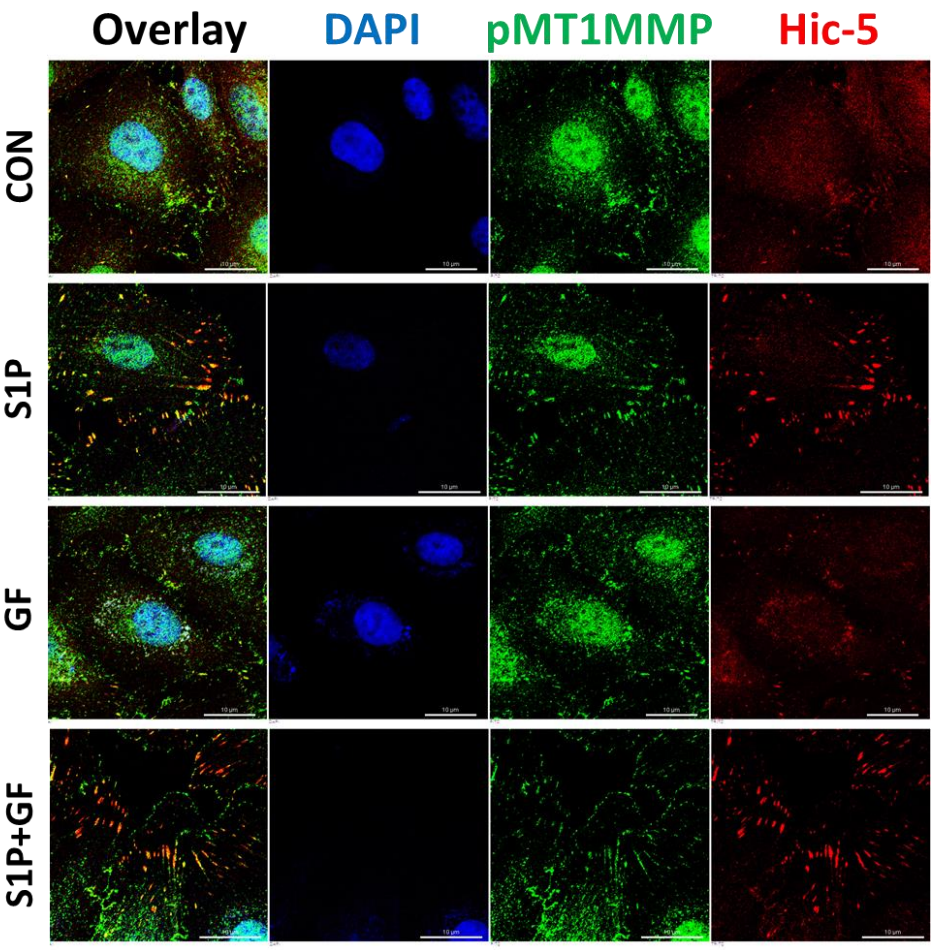

Figure 20. Hic-5 co-localized with activated MT1-MMP in an S1P- dependent manner. ECs seeded on collagen coated coverslips were serum starved for 2h and left untreated (CON) or treated with 1 μM S1P (S1P), or 40 ng/mL VEGF and bFGF (GF) or both (S1P+GF) for 1h. Cells were fixed in 4% paraformaldehyde, stained with anti-Hic-5 and anti-pMT1-MMP and detected with species-specific secondary antibodies. Images were collected using confocal microscopy. Scale bar=10 μm.

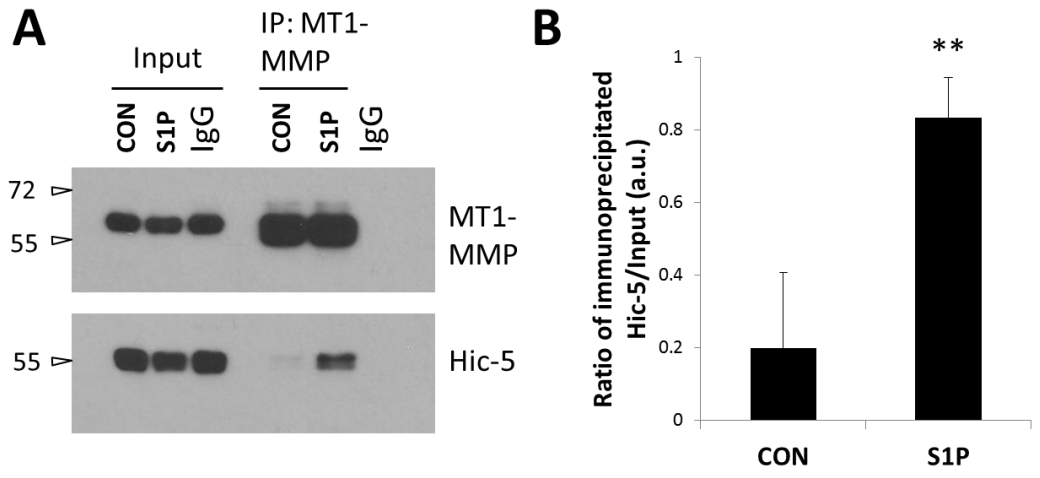

Figure 21. Hic-5 complexed with MT1-MMP in an S1P- dependent manner. (A) ECs cultured in T75 flasks for 3 days were stimulated with nothing (CON) or 1 μM S1P (S1P) for 1 h. Immunoprecipitations were performed using polyclonal MT1-MMP antibody or isotype control (IgG). Eluates were probed with MT1-MMP- and Hic-5- specific antisera using Western blotting. **(B)** Quantification of co-precipitated Hic-5 normalized to starting material from Western blots using Image J software. The results represent average values ± SD in arbitrary units (a.u.) from three independent experiments (Student's t-test, **$p<0.01$, compared to CON).

LIM2 Domain of Hic-5 was Required for Binding to MT1-MMP

Based on the above data that Hic-5 complexed with MT1-MMP in ECs, we next determined MT1-MMP binding site on Hic-5 with various Hic-5 mutant proteins outlined in Table 6. Initially, full-length (FL) His-tagged MT1-MMP was co-transfected with FL FLAG-tagged Hic-5, N-terminal FLAG-tagged Hic-5, C-terminal FLAG-tagged Hic-5, or GFP in 293 cells (Fig. 22A). Immunoprecipitation experiments were performed by incubating lysates with MT1-MMP- or species-specific IgG antisera.

Western blot analyses revealed successful expression of MT1-MMP, GFP, and Hic-5 constructs in the starting material. Moreover, we observed successful MT1-MMP complex formation with FL Hic-5 and C-terminal Hic-5 constructs, but not with N-terminal Hic-5 (Fig. 22A). These data suggested that one or more LIM domains at the C-terminus of Hic-5 may be involved in MT1-MMP binding. To identify the specific domain(s) involved in MT1-MMP binding, additional FLAG-tagged truncation and deletion constructs of Hic-5 were generated (see Table 6). FL His-tagged MT1-MMP was co-transfected with FL Hic-5, LIM1-2-3, LIM1-2, LIM1, ΔLIM2, or ΔLIM3 in 293 cells (Fig. 22B). Western blot analyses revealed no complex formation with LIM1 or ΔLIM2 constructs and MT1-MMP. However, successful MT1-MMP association was observed with FL Hic-5, LIM1-2-3, LIM1-2, and ΔLIM3 constructs (Fig. 22B). These data indicated that the LIM2 domain within the C-terminus of Hic-5 was essential for MT1-MMP binding.

Table 6. Summary of MT1-MMP and Hic-5 binding studies

FLAG-Hic-5 constructs		Binding to His-MT1-MMP
FL Hic-5	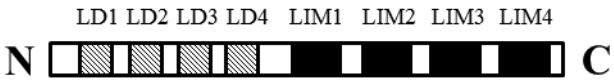	+++
N-Hic-5		-
C-Hic-5		+++
LIM1-2-3		+++
LIM1-2		+
LIM1		-
ΔLIM2		-
ΔLIM3		+

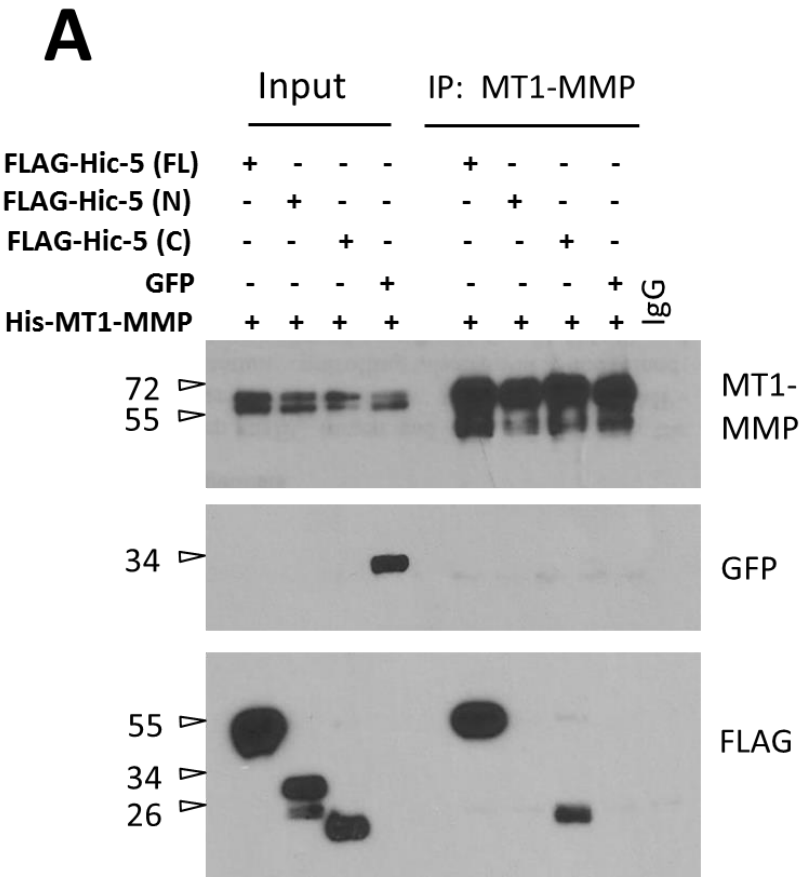

Figure 22. The LIM2 domain of Hic-5 was required for MT1-MMP binding. **(A)** 293 cells were co-transfected with His-MT1-MMP and GFP or FLAG-tagged FL-Hic-5 (full-length), N-Hic-5 (N-terminal) or C-Hic-5 (C-terminal) constructs. Immunoprecipitation experiments were performed using polyclonal MT1-MMP antibody or isotype control (IgG). Eluates were probed with MT1-MMP-, GFP- and FLAG- specific antisera using Western blotting. **(B)** 293 cells were co-transfected with His-MT1-MMP and FLAG-tagged FL-Hic-5 (full-length), LIM1-2-3, LIM1-2, LIM1, ΔLIM2, and ΔLIM3 constructs. Immunoprecipitation experiments were performed using polyclonal MT1-MMP antibody or isotype control (IgG). Eluates were probed with MT1-MMP- and FLAG- specific antisera using Western blotting.

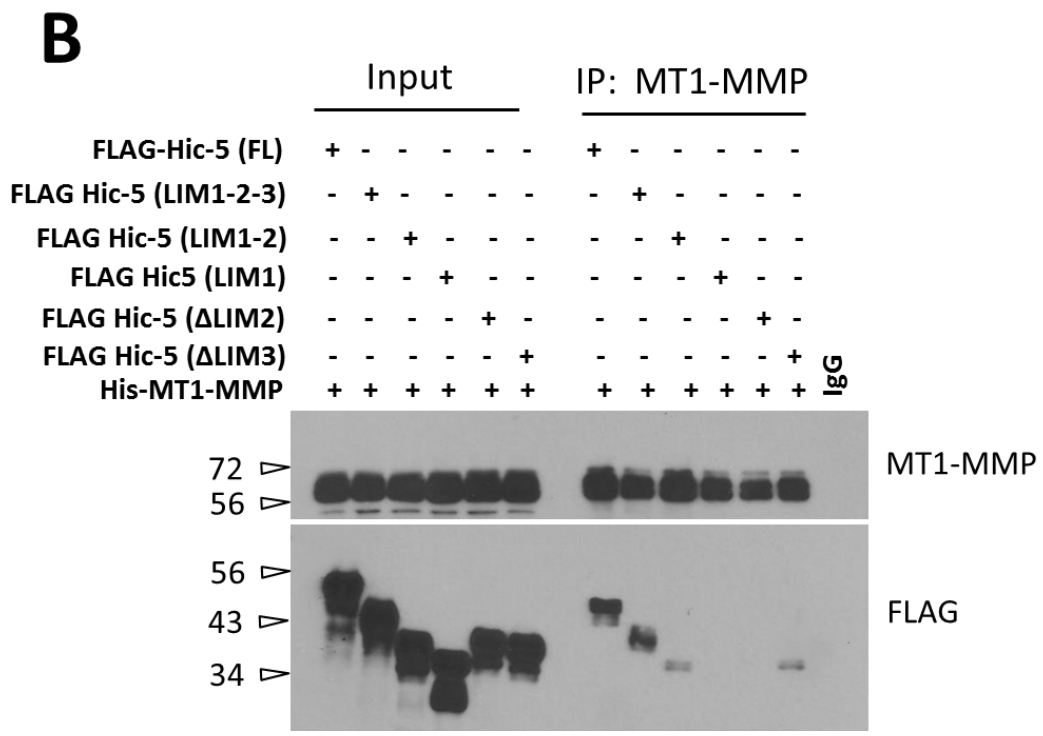

Figure 22. Continued

MT1-MMP and Hic-5 Were More Resistant to Detergent Extraction during Endothelial Invasion

To determine whether MT1-MMP, Hic-5, and FAK complex assembly was altered in non-invading versus invading cells, invading cultures were not treated (CON) or stimulated with 1 μM S1P and 40 ng/mL GFs (S1P+GF), respectively. Extracts were made at 6 h by washing collagen matrices with increasing concentrations of TX-100 (0.05%, 0.1% and 0.5%) and remaining material was collected, solubilized, and designated as detergent resistant membrane (DRM) extracts. In agreement with previous

reports [216, 217], we observed successful upregulation of MT1-MMP in DRM extracts in invading ECs stimulated with S1P and GF (Fig. 23A), and we also observed an increase in the levels of Hic-5 in DRM extracts collected from sprouting ECs that followed the MT1-MMP pattern. Interestingly, FAK levels in DRM extracts were not significantly elevated by S1P and GF treatment. The β1 integrin and αV integrin subunits were also upregulated in DRM fractions of invading ECs, while levels of vinculin and actin and remained unchanged. GAPDH was not detected in DRMs supporting successful isolation of DRM fractions (Fig. 23A). Quantification of MT1-MMP, FAK, and Hic-5 levels in DRMs from three independent experiments revealed a significant increase of MT1-MMP and Hic-5 levels, but not FAK, in DRM extracts in invading versus non-invading cells (Fig. 23B). Overall, these data indicate that the MT1-MMP and Hic-5 complex is more resistant to detergent extraction in invading cells suggesting the formation of this complex within the membrane facilitates EC sprouting responses in 3D collagen matrices.

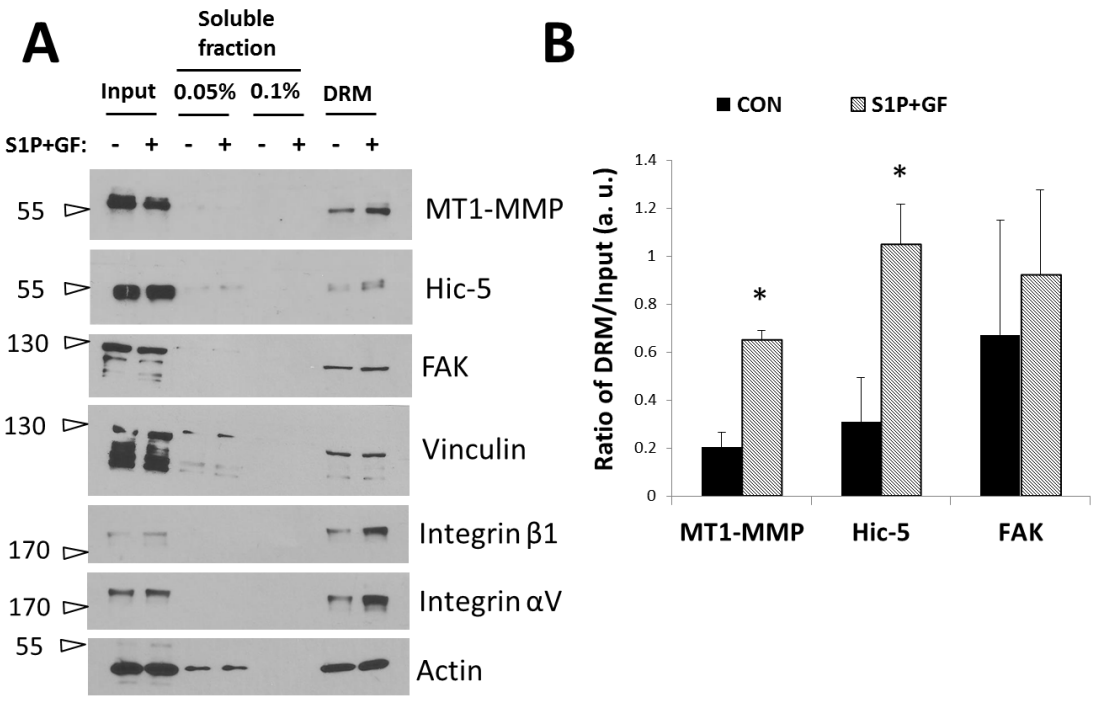

Figure 23. Hic-5 and MT1-MMP were more resistant to detergent extraction during endothelial invasion. (A) Detergent resistant membrane (DRM) extracts were isolated from invasion cultures without (CON) or with (S1P+GF) 1 μM S1P and 40 ng/mL GFs. Starting material lysates, soluble lysates (obtained with 0.05% and 0.1% TX-100 treatment) and DRM extracts and were analyzed by western blotting and probed with FAK-, MT1-MMP-, Hic-5-, vinculin-, integrin β1-, integrin αV-, actin-, and GAPDH- specific antisera. Quantification of **(B)** MT1-MMP, Hic-5, and FAK levels in DRM normalized to starting material from Western blots using Image J software. The results represent average values ± SD in arbitrary units (a.u.) from three independent experiments (Student's t-test, *$p<0.05$, compared to CON).

Hic-5 Silencing Interfered with MT1-MMP Membrane Translocation

The data shown above demonstrate Hic-5 was required for sprouting and formed a complex with MT1-MMP that was enhanced by S1P and more resistant to detergent

extraction. S1P has been shown to stimulate MT1-MMP membrane translocation during angiogenesis [66, 218]. To test whether Hic-5 was needed for membrane localization of activated MT1-MMP, ECs expressing shRNA directed to β2M (shβ2M) and Hic-5 (shHic-5) were seeded on collagen coated coverslips, serum starved, and treated with S1P. Coverslips were stained with VE-cadherin- and pMT1-MMP (Y573)-specific antisera. We observed successful membrane translocation of pMT1-MMP in shβ2M control at 60 min of S1P stimulation. However, Hic-5 silencing reduced co-localization of MT1-MMP with VE-Cadherin (Fig. 24A and 24B). Endothelial junctions visualized by VE-cadherin staining were unaffected with Hic-5 knockdown. Quantification of colocalization between VE-cadherin and pMT1-MMP revealed a significant decrease in overlap with Hic-5 silencing at 60 min of S1P stimulation (Fig. 24C). To confirm these observations, membrane fractions were isolated from shβ2M and shHic-5 cells treated with 0 or 60 min of S1P. Analysis of membrane extracts by western blotting revealed an upregulation of MT1-MMP levels in shβ2M control with S1P treatment but not in the shHic-5 group (Fig. 12A). As observed previously (Fig. 18), FAK levels were reduced with Hic-5 silencing. Also, cytoplasmic proteins like actin, tubulin, and GAPDH were not detected in membrane fractions, but PECAM-1 and VE-Cadherin were present, supporting successful membrane isolation (Fig. 25A). Quantification of MT1-MMP levels in membrane fractions from three independent experiments with 60 min S1P treatment revealed a significant decrease in MT1-MMP levels with Hic-5 depletion (Fig. 25B). Taken together, these studies suggest that Hic-5 may facilitate MT1-MMP

translocation to the cell surface where MT1-MMP is needed for successful sprouting responses in ECs.

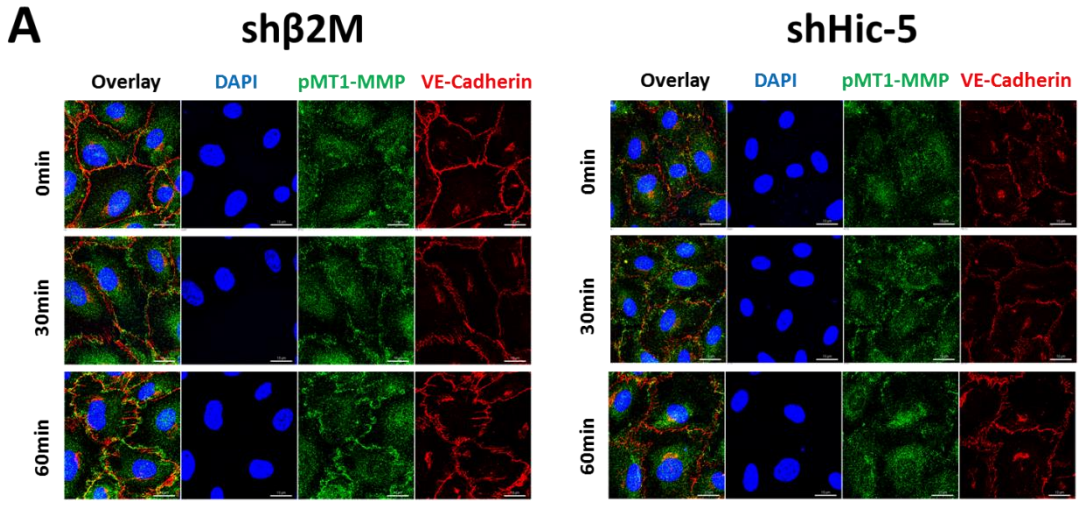

Figure 24. Hic-5 silencing attenuated pMT1-MMP membrane translocation. **(A)** ECs transduced with shRNA directed to β2M (shβ2M) or Hic-5 (shHic-5) were seeded on collagen coated coverslips, serum starved for 2h and treated with 1 μM S1P for the indicated times. After paraformaldehyde fixation, shβ2M and shHic-5 cells were stained with anti-Hic-5 and anti-pMT1-MMP antibodies and detected with species-specific secondary antibodies conjugated to Alexa Fluor 488 and Alexa Fluor 594. Images were collected using confocal microscopy. Scale bar=10 μm. **(B)** 2X magnified images at 60min S1P treatment in shβ2M and shHic-5 groups from **(A)**. **(C)** Quantification of Hic-5 (green) and VE-cadherin (red) co-localization using Pearson's correlation coefficient. The results represent average values ± SD from each treatment group (n>10 fields) for a representative experiment (n=4) (Student's t-test, ***p<0.001, compared to shβ2M).

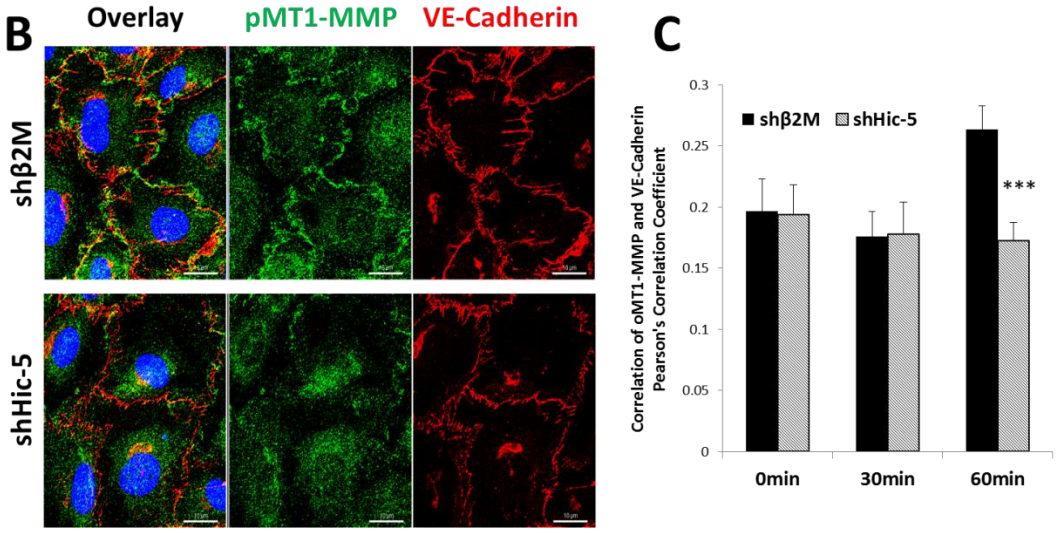

Figure 24. Continued

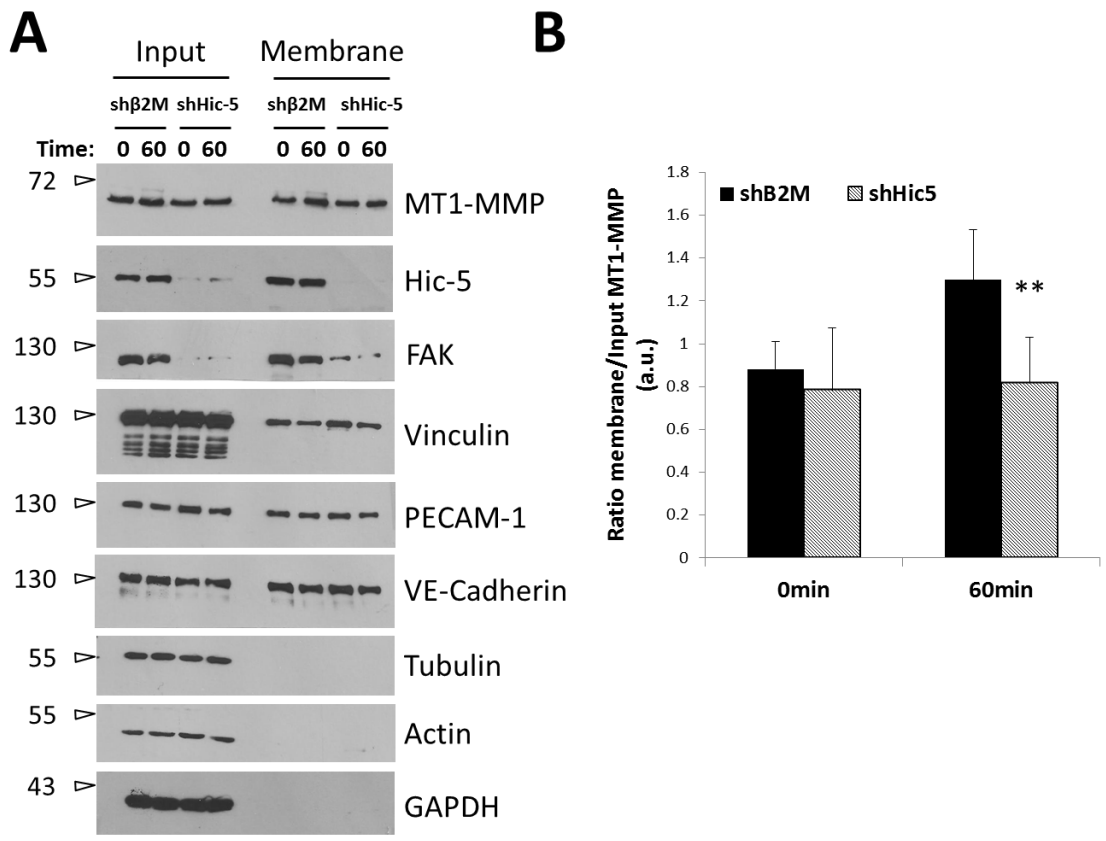

Figure 25. Hic-5 depletion resulted in decreased levels of MT1-MMP at the endothelial membrane following S1P treatment. (A) Membrane fractions were isolated from ECs transduced with shRNA directed to β2M (shβ2M) or Hic-5 (shHic-5), serum starved for 2h and treated with 0 or 1μM S1P for 1h. Membrane fractions and starting materials were analyzed by western blotting and probed with MT1-MMP-, Hic-5-, FAK-, vinculin-, PECAM-1-, VE-cadherin-, tubulin-, actin-, and GAPDH- specific antisera. **(B)** Quantification of MT1-MMP in membrane fraction normalized to starting material from Western blots using Image J software. The results represent average values ± SD in arbitrary units (a.u.) from three independent experiments (Student's t-test, **$p<0.01$, compared to shβ2M).

Hic-5 Enhanced Complex Formation Between FAK and MT1-MMP

McNiven and colleagues have reported that that complex formation between FAK and MT1-MMP is crucial for matrix degradation at focal adhesion sites [205]. Like other paxillin family members, Hic-5 mediates multiple protein-protein interactions at adhesion sites via its LD and LIM domains [219, 220]. Our data clearly suggests a complex forms between MT1-MMP and Hic-5 in ECs. Also, MT1-MMP and Hic-5 levels increased in DRMs of invading ECs. Therefore, we further investigated whether Hic-5 mediated MT1-MMP and FAK binding. To address this question, we combined cell lysates expressing constitutively active FAK with separate lysates containing FL His-tagged MT1-MMP co-transfected GFP, FL FLAG-tagged Hic-5, or ΔLIM2. Immunoprecipitations were performed with FAK-specific antisera and eluates were probed for MT1-MMP, Hic-5, and FAK using Western blot analyses. We observed robust complex formation between MT1-MMP and FAK in the presence of FL Hic-5 compared to GFP or ΔLIM2 (Fig. 26A). Equivalent amounts of FAK were immunoprecipitated in all conditions (Fig 26A). Interestingly, we observed a weak association of ΔLIM2 and FAK as compared to FL Hic-5 (Fig. 26A), which agreed with a previous report which showed that although Hic-5 interacted with FAK via its N-terminal LD domains, the C-terminal LIM domains were required for targeting Hic-5 to focal adhesion sites [174]. Quantification of western blots from three independent experiments revealed that the presence of FL Hic-5 significantly increased MT1-MMP complex formation with FAK compared to GFP and ΔLIM2 controls (Fig. 26B). In

conclusion, these results suggested that Hic-5 enhanced complex formation between MT1-MMP and FAK.

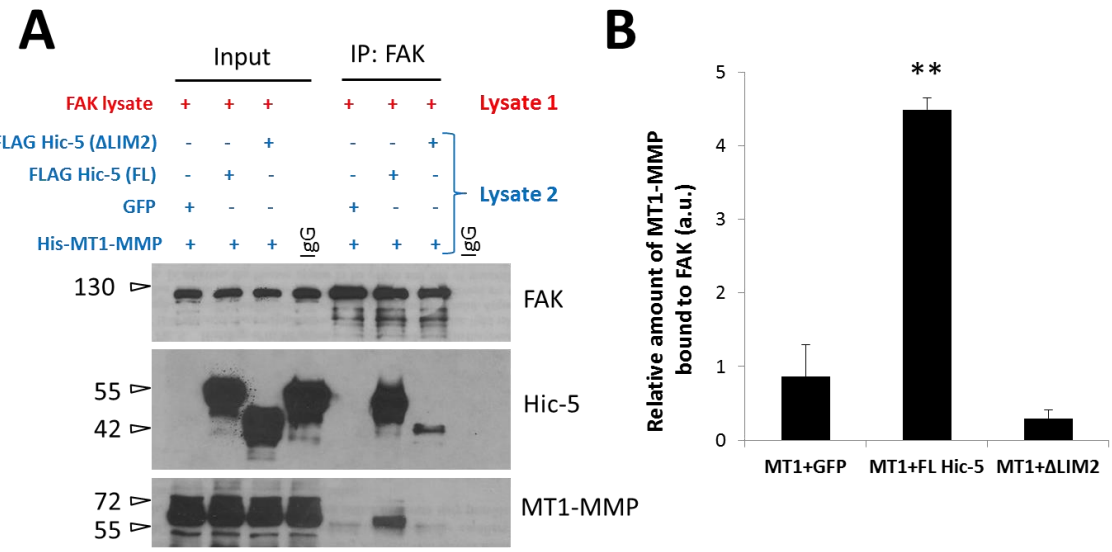

Figure 26. Hic-5 mediated complex formation between FAK and MT1-MMP. **(A)** 293 cells were co-transfected with His-MT1-MMP and GFP, FL-Hic-5, or ΔLIM2 constructs in 6 well plates (Lysate 2). Constitutively active FAK (CD2FAK) was overexpressed separately in 293 cells (Lysate 1). 700 uL lysates were prepared from each well for all treatment groups. Equal amounts of lysate 1 and lysate 2 were allowed to mix for 2h at 4°C before immunoprecipitating with 1 µg monoclonal FAK antibody or isotype control (IgG) antibodies. Eluates were probed with FAK-, Hic-5- and MT1-MMP- specific antisera using western blotting. **(B)** Quantification of co-precipitated MT1-MMP normalized to starting material from Western blots using Image J software. The results represent average values ± SD in arbitrary units (a.u.) from three independent experiments (Student's t-test, **p<0.01, compared to MT1+GFP and MT1+ΔLIM2 controls).

DISCUSSION

We have investigated and report a new regulatory role of the focal adhesion scaffold protein Hic-5 during sprouting angiogenesis in 3D collagen matrices. Our results suggested that Hic-5 regulated endothelial sprouting reponses by (i) regulating FAK expression and activation, (ii) associating with MT1-MMP, (iii) regulating MT1-MMP membrane translocation, and (iv) mediating FAK and MT1-MMP interactions.

Our results are the first to demonstrate a complex formation between Hic-5 and MT1-MMP during endothelial sprouting. Hic-5 was discovered as a cDNA clone induced by TGFβ stimulation [171]. Further studies described Hic-5 as a focal adhesion scaffold protein based on a lack of enzymatic activity, homology to paxillin, localization at FA sites, and interaction with FA proteins [220]. Like other LIM proteins, Hic-5 was found to translocate into the nucleus and regulate gene expression upon oxidative stress [181, 221]. Hic-5 acts as a transcriptional co-activator for glucocorticoid receptor [65, 66], endogeneous c-Fos [37], specificity protein 1 (Sp1) [38], and Peroxisome proliferator-activated receptor γ (PPARγ) [67]. Hic-5 has also been reported to act as repressor for lymphoid enhancer-binding factor and transcriptional factor (LEF/TCF) driven transcription [68]. Evidence from cancer cells suggests that Hic-5 may be important during cell migration [186, 211, 222]. However, the molecular mechanisms that define the function of Hic-5 in regulating cell migration and focal adhesion assembly are not fully understood. Also, a role for Hic-5 during angiogenesis and endothelial sprouting remains unexplored. We show here for the first time a requirement

for Hic-5 during endothelial sprouting and lumen formation in 3D matrices. Our data demonstrate that S1P stimulation increased Hic-5 complex formation with MT1-MMP during EC sprouting. MT1-MMP is a major membrane bound metalloprotease that is involved in enzymatic breakdown of surrounding ECM proteins to facilitate cell invasion in 3D matrices [191, 192]. Several studies have demonstrated a requirement for MT1-MMP in directing successful endothelial sprouting and lumen formation as well as cancer cell invasion [193, 196, 223]. Previous work from our laboratory indicated that proper membrane translocation of MT1-MMP, occurred when soluble vimentin was liberated in activated ECs, facilitating successful endothelial sprout formation [66]. We find here that Hic-5 regulated EC invasion through a unique pathway involving MT1-MMP and FAK.

FAK is a major focal kinase protein that plays a key role in cell migration and endothelial morphogenesis [136, 224]. Numerous studies have reported that FAK is essential for embryogenesis, cardiovascular development, EC survival, endothelial morphogenesis and angiogenesis [139-142, 198, 199]. In agreement with these data, we have previously observed that blocking FAK activation completely inhibited sprouting in ECs [210]. Recent studies by Deakin and Turner suggest that Hic-5 depletion in tumor cells significantly hampered focal adhesion formation in 3D ECM and decreased FAK phosphorylation [211]. In this study, we find that Hic-5 silencing attenuated FAK phosphorylation (Y397) and expression in ECs. These results help explain, in part, the requirement of Hic-5 for successful endothelial sprouting.

S1P is a bioactive sphingolipid that increases EC proliferation, barrier enhancement, and stimulates endothelial sprouting [59-62]. Others have reported that S1P directed rapid translocation of FA to proteins FA sites [65]. In agreement with these data, we observed rapid translocation of Hic-5 to FA sites as well as EC junctions. Interestingly, S1P is also known to activate MT1-MMP and mediate its membrane translocation [225]. Studies by Pignatelli *et al*., have demonstrated in tumor cells that Hic-5 was required for successful matrix degradation [186]. Our results indicated that Hic-5 knockdown interfered with lumen formation in endothelial sprouts, which is MT1-MMP dependent. Wang and McNiven have reported that FAs are potential sites for MT1-MMP dependent invasive matrix degradation [205]. Our immunofluorescence data revealed that S1P induced co-localization between these proteins at punctate FA sites at the endothelial cell periphery. Immunoprecipitation studies confirmed an up-regulation of Hic-5 and MT1-MMP complex formation with S1P stimulation. Moreover, we also observed that MT1-MMP and Hic-5 levels were enhanced in DRM fractions of invading ECs, indicative of their interplay during endothelial sprouting in response to S1P and pro-angiogenic GFs. Our results are the first to report an S1P- dependent complex formation between Hic-5 and MT1-MMP in ECs.

Both LD and LIM domains in Hic-5 participate actively in protein binding [175]. To further investigate the MT1-MMP binding domain in Hic-5, we used *in vitro* binding studies. Our results indicated that the LIM2 domain of Hic-5 was required in binding with MT1-MMP. Interestingly, we also observed weak MT1-MMP association with

LIM3 deletion, suggesting that LIM3 was not required but enhanced MT1-MMP binding to Hic-5. LIM3 has been implicated in successful targeting of Hic-5 to FA sites [174] and Hic-5 constructs bearing mutations in the LIM3 site (C369A/C372A) fail to localize to FAs upon LPA stimulation [185]. Thus, we speculate that successful targeting of Hic-5 to FAs improves interaction with MT1-MMP. To determine the role of Hic-5 in MT1-MMP signaling, we looked at levels of MT1-MMP at the endothelial membrane following S1P stimulation. Our results indicated that Hic-5 depletion significantly attenuated S1P- mediated MT1-MMP membrane translocation. These results suggested that Hic-5 acted as a molecular adaptor in transporting MT1-MMP to plasma membrane for successful sprouting responses.

Several reports have implicated the importance of MT1-MMP and FAK crosstalk during cell migration [204, 206, 207]. Studies by Wang and McNiven have demonstrated that the interaction between MT1-MMP and FAK is essential for mediating matrix degradation at FA sites [205]. Their results indicate p130Cas mediates MT1-MMP and FAK interactions [205]. Moreover, S1P is known to stimulate binding between MT1-MMP and p130Cas in ECs [218]. Since Hic-5 is a scaffold protein known to mediate protein interactions at FAs, we investigated whether Hic-5 regulated MT1-MMP and FAK interactions. Our data from *in vitro* binding studies indicated that the presence of full-length Hic-5 enhanced MT1-MMP and FAK interactions by more than 4-fold. These results indicate that Hic-5 acted as a scaffold to enhance interaction between MT1-MMP and FAK.

In summary, our findings reveal novel functions of Hic-5 in mediating endothelial sprouting. Following S1P stimulation, Hic-5 is translocated to FAs and complexes with MT1-MMP; which is required for optimal interactions between MT1-MMP [226, 227] and FAK [228, 229] to mediate matrix degradation at FA sites. In addition, our results demonstrate that Hic-5 is also required for FAK activation and expression as well as MT1-MMP membrane translocation [186, 211]. Several reports have implicated a role for MT1-MMP and FAK during tumor progression and invasion in 3D ECM. Recent studies have determined a role for Hic-5 in tumor cell attachment, matrix degradation, migration and invasion. Our results provide new information on the interplay of these molecules and may be relevant in regulating metastatic behavior of cancer cells.

CHAPTER IV

CONCLUSIONS AND FUTURE DIRECTIONS

In conclusion, we have demonstrated that both RACK1 and Hic-5, scaffold proteins known to be associated with focal adhesions, are required for S1P- and GF-induced sprouting angiogenesis. RACK1 is up-regulated along with vimentin, in sprouting versus quiescent ECs. Moreover, RACK1 and vimentin, both complex together in GF- dependent manner and regulate FAK in ECs. Silencing of either RACK1 or vimentin attenuated cell attachment and disturbed focal adhesion distribution. RACK1, vimentin, and FAK formed a complex during endothelial sprout formation in 3D collagen matrices. RACK1, vimentin and FAK activation were required for successful endothelial sprouting. Also RACK1 silencing decreased complex formation between vimentin and FAK. These data added new insights into the role of RACK1 during angiogenesis.

Like RACK1 and vimentin, we observed that focal adhesion scaffold protein Hic-5 also regulated FAK expression and activation. S1P induced Hic-5 translocation at adhesion sites in ECs. Moreover, Hic-5 silencing decreased endothelial sprouting and lumen formation in S1P- and GF- mediated angiogenesis. Interestingly, S1P induced complex formation between Hic-5 and MT1-MMP, a surface metalloproteinase known to drive ECM degradation at focal adhesion sites as well as invadopodia [205]. We identified the MT1-MMP binding domain on Hic-5 to be LIM2. Also, our results indicated that Hic-5 regulated MT1-MMP membrane translocation. Hic-5 and MT1-

MMP were enriched in detergent resistant lipid rafts of invading ECs. Association between MT1-MMP and FAK was increased over three folds in presence of Hic-5, suggesting that Hic-5 adapted MT1-MMP to FAK. These evidences uncover novel functions of Hic-5 during endothelial invasion and lumen formation. Taken together, these studies shed light on the roles of RACK1 and Hic-5 during angiogenesis (Fig. 27).

Several studies have demonstrated that MT1-MMP, FAK [164, 165], RACK1 [128, 166, 167], and vimentin [168, 169] are up-regulated during tumor formation, invasion and metastasis. Moreover, recent studies have implicated a requirement of Hic-5 during breast cancer cell migration and invasion in 3D ECM [186, 211]. Since expression of all these molecules is altered during malignant disease, these pathways may regulate invasive, metastatic cell behavior. Our data provide novel insights into the role of RACK1 and Hic-5 during endothelial invasion in 3D collagen matrices.

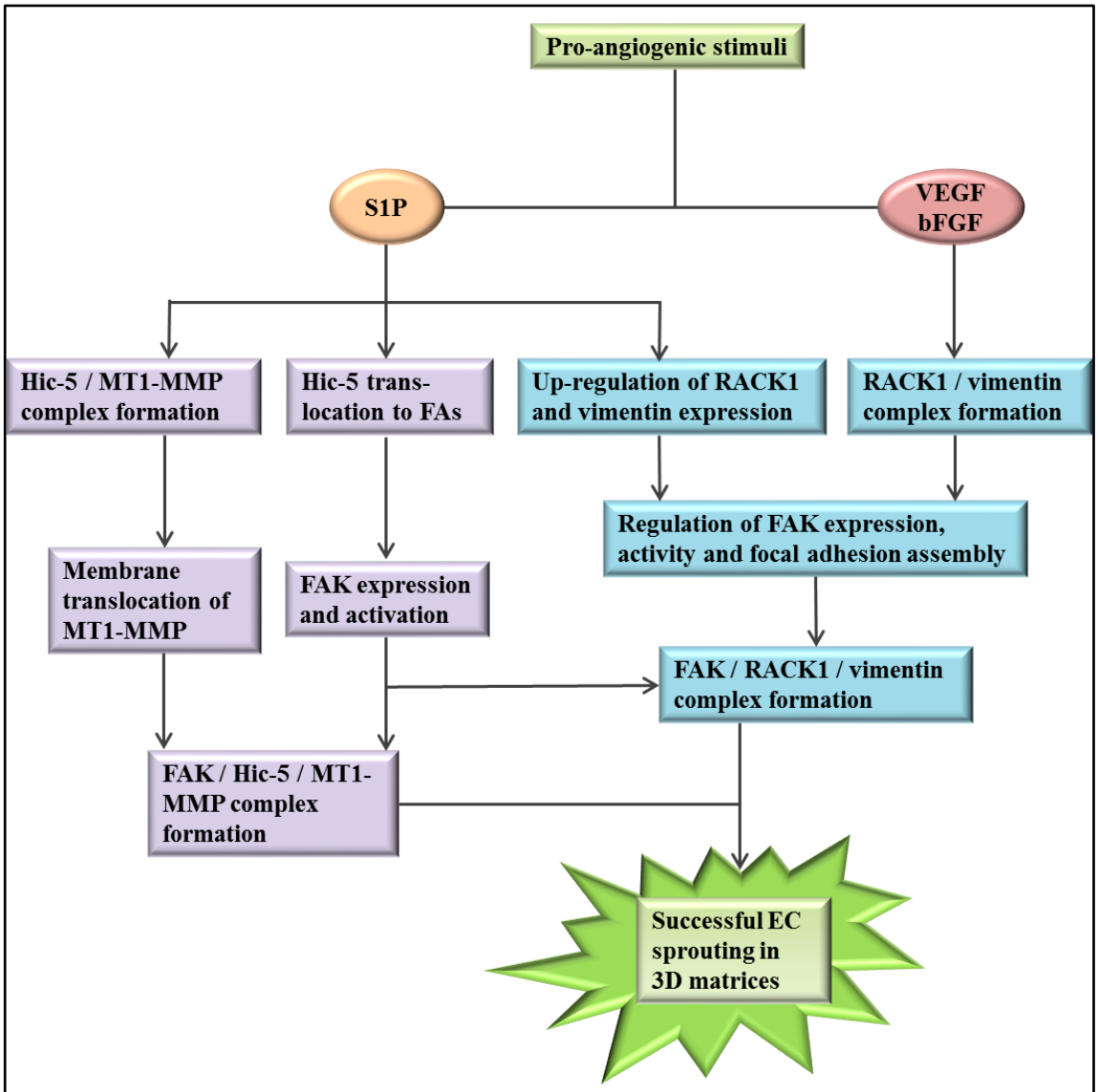

Figure 27. Roles of scaffold proteins RACK1 and Hic-5 during endothelial sprouting

FUTURE DIRECTIONS

In this study, we have elucidated two pathways that contribute towards successful endothelial sprouting responses in 3D collagen matrices. Our results are stepping stones towards a number of potential investigations. One interesting possibility would be to explore cross talk between RACK1 and Hic-5 pathways. Several lines of evidence suggest common characteristics between RACK1 and Hic-5. Both of these proteins are molecular scaffolds that lack enzymatic activity and majorly function as mediators of protein-protein interactions. RACK1 structure has characteristic WD repeat motif [127] while Hic-5 has LD and LIM domains to enable multiple protein interactions [176, 221]. Both Hic-5 [174] and RACK1 [230] are localized at focal adhesions and are known to interact with FAK. RACK1 is required for achieving optimal FAK activation following ECM engagement [122, 126] while Hic-5 silencing attenuates FAK expression as well as activation. Our results indicate that RACK1 and Hic-5 are required for successful sprouting responses in ECs. Moreover, their expression profiles or localization is altered with pro-angiogenic stimuli. RACK1 is up-regulated during S1P- and GF- induced angiogenesis while Hic-5 is localized to focal adhesion sites with S1P treatment. Our data revealed that RACK1 and Hic-5 complexed with important regulators of angiogenesis in ECs. Pro-angiogenic GFs induced complex formation between RACK1 and vimentin, while Hic-5 complexed with MT1-MMP in S1P-dependent manner. Interestingly, previous studies from our laboratory have revealed that soluble vimentin filaments transport MT1-MMP to endothelial surface in response to

pro-angiogenic stimuli to direct matrix degradation and sprouting [66]. Keeping in mind this evidence, an intriguing possibility would be to determine if Hic-5 and/or RACK1 is transported along with MT1-MMP to focal adhesion sites via vimentin filaments. In support of this theory, we find that Hic-5 is required for successful membrane translocation of MT1-MMP. Whether RACK1 affects MT1-MMP regulation is ECs remains to be determined. Since calpains are known to cleave vimentin, it would be interesting to test if calpains are involved upstream of this pathway.

Another potential area of investigation would be to probe for the phosphorylation states of RACK1 and Hic-5 in invading endothelial cells. RACK1 structure consists of six tyrosine residues that are known to be phosphorylated to mediate varied RACK1 functions. Insulin like growth factor 1 (IGF-1) mediated phosphorylation of RACK1 at Y52 by c-Abl mediates its interaction with FAK at focal adhesion sites [122]. This interaction between RACK1 and FAK is important to mediate adhesion signaling downstream of ECM engagement and integrin ligation [122]. Interestingly, c-Abl is known to participate in endothelial barrier enhancement, downstream of S1P signaling [163, 231-233]. Y302 phosphorylation on RACK1 directs its association with protein phosphatase 2A (PP2A) and integrin β1 which is important for regulation of PP2A activity and IGF-1 induced cell migration [144, 146]. Thus, RACK1 phosphorylation seems to correlate with cell migration. Src kinase is also known to phosphorylate RACK1 at residues Y228 and Y246 which in turn mediates RACK1 association with Src [149]. Interestingly, Hic-5 is also tyrosine phosphorylated at residues Y38 and Y60 in

Src- dependent manner in response to epidermal growth factor (EGF) stimulation [234]. Other stimuli including TGFβ, serum, integrin ligation, LPA and osmotic stress have been reported to enhance Hic-5 phosphorylation [170, 174, 176, 234, 235]. Moreover, studies in breast cancer cells have shown that Src- mediated Hic-5 phosphorylation is required for matrix degradation and invasion [186]. Interestingly, Src is also known to phosphorylate and activate MT1-MMP [236] as well as FAK [237, 238]. From previous studies we know that blocking Src activity using pharmacological inhibitor inhibits capillary morphogenesis and lumen formation in invading ECs [239, 240]. Thus, based on our results, we can speculate that pro-angiogenic stimuli would induce Src- mediated phosphorylation of RACK1 and Hic-5 to direct sprouting in 3D matrices. However, biochemical evidence to confirm a requirement of RACK1 and Hic-5 phosphorylation during sprouting is warranted.

Our data reveal, for the first time, two new protein interactions which point towards the possibility of a large macromolecular complex formation between RACK1, vimentin, MT1-MMP, FAK and Hic-5. All of these molecules are required for angiogenesis and have also been implicated in cancer. MT1-MMP [226, 227, 241-243] and FAK [228, 229, 244, 245] have been well distinguished as primary targets for anti-cancer drugs. Several studies demonstrate up-regulation of vimentin during epithelial to mesenchymal transition (EMT) [246] and cancer [247-249]. RACK1 is used as a prognostic indicator for breast cancer [166, 167, 250, 251] and has also been reported to be up-regulated during human carcinomas [128, 252-256]. Hic-5 has been recently

shown to be required for breast cancer cell attachment, motility, invasion, matrix degradation, and metastasis [186, 211]. Our data identify RACK1 and Hic-5 to be critical regulators of angiogenesis, and help explain their possible roles in tumor vascularization, a key step towards tumor growth and progression. Studies in animal models designed to test the effect of RACK1 or Hic-5 inhibition on tumor vascularization would be highly informative in determining the role of these molecules during malignant disease. These experiments would basically involve generation of RACK1 or Hic-5 depleted tumor cells using siRNA or shRNA mediated gene silencing along with appropriate controls. Injection of tumor cells in immunocompromised animals and study of tumor growth rate, metastasis and tumor morphology would provide detailed information on the effect of RACK1 or Hic-5 depletion during cancer. From our results, we speculate that silencing these molecules would decrease tumor progression rate and angiogenesis in tumor microenvironment. Designing small molecule inhibitors specific to RACK1 or Hic-5 provides another promising and exciting area for future investigation.

REFERENCES

[1] Carmeliet, P., *Angiogenesis in health and disease.* Nat Med, 2003. **9**(6): p. 653-60.

[2] Folkman, J. and P.A. D'Amore, *Blood vessel formation: what is its molecular basis?* Cell, 1996. **87**(7): p. 1153-5.

[3] Harper, J. and M.A. Moses, *Molecular regulation of tumor angiogenesis: mechanisms and therapeutic implications.* EXS, 2006(96): p. 223-68.

[4] Folkman, J., *Angiogenesis in cancer, vascular, rheumatoid and other disease.* Nat Med, 1995. **1**(1): p. 27-31.

[5] Azizi, G., R. Boghozian, and A. Mirshafiey, *The potential role of angiogenic factors in rheumatoid arthritis.* Int J Rheum Dis, 2014. **17**(4): p. 369-83.

[6] Khurana, R., et al., *Role of angiogenesis in cardiovascular disease: a critical appraisal.* Circulation, 2005. **112**(12): p. 1813-24.

[7] Simons, M. and J.A. Ware, *Therapeutic angiogenesis in cardiovascular disease.* Nat Rev Drug Discov, 2003. **2**(11): p. 863-71.

[8] de la Torre, J.C., *Alzheimer's disease: how does it start?* J Alzheimers Dis, 2002. **4**(6): p. 497-512.

[9] Krupinski, J., et al., *Role of angiogenesis in patients with cerebral ischemic stroke.* Stroke, 1994. **25**(9): p. 1794-8.

[10] Waltenberger, J., *Impaired collateral vessel development in diabetes: potential cellular mechanisms and therapeutic implications.* Cardiovasc Res, 2001. **49**(3): p. 554-60.

[11] Rivard, A., et al., *Rescue of diabetes-related impairment of angiogenesis by intramuscular gene therapy with adeno-VEGF.* Am J Pathol, 1999. **154**(2): p. 355-63.

[12] Van Belle, E., et al., *Hypercholesterolemia attenuates angiogenesis but does not preclude augmentation by angiogenic cytokines.* Circulation, 1997. **96**(8): p. 2667-74.

[13] Ambati, J. and B.J. Fowler, *Mechanisms of age-related macular degeneration.* Neuron, 2012. **75**(1): p. 26-39.

[14] Gariano, R.F. and T.W. Gardner, *Retinal angiogenesis in development and disease.* Nature, 2005. **438**(7070): p. 960-6.

[15] Boudier, H.A., *Arteriolar and capillary remodelling in hypertension.* Drugs, 1999. **58 Spec No 1**: p. 37-40.

[16] Tonnesen, M.G., X. Feng, and R.A. Clark, *Angiogenesis in wound healing.* J Investig Dermatol Symp Proc, 2000. **5**(1): p. 40-6.

[17] Jenkinson, L., et al., *Helicobacter pylori prevents proliferative stage of angiogenesis in vitro: role of cytokines.* Dig Dis Sci, 2002. **47**(8): p. 1857-62.

[18] Iruela-Arispe, M.L. and G.E. Davis, *Cellular and molecular mechanisms of vascular lumen formation.* Dev Cell, 2009. **16**(2): p. 222-31.

[19] Adams, R.H. and K. Alitalo, *Molecular regulation of angiogenesis and lymphangiogenesis.* Nat Rev Mol Cell Biol, 2007. **8**(6): p. 464-78.

[20] Davis, G.E. and C.W. Camarillo, *An alpha 2 beta 1 integrin-dependent pinocytic mechanism involving intracellular vacuole formation and coalescence regulates capillary lumen and tube formation in three-dimensional collagen matrix.* Exp Cell Res, 1996. **224**(1): p. 39-51.

[21] Kalluri, R., *Basement membranes: structure, assembly and role in tumour angiogenesis.* Nat Rev Cancer, 2003. **3**(6): p. 422-33.

[22] Ferrara, N., *Vascular endothelial growth factor and the regulation of angiogenesis.* Recent Prog Horm Res, 2000. **55**: p. 15-35; discussion 35-6.

[23] Ferrara, N., *Vascular endothelial growth factor as a target for anticancer therapy.* Oncologist, 2004. **9 Suppl 1**: p. 2-10.

[24] Gospodarowicz, D., et al., *Basic fibroblast growth factor: expression in cultured bovine vascular smooth muscle cells.* Eur J Cell Biol, 1988. **46**(1): p. 144-51.

[25] Battegay, E.J., et al., *PDGF-BB modulates endothelial proliferation and angiogenesis in vitro via PDGF beta-receptors.* J Cell Biol, 1994. **125**(4): p. 917-28.

[26] Saunders, W.B., et al., *Coregulation of vascular tube stabilization by endothelial cell TIMP-2 and pericyte TIMP-3.* J Cell Biol, 2006. **175**(1): p. 179-91.

[27] Bayless, K.J. and G.E. Davis, *Sphingosine-1-phosphate markedly induces matrix metalloproteinase and integrin-dependent human endothelial cell invasion and lumen formation in three-dimensional collagen and fibrin matrices.* Biochem Biophys Res Commun, 2003. **312**(4): p. 903-13.

[28] Garcia, J.G., et al., *Sphingosine 1-phosphate promotes endothelial cell barrier integrity by Edg-dependent cytoskeletal rearrangement.* J Clin Invest, 2001. **108**(5): p. 689-701.

[29] Kaunas, R., H. Kang, and K.J. Bayless, *Synergistic Regulation of Angiogenic Sprouting by Biochemical Factors and Wall Shear Stress.* Cell Mol Bioeng, 2011. **4**(4): p. 547-559.

[30] Kang, H., et al., *Fluid shear stress and sphingosine 1-phosphate activate calpain to promote membrane type 1 matrix metalloproteinase (MT1-MMP) membrane translocation and endothelial invasion into three-dimensional collagen matrices.* J Biol Chem, 2011. **286**(49): p. 42017-26.

[31] Dimmeler, S., et al., *Fluid shear stress stimulates phosphorylation of Akt in human endothelial cells: involvement in suppression of apoptosis.* Circ Res, 1998. **83**(3): p. 334-41.

[32] Wu, H., et al., *Differentiation and proliferation of endothelial progenitor cells from canine peripheral blood mononuclear cells.* J Surg Res, 2005. **126**(2): p. 193-8.

[33] Folkman, J., *The role of angiogenesis in tumor growth.* Semin Cancer Biol, 1992. **3**(2): p. 65-71.

[34] Richardson, M. and G. Singh, *Observations on the use of the avian chorioallantoic membrane (CAM) model in investigations into angiogenesis.* Curr Drug Targets Cardiovasc Haematol Disord, 2003. **3**(2): p. 155-85.

[35] Gimbrone, M.A., Jr., et al., *Tumor growth and neovascularization: an experimental model using the rabbit cornea.* J Natl Cancer Inst, 1974. **52**(2): p. 413-27.

[36] Udan, R.S., J.C. Culver, and M.E. Dickinson, *Understanding vascular development.* Wiley Interdiscip Rev Dev Biol, 2013. **2**(3): p. 327-46.

[37] Larson, J.D., et al., *Expression of VE-cadherin in zebrafish embryos: a new tool to evaluate vascular development.* Dev Dyn, 2004. **231**(1): p. 204-13.

[38] Vogel, A.M. and B.M. Weinstein, *Studying vascular development in the zebrafish.* Trends Cardiovasc Med, 2000. **10**(8): p. 352-60.

[39] Montesano, R., et al., *Phorbol ester induces cultured endothelial cells to invade a fibrin matrix in the presence of fibrinolytic inhibitors.* J Cell Physiol, 1987. **132**(3): p. 509-16.

[40] Vernon, R.B. and E.H. Sage, *A novel, quantitative model for study of endothelial cell migration and sprout formation within three-dimensional collagen matrices.* Microvasc Res, 1999. **57**(2): p. 118-33.

[41] Nicosia, R.F. and A. Ottinetti, *Growth of microvessels in serum-free matrix culture of rat aorta. A quantitative assay of angiogenesis in vitro.* Lab Invest, 1990. **63**(1): p. 115-22.

[42] Nakatsu, M.N. and C.C. Hughes, *An optimized three-dimensional in vitro model for the analysis of angiogenesis.* Methods Enzymol, 2008. **443**: p. 65-82.

[43] Davis, G.E., et al., *Molecular basis for endothelial lumen formation and tubulogenesis during vasculogenesis and angiogenic sprouting.* Int Rev Cell Mol Biol, 2011. **288**: p. 101-65.

[44] Hoying, J.B., C.A. Boswell, and S.K. Williams, *Angiogenic potential of microvessel fragments established in three-dimensional collagen gels.* In Vitro Cell Dev Biol Anim, 1996. **32**(7): p. 409-19.

[45] Bayless, K.J., H.I. Kwak, and S.C. Su, *Investigating endothelial invasion and sprouting behavior in three-dimensional collagen matrices.* Nat Protoc, 2009. **4**(12): p. 1888-98.

[46] Montesano, R., L. Orci, and P. Vassalli, *In vitro rapid organization of endothelial cells into capillary-like networks is promoted by collagen matrices.* J Cell Biol, 1983. **97**(5 Pt 1): p. 1648-52.

[47] Browder, T., J. Folkman, and S. Pirie-Shepherd, *The hemostatic system as a regulator of angiogenesis.* J Biol Chem, 2000. **275**(3): p. 1521-4.

[48] English, D., et al., *Sphingosine 1-phosphate released from platelets during clotting accounts for the potent endothelial cell chemotactic activity of blood serum and provides a novel link between hemostasis and angiogenesis.* FASEB J, 2000. **14**(14): p. 2255-65.

[49] Yatomi, Y., et al., *Sphingosine 1-phosphate as a major bioactive lysophospholipid that is released from platelets and interacts with endothelial cells.* Blood, 2000. **96**(10): p. 3431-8.

[50] Mohle, R., et al., *Constitutive production and thrombin-induced release of vascular endothelial growth factor by human megakaryocytes and platelets.* Proc Natl Acad Sci U S A, 1997. **94**(2): p. 663-8.

[51] Wartiovaara, U., et al., *Peripheral blood platelets express VEGF-C and VEGF which are released during platelet activation.* Thromb Haemost, 1998. **80**(1): p. 171-5.

[52] English, D., et al., *Lipid mediators of angiogenesis and the signalling pathways they initiate.* Biochim Biophys Acta, 2002. **1582**(1-3): p. 228-39.

[53] Hla, T., *Physiological and pathological actions of sphingosine 1-phosphate.* Semin Cell Dev Biol, 2004. **15**(5): p. 513-20.

[54] Langlois, S., D. Gingras, and R. Beliveau, *Membrane type 1-matrix metalloproteinase (MT1-MMP) cooperates with sphingosine 1-phosphate to induce endothelial cell migration and morphogenic differentiation.* Blood, 2004. **103**(8): p. 3020-8.

[55] Spiegel, S., D. English, and S. Milstien, *Sphingosine 1-phosphate signaling: providing cells with a sense of direction.* Trends Cell Biol, 2002. **12**(5): p. 236-42.

[56] Spiegel, S. and S. Milstien, *Sphingosine-1-phosphate: an enigmatic signalling lipid.* Nat Rev Mol Cell Biol, 2003. **4**(5): p. 397-407.

[57] Kaslow, H.R. and D.L. Burns, *Pertussis toxin and target eukaryotic cells: binding, entry, and activation.* Faseb J, 1992. **6**(9): p. 2684-90.

[58] Liu, Y., et al., *Edg-1, the G protein-coupled receptor for sphingosine-1-phosphate, is essential for vascular maturation.* J Clin Invest, 2000. **106**(8): p. 951-61.

[59] Rosen, H. and E.J. Goetzl, *Sphingosine 1-phosphate and its receptors: an autocrine and paracrine network.* Nat Rev Immunol, 2005. **5**(7): p. 560-70.

[60] Rivera, J., R.L. Proia, and A. Olivera, *The alliance of sphingosine-1-phosphate and its receptors in immunity.* Nat Rev Immunol, 2008. **8**(10): p. 753-63.

[61] Taha, T.A., T.D. Mullen, and L.M. Obeid, *A house divided: ceramide, sphingosine, and sphingosine-1-phosphate in programmed cell death.* Biochim Biophys Acta, 2006. **1758**(12): p. 2027-36.

[62] Peters, S.L. and A.E. Alewijnse, *Sphingosine-1-phosphate signaling in the cardiovascular system.* Curr Opin Pharmacol, 2007. **7**(2): p. 186-92.

[63] Lee, M.J., et al., *Vascular endothelial cell adherens junction assembly and morphogenesis induced by sphingosine-1-phosphate.* Cell, 1999. **99**(3): p. 301-12.

[64] Bayless, K.J. and G.E. Davis, *The Cdc42 and Rac1 GTPases are required for capillary lumen formation in three-dimensional extracellular matrices.* J Cell Sci, 2002. **115**(Pt 6): p. 1123-36.

[65] Sun, X., et al., *Enhanced interaction between focal adhesion and adherens junction proteins: involvement in sphingosine 1-phosphate-induced endothelial barrier enhancement.* Microvasc Res, 2009. **77**(3): p. 304-13.

[66] Kwak, H.I., et al., *Calpain-mediated vimentin cleavage occurs upstream of MT1-MMP membrane translocation to facilitate endothelial sprout initiation.* Angiogenesis, 2012. **15**(2): p. 287-303.

[67] Su, S.C., S.A. Maxwell, and K.J. Bayless, *Annexin 2 regulates endothelial morphogenesis by controlling AKT activation and junctional integrity.* J Biol Chem. **285**(52): p. 40624-34.

[68] Kang, H., K.J. Bayless, and R. Kaunas, *Fluid shear stress modulates endothelial cell invasion into three-dimensional collagen matrices.* Am J Physiol Heart Circ Physiol, 2008. **295**(5): p. H2087-97.

[69] Park, J.E., G.A. Keller, and N. Ferrara, *The vascular endothelial growth factor (VEGF) isoforms: differential deposition into the subepithelial extracellular matrix and bioactivity of extracellular matrix-bound VEGF.* Mol Biol Cell, 1993. **4**(12): p. 1317-26.

[70] Senger, D.R., et al., *Tumor cells secrete a vascular permeability factor that promotes accumulation of ascites fluid.* Science, 1983. **219**(4587): p. 983-5.

[71] Hoeben, A., et al., *Vascular endothelial growth factor and angiogenesis.* Pharmacol Rev, 2004. **56**(4): p. 549-80.

[72] Neufeld, G., et al., *Vascular endothelial growth factor (VEGF) and its receptors.* Faseb J, 1999. **13**(1): p. 9-22.

[73] Alitalo, K. and P. Carmeliet, *Molecular mechanisms of lymphangiogenesis in health and disease.* Cancer Cell, 2002. **1**(3): p. 219-27.

[74] Karkkainen, M.J., et al., *Vascular endothelial growth factor C is required for sprouting of the first lymphatic vessels from embryonic veins.* Nat Immunol, 2004. **5**(1): p. 74-80.

[75] Ferrara, N., et al., *Targeting VEGF-A to treat cancer and age-related macular degeneration.* Annu Rev Med, 2007. **58**: p. 491-504.

[76] Ray, D., et al., *Association of the VEGF gene with proliferative diabetic retinopathy but not proteinuria in diabetes.* Diabetes, 2004. **53**(3): p. 861-4.

[77] Afuwape, A.O., S. Kiriakidis, and E.M. Paleolog, *The role of the angiogenic molecule VEGF in the pathogenesis of rheumatoid arthritis.* Histol Histopathol, 2002. **17**(3): p. 961-72.

[78] Gupta, P.K., et al., *Vascular endothelial growth factor-A and chemokine ligand (CCL2) genes are upregulated in peripheral blood mononuclear cells in Indian amyotrophic lateral sclerosis patients.* J Neuroinflammation, 2011. **8**: p. 114.

[79] Yuan, A., et al., *Correlation of total VEGF mRNA and protein expression with histologic type, tumor angiogenesis, patient survival and timing of relapse in non-small-cell lung cancer.* Int J Cancer, 2000. **89**(6): p. 475-83.

[80] Yuan, A., et al., *Quantification of VEGF mRNA expression in non-small cell lung cancer using a real-time quantitative reverse transcription-PCR assay and a comparison with quantitative competitive reverse transcription-PCR.* Lab Invest, 2000. **80**(11): p. 1671-80.

[81] Yuan, A., et al., *Vascular endothelial growth factor 189 mRNA isoform expression specifically correlates with tumor angiogenesis, patient survival, and*

postoperative relapse in non-small-cell lung cancer. J Clin Oncol, 2001. **19**(2): p. 432-41.

[82] Dong, J., et al., *VEGF-null cells require PDGFR alpha signaling-mediated stromal fibroblast recruitment for tumorigenesis.* EMBO J, 2004. **23**(14): p. 2800-10.

[83] Liang, W.C., et al., *Cross-species vascular endothelial growth factor (VEGF)-blocking antibodies completely inhibit the growth of human tumor xenografts and measure the contribution of stromal VEGF.* J Biol Chem, 2006. **281**(2): p. 951-61.

[84] Li, B., et al., *VEGF and PlGF promote adult vasculogenesis by enhancing EPC recruitment and vessel formation at the site of tumor neovascularization.* FASEB J, 2006. **20**(9): p. 1495-7.

[85] Carmeliet, P., et al., *Abnormal blood vessel development and lethality in embryos lacking a single VEGF allele.* Nature, 1996. **380**(6573): p. 435-9.

[86] Robinson, C.J. and S.E. Stringer, *The splice variants of vascular endothelial growth factor (VEGF) and their receptors.* J Cell Sci, 2001. **114**(Pt 5): p. 853-65.

[87] Olsson, A.K., et al., *VEGF receptor signalling - in control of vascular function.* Nat Rev Mol Cell Biol, 2006. **7**(5): p. 359-71.

[88] Bekhite, M.M., et al., *VEGF-mediated PI3K class IA and PKC signaling in cardiomyogenesis and vasculogenesis of mouse embryonic stem cells.* J Cell Sci, 2011. **124**(Pt 11): p. 1819-30.

[89] Doanes, A.M., et al., *VEGF stimulates MAPK through a pathway that is unique for receptor tyrosine kinases.* Biochem Biophys Res Commun, 1999. **255**(2): p. 545-8.

[90] Shing, Y., et al., *Heparin affinity: purification of a tumor-derived capillary endothelial cell growth factor.* Science, 1984. **223**(4642): p. 1296-9.

[91] Shing, Y., et al., *Angiogenesis is stimulated by a tumor-derived endothelial cell growth factor.* J Cell Biochem, 1985. **29**(4): p. 275-87.

[92] Presta, M., et al., *Fibroblast growth factor/fibroblast growth factor receptor system in angiogenesis.* Cytokine Growth Factor Rev, 2005. **16**(2): p. 159-78.

[93] Presta, M., et al., *Purification from a human hepatoma cell line of a basic fibroblast growth factor-like molecule that stimulates capillary endothelial cell plasminogen activator production, DNA synthesis, and migration.* Mol Cell Biol, 1986. **6**(11): p. 4060-6.

[94] Taraboletti, G., et al., *Shedding of the matrix metalloproteinases MMP-2, MMP-9, and MT1-MMP as membrane vesicle-associated components by endothelial cells.* Am J Pathol, 2002. **160**(2): p. 673-80.

[95] Bikfalvi, A., et al., *New insights in the biology of fibroblast growth factor-2.* Angiogenesis, 1998. **1**(2): p. 155-73.

[96] Gualandris, A., et al., *Interaction of high-molecular-weight basic fibroblast growth factor with endothelium: biological activity and intracellular fate of human recombinant M(r) 24,000 bFGF.* J Cell Physiol, 1994. **161**(1): p. 149-59.

[97] Ozaki, H., et al., *Basic fibroblast growth factor is neither necessary nor sufficient for the development of retinal neovascularization.* Am J Pathol, 1998. **153**(3): p. 757-65.

[98] Tobe, T., et al., *Targeted disruption of the FGF2 gene does not prevent choroidal neovascularization in a murine model.* Am J Pathol, 1998. **153**(5): p. 1641-6.

[99] Zhou, M., et al., *Fibroblast growth factor 2 control of vascular tone.* Nat Med, 1998. **4**(2): p. 201-7.

[100] Miller, D.L., et al., *Compensation by fibroblast growth factor 1 (FGF1) does not account for the mild phenotypic defects observed in FGF2 null mice.* Mol Cell Biol, 2000. **20**(6): p. 2260-8.

[101] Ornitz, D.M., et al., *Receptor specificity of the fibroblast growth factor family.* J Biol Chem, 1996. **271**(25): p. 15292-7.

[102] Fantl, W.J., et al., *Distinct phosphotyrosines on a growth factor receptor bind to specific molecules that mediate different signaling pathways.* Cell, 1992. **69**(3): p. 413-23.

[103] Javerzat, S., P. Auguste, and A. Bikfalvi, *The role of fibroblast growth factors in vascular development.* Trends Mol Med, 2002. **8**(10): p. 483-9.

[104] Dell'Era, P., et al., *Paracrine and autocrine effects of fibroblast growth factor-4 in endothelial cells.* Oncogene, 2001. **20**(21): p. 2655-63.

[105] Eswarakumar, V.P., I. Lax, and J. Schlessinger, *Cellular signaling by fibroblast growth factor receptors.* Cytokine Growth Factor Rev, 2005. **16**(2): p. 139-49.

[106] Mohammadi, M., et al., *Identification of six novel autophosphorylation sites on fibroblast growth factor receptor 1 and elucidation of their importance in receptor activation and signal transduction.* Mol Cell Biol, 1996. **16**(3): p. 977-89.

[107] Dell'Era, P., M. Mohammadi, and M. Presta, *Different tyrosine autophosphorylation requirements in fibroblast growth factor receptor-1 mediate urokinase-type plasminogen activator induction and mitogenesis.* Mol Biol Cell, 1999. **10**(1): p. 23-33.

[108] Larsson, H., et al., *Fibroblast growth factor receptor-1-mediated endothelial cell proliferation is dependent on the Src homology (SH) 2/SH3 domain-containing adaptor protein Crk.* J Biol Chem, 1999. **274**(36): p. 25726-34.

[109] Tanghetti, E., et al., *Biological activity of substrate-bound basic fibroblast growth factor (FGF2): recruitment of FGF receptor-1 in endothelial cell adhesion contacts.* Oncogene, 2002. **21**(24): p. 3889-97.

[110] Mohammadi, M., et al., *A tyrosine-phosphorylated carboxy-terminal peptide of the fibroblast growth factor receptor (Flg) is a binding site for the SH2 domain of phospholipase C-gamma 1.* Mol Cell Biol, 1991. **11**(10): p. 5068-78.

[111] Ong, S.H., et al., *Stimulation of phosphatidylinositol 3-kinase by fibroblast growth factor receptors is mediated by coordinated recruitment of multiple docking proteins.* Proc Natl Acad Sci U S A, 2001. **98**(11): p. 6074-9.

[112] Rieck, P.W., S. Cholidis, and C. Hartmann, *Intracellular signaling pathway of FGF-2-modulated corneal endothelial cell migration during wound healing in vitro.* Exp Eye Res, 2001. **73**(5): p. 639-50.

[113] Cross, M.J., et al., *The Shb adaptor protein binds to tyrosine 766 in the FGFR-1 and regulates the Ras/MEK/MAPK pathway via FRS2 phosphorylation in endothelial cells.* Mol Biol Cell, 2002. **13**(8): p. 2881-93.

[114] Giuliani, R., et al., *Role of endothelial cell extracellular signal-regulated kinase1/2 in urokinase-type plasminogen activator upregulation and in vitro angiogenesis by fibroblast growth factor-2.* J Cell Sci, 1999. **112 (Pt 15)**: p. 2597-606.

[115] Eliceiri, B.P., et al., *Integrin alphavbeta3 requirement for sustained mitogen-activated protein kinase activity during angiogenesis.* J Cell Biol, 1998. **140**(5): p. 1255-63.

[116] McCahill, A., et al., *The RACK1 scaffold protein: a dynamic cog in cell response mechanisms.* Mol Pharmacol, 2002. **62**(6): p. 1261-73.

[117] Sklan, E.H., E. Podoly, and H. Soreq, *RACK1 has the nerve to act: structure meets function in the nervous system.* Prog Neurobiol, 2006. **78**(2): p. 117-34.

[118] Chen, J.G., et al., *RACK1 mediates multiple hormone responsiveness and developmental processes in Arabidopsis.* J Exp Bot, 2006. **57**(11): p. 2697-708.

[119] Guo, J. and J.G. Chen, *RACK1 genes regulate plant development with unequal genetic redundancy in Arabidopsis.* BMC Plant Biol, 2008. **8**: p. 108.

[120] Wehner, P., et al., *RACK1 is a novel interaction partner of PTK7 that is required for neural tube closure.* Development, 2011. **138**(7): p. 1321-7.

[121] Hermanto, U., et al., *RACK1, an insulin-like growth factor I (IGF-I) receptor-interacting protein, modulates IGF-I-dependent integrin signaling and promotes cell spreading and contact with extracellular matrix.* Mol Cell Biol, 2002. **22**(7): p. 2345-65.

[122] Kiely, P.A., et al., *Phosphorylation of RACK1 on tyrosine 52 by c-Abl is required for insulin-like growth factor I-mediated regulation of focal adhesion kinase.* J Biol Chem, 2009. **284**(30): p. 20263-74.

[123] Kiely, P.A., et al., *RACK1-mediated integration of adhesion and insulin-like growth factor I (IGF-I) signaling and cell migration are defective in cells expressing an IGF-I receptor mutated at tyrosines 1250 and 1251.* J Biol Chem, 2005. **280**(9): p. 7624-33.

[124] Kiely, P.A., A. Sant, and R. O'Connor, *RACK1 is an insulin-like growth factor 1 (IGF-1) receptor-interacting protein that can regulate IGF-1-mediated Akt activation and protection from cell death.* J Biol Chem, 2002. **277**(25): p. 22581-9.

[125] Neer, E.J., et al., *The ancient regulatory-protein family of WD-repeat proteins.* Nature, 1994. **371**(6495): p. 297-300.

[126] Onishi, I., et al., *RACK1 associates with NHE5 in focal adhesions and positively regulates the transporter activity.* Cell Signal, 2007. **19**(1): p. 194-203.

[127] Adams, D.R., D. Ron, and P.A. Kiely, *RACK1, A multifaceted scaffolding protein: Structure and function.* Cell Commun Signal, 2011. **9**: p. 22.

[128] Berns, H., et al., *RACK1 is up-regulated in angiogenesis and human carcinomas.* Faseb J, 2000. **14**(15): p. 2549-58.

[129] Burgstaller, G., et al., *Keeping the vimentin network under control: cell-matrix adhesion-associated plectin 1f affects cell shape and polarity of fibroblasts.* Mol Biol Cell, 2010. **21**(19): p. 3362-75.

[130] Tsuruta, D. and J.C. Jones, *The vimentin cytoskeleton regulates focal contact size and adhesion of endothelial cells subjected to shear stress.* J Cell Sci, 2003. **116**(Pt 24): p. 4977-84.

[131] Romer, L.H., K.G. Birukov, and J.G. Garcia, *Focal adhesions: paradigm for a signaling nexus.* Circ Res, 2006. **98**(5): p. 606-16.

[132] Petit, V. and J.P. Thiery, *Focal adhesions: structure and dynamics.* Biol Cell, 2000. **92**(7): p. 477-94.

[133] Martin, G.M., *Fak and focal adhesions.* Jpn J Cancer Res, 1996. **87**(3): p. inside front cover.

[134] Burridge, K., M. Chrzanowska-Wodnicka, and C. Zhong, *Focal adhesion assembly.* Trends Cell Biol, 1997. **7**(9): p. 342-7.

[135] Burridge, K. and M. Chrzanowska-Wodnicka, *Focal adhesions, contractility, and signaling.* Annu Rev Cell Dev Biol, 1996. **12**: p. 463-518.

[136] Mitra, S.K. and D.D. Schlaepfer, *Integrin-regulated FAK-Src signaling in normal and cancer cells.* Curr Opin Cell Biol, 2006. **18**(5): p. 516-23.

[137] Guan, J.L., *Integrin signaling through FAK in the regulation of mammary stem cells and breast cancer.* IUBMB Life. **62**(4): p. 268-76.

[138] Arold, S.T., *How focal adhesion kinase achieves regulation by linking ligand binding, localization and action.* Curr Opin Struct Biol, 2011. **21**(6): p. 808-13.

[139] Braren, R., et al., *Endothelial FAK is essential for vascular network stability, cell survival, and lamellipodial formation.* J Cell Biol, 2006. **172**(1): p. 151-62.

[140] Hakim, Z.S., et al., *Conditional deletion of focal adhesion kinase leads to defects in ventricular septation and outflow tract alignment.* Mol Cell Biol, 2007. **27**(15): p. 5352-64.

[141] Peng, X., et al., *Cardiac developmental defects and eccentric right ventricular hypertrophy in cardiomyocyte focal adhesion kinase (FAK) conditional knockout mice.* Proc Natl Acad Sci U S A, 2008. **105**(18): p. 6638-43.

[142] Shen, T.L., et al., *Conditional knockout of focal adhesion kinase in endothelial cells reveals its role in angiogenesis and vascular development in late embryogenesis.* J Cell Biol, 2005. **169**(6): p. 941-52.

[143] Su, S.C., et al., *Molecular profile of endothelial invasion of three-dimensional collagen matrices: insights into angiogenic sprout induction in wound healing.* Am J Physiol Cell Physiol, 2008. **295**(5): p. C1215-29.

[144] Kiely, P.A., et al., *Insulin-like growth factor I controls a mutually exclusive association of RACK1 with protein phosphatase 2A and beta1 integrin to promote cell migration.* Mol Cell Biol, 2006. **26**(11): p. 4041-51.

[145] Serrels, A., et al., *Src/FAK-mediated regulation of E-cadherin as a mechanism for controlling collective cell movement: insights from in vivo imaging.* Cell Adh Migr, 2011. **5**(4): p. 360-5.

[146] Kiely, P.A., et al., *Tyrosine 302 in RACK1 is essential for insulin-like growth factor-I-mediated competitive binding of PP2A and beta1 integrin and for tumor cell proliferation and migration.* J Biol Chem, 2008. **283**(34): p. 22952-61.

[147] Burridge, K., et al., *Focal adhesions: transmembrane junctions between the extracellular matrix and the cytoskeleton.* Annu Rev Cell Biol, 1988. **4**: p. 487-525.

[148] Bayless, K.J., Davis, G. E., and Meininger, G. A. , *Protein expression and purification* 1997. **9**: p. 309-314.

[149] Chang, B.Y., R.A. Harte, and C.A. Cartwright, *RACK1: a novel substrate for the Src protein-tyrosine kinase.* Oncogene, 2002. **21**(50): p. 7619-29.

[150] Yaka, R., et al., *NMDA receptor function is regulated by the inhibitory scaffolding protein, RACK1.* Proc Natl Acad Sci U S A, 2002. **99**(8): p. 5710-5.

[151] Koehler, J.A. and M.F. Moran, *RACK1, a protein kinase C scaffolding protein, interacts with the PH domain of p120GAP.* Biochem Biophys Res Commun, 2001. **283**(4): p. 888-95.

[152] Rodriguez, M.M., et al., *RACK1, a protein kinase C anchoring protein, coordinates the binding of activated protein kinase C and select pleckstrin homology domains in vitro.* Biochemistry, 1999. **38**(42): p. 13787-94.

[153] Usacheva, A., et al., *The WD motif-containing protein RACK-1 functions as a scaffold protein within the type I IFN receptor-signaling complex.* J Immunol, 2003. **171**(6): p. 2989-94.

[154] Liliental, J. and D.D. Chang, *Rack1, a receptor for activated protein kinase C, interacts with integrin beta subunit.* J Biol Chem, 1998. **273**(4): p. 2379-83.

[155] Lee, H.S., et al., *Activation of Integrin-RACK1/PKCalpha signalling in human articular chondrocyte mechanotransduction.* Osteoarthritis Cartilage, 2002. **10**(11): p. 890-7.

[156] Rigas, A.C., et al., *The scaffolding protein RACK1 interacts with androgen receptor and promotes cross-talk through a protein kinase C signaling pathway.* J Biol Chem, 2003. **278**(46): p. 46087-93.

[157] Helfand, B.T., et al., *Intermediate filament proteins participate in signal transduction.* Trends Cell Biol, 2005. **15**(11): p. 568-70.

[158] Ivaska, J., et al., *Novel functions of vimentin in cell adhesion, migration, and signaling.* Exp Cell Res, 2007. **313**(10): p. 2050-62.

[159] Oriolo, A.S., et al., *Intermediate filaments: a role in epithelial polarity.* Exp Cell Res, 2007. **313**(10): p. 2255-64.

[160] Bershadsky, A.D., I.S. Tint, and T.M. Svitkina, *Association of intermediate filaments with vinculin-containing adhesion plaques of fibroblasts.* Cell Motil Cytoskeleton, 1987. **8**(3): p. 274-83.

[161] Gonzales, M., et al., *Structure and function of a vimentin-associated matrix adhesion in endothelial cells.* Mol Biol Cell, 2001. **12**(1): p. 85-100.

[162] Ilic, D., et al., *Reduced cell motility and enhanced focal adhesion contact formation in cells from FAK-deficient mice.* Nature, 1995. **377**(6549): p. 539-44.

[163] Zhao, J., et al., *Phosphotyrosine protein dynamics in cell membrane rafts of sphingosine-1-phosphate-stimulated human endothelium: role in barrier enhancement.* Cell Signal, 2009. **21**(12): p. 1945-60.

[164] Owens, L.V., et al., *Focal adhesion kinase as a marker of invasive potential in differentiated human thyroid cancer.* Ann Surg Oncol, 1996. **3**(1): p. 100-5.

[165] Tremblay, L., et al., *Focal adhesion kinase (pp125FAK) expression, activation and association with paxillin and p50CSK in human metastatic prostate carcinoma.* Int J Cancer, 1996. **68**(2): p. 164-71.

[166] Al-Reefy, S. and K. Mokbel, *The role of RACK1 as an independent prognostic indicator in human breast cancer.* Breast Cancer Res Treat, 2010. **123**(3): p. 911; author reply 912.

[167] Cao, X.X., et al., *RACK1 promotes breast carcinoma proliferation and invasion/metastasis in vitro and in vivo.* Breast Cancer Res Treat, 2010. **123**(2): p. 375-86.

[168] Singh, S., et al., *Overexpression of vimentin: role in the invasive phenotype in an androgen-independent model of prostate cancer.* Cancer Res, 2003. **63**(9): p. 2306-11.

[169] Alfonso, P., et al., *Proteomic expression analysis of colorectal cancer by two-dimensional differential gel electrophoresis.* Proteomics, 2005. **5**(10): p. 2602-11.

[170] Matsuya, M., et al., *Cell adhesion kinase beta forms a complex with a new member, Hic-5, of proteins localized at focal adhesions.* J Biol Chem, 1998. **273**(2): p. 1003-14.

[171] Shibanuma, M., et al., *Characterization of the TGF beta 1-inducible hic-5 gene that encodes a putative novel zinc finger protein and its possible involvement in cellular senescence.* J Biol Chem, 1994. **269**(43): p. 26767-74.

[172] Turner, C.E., *Paxillin and focal adhesion signalling.* Nat Cell Biol, 2000. **2**(12): p. E231-6.

[173] Brown, M.C. and C.E. Turner, *Paxillin: adapting to change.* Physiol Rev, 2004. **84**(4): p. 1315-39.

[174] Fujita, H., et al., *Interaction of Hic-5, A senescence-related protein, with focal adhesion kinase.* J Biol Chem, 1998. **273**(41): p. 26516-21.

[175] Deakin, N.O., C. Ballestrem, and C.E. Turner, *Paxillin and Hic-5 interaction with vinculin is differentially regulated by Rac1 and RhoA.* PLoS One, 2012. **7**(5): p. e37990.

[176] Thomas, S.M., M. Hagel, and C.E. Turner, *Characterization of a focal adhesion protein, Hic-5, that shares extensive homology with paxillin.* J Cell Sci, 1999. **112 (Pt 2)**: p. 181-90.

[177] Nishiya, N., et al., *Hic-5 interacts with GIT1 with a different binding mode from paxillin.* J Biochem, 2002. **132**(2): p. 279-89.

[178] Nishiya, N., et al., *Hic-5, a paxillin homologue, binds to the protein-tyrosine phosphatase PEST (PTP-PEST) through its LIM 3 domain.* J Biol Chem, 1999. **274**(14): p. 9847-53.

[179] Jia, Y., et al., *Identification and characterization of hic-5/ARA55 as an hsp27 binding protein.* J Biol Chem, 2001. **276**(43): p. 39911-8.

[180] Kim, K., Jr., M. Shibanuma, and K. Nose, *Transcriptional activation of the c-fos gene by a LIM protein, Hic-5.* Biochem Biophys Res Commun, 2002. **299**(3): p. 360-5.

[181] Shibanuma, M., et al., *Hic-5 communicates between focal adhesions and the nucleus through oxidant-sensitive nuclear export signal.* Mol Biol Cell, 2003. **14**(3): p. 1158-71.

[182] Shibanuma, M., et al., *A LIM protein, Hic-5, functions as a potential coactivator for Sp1.* J Cell Biochem, 2004. **91**(3): p. 633-45.

[183] Kim-Kaneyama, J.R., et al., *Hydrogen peroxide-inducible clone 5 (Hic-5) as a potential therapeutic target for vascular and other disorders.* J Atheroscler Thromb, 2012. **19**(7): p. 601-7.

[184] Kim-Kaneyama, J.R., et al., *Hic-5 deficiency enhances mechanosensitive apoptosis and modulates vascular remodeling.* J Mol Cell Cardiol, 2011. **50**(1): p. 77-86.

[185] Avraamides, C., et al., *Hic-5 promotes endothelial cell migration to lysophosphatidic acid.* Am J Physiol Heart Circ Physiol, 2007. **293**(1): p. H193-203.

[186] Pignatelli, J., et al., *Hic-5 promotes invadopodia formation and invasion during TGF-beta-induced epithelial-mesenchymal transition.* J Cell Biol, 2012. **197**(3): p. 421-37.

[187] Wu, R.F., et al., *Subcellular targeting of oxidants during endothelial cell migration.* J Cell Biol, 2005. **171**(5): p. 893-904.

[188] Tumbarello, D.A. and C.E. Turner, *Hic-5 contributes to epithelial-mesenchymal transformation through a RhoA/ROCK-dependent pathway.* J Cell Physiol, 2007. **211**(3): p. 736-47.

[189] Egeblad, M. and Z. Werb, *New functions for the matrix metalloproteinases in cancer progression.* Nat Rev Cancer, 2002. **2**(3): p. 161-74.

[190] Li, X.Y., et al., *Molecular dissection of the structural machinery underlying the tissue-invasive activity of membrane type-1 matrix metalloproteinase.* Mol Biol Cell, 2008. **19**(8): p. 3221-33.

[191] Yana, I. and S.J. Weiss, *Regulation of membrane type-1 matrix metalloproteinase activation by proprotein convertases.* Mol Biol Cell, 2000. **11**(7): p. 2387-401.

[192] Hotary, K., et al., *Regulation of cell invasion and morphogenesis in a three-dimensional type I collagen matrix by membrane-type matrix metalloproteinases 1, 2, and 3.* J Cell Biol, 2000. **149**(6): p. 1309-23.

[193] Hiraoka, N., et al., *Matrix metalloproteinases regulate neovascularization by acting as pericellular fibrinolysins.* Cell, 1998. **95**(3): p. 365-77.

[194] Montesano, R., et al., *Modulation of angiogenesis in vitro.* Exs, 1992. **61**: p. 129-36.

[195] Yana, I., et al., *Crosstalk between neovessels and mural cells directs the site-specific expression of MT1-MMP to endothelial tip cells.* J Cell Sci, 2007. **120**(Pt 9): p. 1607-14.

[196] Chun, T.H., et al., *MT1-MMP-dependent neovessel formation within the confines of the three-dimensional extracellular matrix.* J Cell Biol, 2004. **167**(4): p. 757-67.

[197] Artym, V.V., et al., *Dynamic interactions of cortactin and membrane type 1 matrix metalloproteinase at invadopodia: defining the stages of invadopodia formation and function.* Cancer Res, 2006. **66**(6): p. 3034-43.

[198] Peng, X., et al., *Inactivation of focal adhesion kinase in cardiomyocytes promotes eccentric cardiac hypertrophy and fibrosis in mice.* J Clin Invest, 2006. **116**(1): p. 217-27.

[199] Peng, X., et al., *Overexpression of focal adhesion kinase in vascular endothelial cells promotes angiogenesis in transgenic mice.* Cardiovasc Res, 2004. **64**(3): p. 421-30.

[200] Bowden, E.T., et al., *Co-localization of cortactin and phosphotyrosine identifies active invadopodia in human breast cancer cells.* Exp Cell Res, 2006. **312**(8): p. 1240-53.

[201] Hsia, D.A., et al., *Differential regulation of cell motility and invasion by FAK.* J Cell Biol, 2003. **160**(5): p. 753-67.

[202] Chan, K.T., C.L. Cortesio, and A. Huttenlocher, *FAK alters invadopodia and focal adhesion composition and dynamics to regulate breast cancer invasion.* J Cell Biol, 2009. **185**(2): p. 357-70.

[203] Kolli-Bouhafs, K., et al., *FAK competes for Src to promote migration against invasion in melanoma cells.* Cell Death Dis, 2014. **5**: p. e1379.

[204] Takino, T., et al., *Inhibition of membrane-type 1 matrix metalloproteinase at cell-matrix adhesions.* Cancer Res, 2007. **67**(24): p. 11621-9.

[205] Wang, Y. and M.A. McNiven, *Invasive matrix degradation at focal adhesions occurs via protease recruitment by a FAK-p130Cas complex.* J Cell Biol, 2012. **196**(3): p. 375-85.

[206] Takino, T., et al., *Membrane-type 1 matrix metalloproteinase modulates focal adhesion stability and cell migration.* Exp Cell Res, 2006. **312**(8): p. 1381-9.

[207] Wu, X., et al., *FAK-mediated src phosphorylation of endophilin A2 inhibits endocytosis of MT1-MMP and promotes ECM degradation.* Dev Cell, 2005. **9**(2): p. 185-96.

[208] Gonzales, R.C., R.E. Woods, and S.L. Eddins, *Digital Image Processing using MATLAB*, 2009, Gatesmark publishing

[209] Lee, P.F., et al., *Angiogenic responses are enhanced in mechanically and microscopically characterized, microbial transglutaminase crosslinked collagen matrices with increased stiffness.* Acta Biomater, 2013. **9**(7): p. 7178-90.

[210] Dave, J.M., et al., *Proteomic profiling of endothelial invasion revealed receptor for activated C kinase 1 (RACK1) complexed with vimentin to regulate focal adhesion kinase (FAK).* J Biol Chem, 2013. **288**(42): p. 30720-33.

[211] Deakin, N.O. and C.E. Turner, *Distinct roles for paxillin and Hic-5 in regulating breast cancer cell morphology, invasion, and metastasis.* Mol Biol Cell, 2011. **22**(3): p. 327-41.

[212] Sacharidou, A., et al., *Endothelial lumen signaling complexes control 3D matrix-specific tubulogenesis through interdependent Cdc42- and MT1-MMP-mediated events.* Blood, 2010. **115**(25): p. 5259-69.

[213] Stratman, A.N., et al., *Endothelial cell lumen and vascular guidance tunnel formation requires MT1-MMP-dependent proteolysis in 3-dimensional collagen matrices.* Blood, 2009. **114**(2): p. 237-47.

[214] Poincloux, R., F. Lizarraga, and P. Chavrier, *Matrix invasion by tumour cells: a focus on MT1-MMP trafficking to invadopodia.* J Cell Sci, 2009. **122**(Pt 17): p. 3015-24.

[215] Wolf, K. and P. Friedl, *Mapping proteolytic cancer cell-extracellular matrix interfaces.* Clin Exp Metastasis, 2009. **26**(4): p. 289-98.

[216] Shirvaikar, N., et al., *MT1-MMP association with membrane lipid rafts facilitates G-CSF--induced hematopoietic stem/progenitor cell mobilization.* Exp Hematol, 2010. **38**(9): p. 823-35.

[217] Yamaguchi, H., et al., *Lipid rafts and caveolin-1 are required for invadopodia formation and extracellular matrix degradation by human breast cancer cells.* Cancer Res, 2009. **69**(22): p. 8594-602.

[218] Gingras, D., et al., *Sphingosine-1-phosphate induces the association of membrane-type 1 matrix metalloproteinase with p130Cas in endothelial cells.* FEBS Lett, 2008. **582**(3): p. 399-404.

[219] Dawid, I.B., R. Toyama, and M. Taira, *LIM domain proteins.* C R Acad Sci III, 1995. **318**(3): p. 295-306.

[220] Shibanuma, M., K. Mori, and K. Nose, *HIC-5: A Mobile Molecular Scaffold Regulating the Anchorage Dependence of Cell Growth.* Int J Cell Biol, 2012. **2012**: p. 426138.

[221] Shibanuma, M., et al., *Induction of senescence-like phenotypes by forced expression of hic-5, which encodes a novel LIM motif protein, in immortalized human fibroblasts.* Mol Cell Biol, 1997. **17**(3): p. 1224-35.

[222] Noguchi, F., et al., *Hic-5 affects proliferation, migration and invasion of B16 murine melanoma cells.* Pigment Cell Melanoma Res, 2012. **25**(6): p. 773-82.

[223] Yana, I. and M. Seiki, *[Matrix metalloproteinases; the past, present, and future].* Nihon Shokakibyo Gakkai Zasshi, 2003. **100**(2): p. 144-51.

[224] Mitra, S.K., D.A. Hanson, and D.D. Schlaepfer, *Focal adhesion kinase: in command and control of cell motility.* Nat Rev Mol Cell Biol, 2005. **6**(1): p. 56-68.

[225] Langlois, S., et al., *Membrane-type 1 matrix metalloproteinase stimulates cell migration through epidermal growth factor receptor transactivation.* Mol Cancer Res, 2007. **5**(6): p. 569-83.

[226] Zucker, S. and J. Cao, *Selective matrix metalloproteinase (MMP) inhibitors in cancer therapy: ready for prime time?* Cancer Biol Ther, 2009. **8**(24): p. 2371-3.

[227] Sounni, N.E., et al., *Expression of membrane type 1 matrix metalloproteinase (MT1-MMP) in A2058 melanoma cells is associated with MMP-2 activation and increased tumor growth and vascularization.* Int J Cancer, 2002. **98**(1): p. 23-8.

[228] Dunn, K.B., M. Heffler, and V.M. Golubovskaya, *Evolving therapies and FAK inhibitors for the treatment of cancer.* Anticancer Agents Med Chem, 2010. **10**(10): p. 722-34.

[229] McLean, G.W., et al., *The role of focal-adhesion kinase in cancer - a new therapeutic opportunity.* Nat Rev Cancer, 2005. **5**(7): p. 505-15.

[230] Serrels, B., et al., *A complex between FAK, RACK1, and PDE4D5 controls spreading initiation and cancer cell polarity.* Curr Biol, 2010. **20**(12): p. 1086-92.

[231] Wang, L., et al., *FTY720-induced human pulmonary endothelial barrier enhancement is mediated by c-Abl.* Eur Respir J, 2011. **38**(1): p. 78-88.

[232] Chislock, E.M. and A.M. Pendergast, *Abl family kinases regulate endothelial barrier function in vitro and in mice.* PLoS One, 2013. **8**(12): p. e85231.

[233] Dudek, S.M., et al., *Abl tyrosine kinase phosphorylates nonmuscle Myosin light chain kinase to regulate endothelial barrier function.* Mol Biol Cell, 2010. **21**(22): p. 4042-56.

[234] Hetey, S.E., D.P. Lalonde, and C.E. Turner, *Tyrosine-phosphorylated Hic-5 inhibits epidermal growth factor-induced lamellipodia formation.* Exp Cell Res, 2005. **311**(1): p. 147-56.

[235] Ishino, M., et al., *Phosphorylation of Hic-5 at tyrosine 60 by CAKbeta and Fyn.* FEBS Lett, 2000. **474**(2-3): p. 179-83.

[236] Nyalendo, C., et al., *Src-dependent phosphorylation of membrane type I matrix metalloproteinase on cytoplasmic tyrosine 573: role in endothelial and tumor cell migration.* J Biol Chem, 2007. **282**(21): p. 15690-9.

[237] Westhoff, M.A., et al., *SRC-mediated phosphorylation of focal adhesion kinase couples actin and adhesion dynamics to survival signaling.* Mol Cell Biol, 2004. **24**(18): p. 8113-33.

[238] Brunton, V.G., et al., *Identification of Src-specific phosphorylation site on focal adhesion kinase: dissection of the role of Src SH2 and catalytic functions and their consequences for tumor cell behavior.* Cancer Res, 2005. **65**(4): p. 1335-42.

[239] Koh, W., et al., *Formation of endothelial lumens requires a coordinated PKCepsilon-, Src-, Pak- and Raf-kinase-dependent signaling cascade downstream of Cdc42 activation.* J Cell Sci, 2009. **122**(Pt 11): p. 1812-22.

[240] Liu, Y. and D.R. Senger, *Matrix-specific activation of Src and Rho initiates capillary morphogenesis of endothelial cells.* FASEB J, 2004. **18**(3): p. 457-68.

[241] Perentes, J.Y., et al., *Cancer cell-associated MT1-MMP promotes blood vessel invasion and distant metastasis in triple-negative mammary tumors.* Cancer Res, 2011. **71**(13): p. 4527-38.

[242] Munoz-Najar, U.M., et al., *Hypoxia stimulates breast carcinoma cell invasion through MT1-MMP and MMP-2 activation.* Oncogene, 2006. **25**(16): p. 2379-92.

[243] Sounni, N.E., et al., *MT1-MMP expression promotes tumor growth and angiogenesis through an up-regulation of vascular endothelial growth factor expression.* FASEB J, 2002. **16**(6): p. 555-64.

[244] Sulzmaier, F.J., C. Jean, and D.D. Schlaepfer, *FAK in cancer: mechanistic findings and clinical applications.* Nat Rev Cancer, 2014. **14**(9): p. 598-610.

[245] Cabrita, M.A., et al., *Focal adhesion kinase inhibitors are potent anti-angiogenic agents.* Mol Oncol, 2011. **5**(6): p. 517-26.

[246] Mendez, M.G., S. Kojima, and R.D. Goldman, *Vimentin induces changes in cell shape, motility, and adhesion during the epithelial to mesenchymal transition.* FASEB J, 2010. **24**(6): p. 1838-51.

[247] Satelli, A. and S. Li, *Vimentin in cancer and its potential as a molecular target for cancer therapy.* Cell Mol Life Sci, 2011. **68**(18): p. 3033-46.

[248] Kidd, M.E., D.K. Shumaker, and K.M. Ridge, *The role of vimentin intermediate filaments in the progression of lung cancer.* Am J Respir Cell Mol Biol, 2014. **50**(1): p. 1-6.

[249] Lahat, G., et al., *Vimentin is a novel anti-cancer therapeutic target; insights from in vitro and in vivo mice xenograft studies.* PLoS One, 2010. **5**(4): p. e10105.

[250] Al-Reefy, S., et al., *Evidence for a pro-apoptotic function of RACK1 in human breast cancer.* Oncogene, 2010. **29**(41): p. 5651; author reply 5652.

[251] Cao, X.X., et al., *RACK1: A superior independent predictor for poor clinical outcome in breast cancer.* Int J Cancer, 2010. **127**(5): p. 1172-9.

[252] Bourd-Boittin, K., et al., *RACK1, a new ADAM12 interacting protein. Contribution to liver fibrogenesis.* J Biol Chem, 2008. **283**(38): p. 26000-9.

[253] Egidy, G., et al., *Transcription analysis in the MeLiM swine model identifies RACK1 as a potential marker of malignancy for human melanocytic proliferation.* Mol Cancer, 2008. **7**: p. 34.

[254] Lopez-Bergami, P., et al., *Rewired ERK-JNK signaling pathways in melanoma.* Cancer Cell, 2007. **11**(5): p. 447-60.

[255] Williams, S.R., D.S. Son, and P.F. Terranova, *Protein kinase C delta is activated in mouse ovarian surface epithelial cancer cells by 2,3,7,8-tetrachlorodibenzo-p-dioxin (TCDD).* Toxicology, 2004. **195**(1): p. 1-17.

[256] Boner, W. and I.M. Morgan, *Novel cellular interacting partners of the human papillomavirus 16 transcription/replication factor E2.* Virus Res, 2002. **90**(1-2): p. 113-8.